Extra-terrestrial fullerenes as a food source for microorganisms on the early Earth

Elle Bethune

Doctor of Philosophy

The University of Edinburgh

2024

Declaration

I hereby declare that this thesis was written by myself and that the work detailed within is my own unless explicitly stated otherwise. This work has not been submitted for any other degree or professional qualification.

(Elle Bethune, August 2024)

Lay Summary

The origin of life on Earth occurred about 4 billion years ago. During this time, the young Earth was being constantly bombarded by meteorites, many of which contained large amounts of organic material, which is made up of complex carbon compounds of all different structures. Carbon compounds are the main energy source for almost all types of life, and therefore it is possible that the first life to appear on Earth could have used the carbon compounds from meteorites as its food source, and therefore also an energy source. As an astrobiologist, I am interested in understanding how early life on Earth might have used these carbon compounds as a food source for two main reasons; firstly, understanding how the first life on Earth got its energy to grow and evolve will also help us understand how life on other planets might do the same. Secondly, by studying how life uses different carbon compounds from meteorites as food sources, we can narrow down the different types of environments on other planets that might be able to support life.

To understand how carbon compounds from meteorites might have been used as food sources by early life, my approach in this thesis is to test how microorganisms from the modern-day Earth might do so. The first two sections of this thesis detail a series of experiments where multiple different types of microorganisms were grown with some of the carbon compounds found in meteorites. On the early Earth, any organic material present would have been exposed to much higher levels of UV-radiation than it would today, and the atmosphere did not contain oxygen. In my experiments, I exposed meteorite organics to these environmental conditions, which changed their chemistry considerably. I found that after being exposed to these conditions, some microorganisms can use the organics from meteorites as a food source for growth. However, I also found that these same compounds are toxic to other types of more modern microorganisms. This shows that only the microorganisms that are most similar to early life on Earth can use meteorite material as a food source.

The last section of this thesis looks at the metabolomic response of the microorganisms when they are growing with the meteorite carbon as a food source. Metabolomics is the study of all the chemical reactions that take place inside a living organism, whether this is breaking down a food source to release energy, using simple molecules to form larger molecules for different functions or replicating DNA in order to reproduce and grow. In this section of the thesis I show that the microorganisms that are using the carbon compounds as a food source are actually experiencing some stress which is caused by the compounds themselves. This is a very interesting result because it shows these carbon compounds can simultaneously be used as a food source, while also harming the microorganisms- just enough to cause them stress, but not enough to slow down their growth.

This thesis establishes the effect that carbon compounds from meteorites have on a range of different types of microorganisms. The collective findings presented indicate that carbon compounds from meteorites, while they can be used as a food source by microorganisms, do not necessarily always mean that the environments they are found in are good places to search for life.

Abstract

The search for extra-terrestrial life is an ever-evolving field of research that seeks to identify and understand life elsewhere in the universe. In order to narrow down this expansive search it is necessary to establish a set of parameters pertaining to habitability. It is therefore of significant interest for astrobiologists to study the conditions extra-terrestrial life may need to arise. Earth is the only planet currently known to host life and therefore provides an excellent model system as a case study for astrobiologists seeking to search for and understand life on distant planets. Very little is currently known about primitive terrestrial microorganisms, particularly with regard to their energetic processes and metabolism. It is well established that the origin of terrestrial life occurred simultaneously with the Late Heavy Bombardment, during which time a massive amount of organic-rich meteoritic material was accreted. This likely resulted in the accumulation of a large reservoir of extra-terrestrial carbon on the early Earth around the time primitive microorganisms were evolving more advanced metabolic processes. While it was previously assumed early life must have been purely autotrophic, the presence of potentially biologically accessible organics in the early Earth environment introduces the possibility that primitive microbes may have evolved to exploit these resources and develop early heterotrophic mechanisms much earlier than is currently postulated.

Fullerenes are found in abundance in carbonaceous chondrites and were therefore almost certainly present in relatively high amounts on the early Earth. Very little is known about the effect of fullerenes and their naturally occurring water-soluble derivatives, fullerols, on microorganisms, particularly in anoxic environments, and therefore very limited conclusions can be drawn for their potential effects on primitive microbes. Furthermore, the effects of the extreme early Earth environmental conditions, such as short-wave UV exposure, on the chemical properties of fullerenes and their derivatives are yet to be characterised; yet investigating this is critical in understanding how fullerenes may have fulfilled an important ecological niche.

In this thesis, I will explore the effect of fullerenes C_{60} and C_{70} and their fullerol derivatives on microorganisms and their potential as carbon sources for heterotrophic metabolism. An anaerobic community was studied as an analogue of a primitive microbial system, with an isolate derived from this community used for further, more comprehensive analyses of biological fullerene interactions. Furthermore, the effect of fullerenes and fullerols on select aerobic environmental isolates and model species *E. coli* was examined. With these microbiology studies, I show that fullerene response is highly species-specific and closely linked to the growth environment. It is demonstrated that fullerene C_{60}, while inaccessible in its native form, can be converted to a highly accessible carbon source for anaerobic microorganisms when exposed to the high UV and anoxic conditions found on early Earth. To further understand the biodegradation pathways involved in C_{60} utilisation and the mechanism of toxicity to aerobic species, a comprehensive metabolomics study was carried out in which I present a novel set of results describing the innate biological effect of fullerenes on both an aerobic and anaerobic microorganism. The results presented in this thesis in their entirety give a clearer picture of how fullerenes on the early Earth and other habitable planets could provide primitive microbes with a previously undescribed source of carbon and energy.

Acknowledgements

I would first like to express my deepest gratitude towards my supervisor, Professor Charles Cockell, for his mentorship and guidance throughout my entire PhD process. Thank you for always providing me with the help and support I need while allowing me the freedom to explore my academic interests. A huge thank you to my second supervisor, Professor Eleanor Campbell, for her constant input and support, particularly with the chemistry side of my projects. Additionally, I would like to thank my collaborator Andrei Gromov for his help with the chemistry experiments.

I would like to extend a huge thank you to the entire UK Centre for Astrobiology group for creating such an encouraging work environment and for all the help and advice offered to me over these four years. I would also like to acknowledge my office mates, past and present, for supporting me through the hardest of days with endless coffee breaks.

I am so grateful to my best friends, Leo, Martina, Sam and Joe; thank you for being there unconditionally, for annoying me into smiling when I want to cry, for indulging my caffeine addiction and for throwing sugary snacks at me when I'm stressed. You all mean the world to me.

To my partner, Jonathan, thank you for loving me at my best and my worst, for never complaining about my singing in the car, for secretly loving my cats as much as I do and for waking me up every morning with the world's best coffee. I love you to Saturn and back.

I would like to thank my family for their constant support throughout my entire academic career: my grandparents, Nan and George, my uncle Graeme, my brother, Alex and mum, Lesley. Thank you for everything, I love you.

To Ms T. A. Swift, thank you for writing your discography; this entire thesis was written with the Anthology as the soundtrack.

Finally, and most importantly, I'd like to thank the most beautiful of boys Mr Spock, Calgacus and Agricola, for endless on-demand kitty cuddles and emotional support.

Contents

List of Figures

List of Tables

Chapter 1 Introduction

Habitability is one of the most important concepts in astrobiology research, as it encompasses the study of all the conditions which must be met for life to evolve, survive and proliferate in extra-terrestrial environments. Despite this, we still have a very limited understanding of the environments which can sustain life and no clear definition of the conditions necessary to make an environment habitable. Research which elucidates and refines our knowledge of habitability is therefore critical in the search for extra-terrestrial life and for the exploitation of terrestrial microflora for anthropogenic activities in space.

We are yet to discover conclusive evidence of extra-terrestrial life, therefore Earth remains the only planet on which the spontaneous appearance of living cells is confirmed. Thus, Earth provides us with the only existing case study with which to examine the origin of life and further constrain the conditions that made it habitable for primitive microorganisms.

All currently defined biology is made up primarily of carbon-based molecules, and therefore carbon is indisputably one of, if not the most, important element for life. Living cells use carbon for energy and growth by either fixing it from sources such as CO_2 or by consuming biologically accessible organic compounds. It is presumed that early life on Earth must also have used one of these two mechanisms to acquire energy and synthesise cellular components. It has been postulated that the earliest microbial life must have been autotrophic and synthesised its carbon compounds from CO_2 as, until a significant biological ecosystem was established, there was not enough organic carbon on the early Earth to sustain it otherwise. However, more recent evidence shows that there may indeed have been a large reservoir of biologically available carbon on the early Earth originating from organic-rich meteorites, a huge number of which were accreted around the time life first appeared. If primitive microorganisms had access to these extra-terrestrial compounds, they may have been able to utilise them as their primary source of carbon and energy.

The range of organics found in carbonaceous meteorites has only recently been characterised, and the effect of large fractions of these compounds on microorganisms is still unknown. However, if a significant proportion of these organics is shown to provide an accessible carbon source for primitive microorganisms, this will have a huge impact on our current understanding of exoplanet habitability. Many other Earth-like rocky exoplanets have a similar organic profile to that of the early Earth. Therefore, if these organics prove to be a sufficient carbon and energy source for microorganisms, it may indicate that these planets can sustain life, which will significantly narrow the ongoing search for habitable exoplanets and potentially lead to the first discovery of alien life.

1.1 Thesis scope and outline

In this thesis, I aim to address a significant knowledge gap concerning the potential for microorganisms to use extra-terrestrial organics as carbon and energy sources. The following work specifically focuses on a class of organics called fullerenes, which are found abundantly in carbonaceous meteorites and therefore would have been present as a potential carbon source on the early Earth. In each chapter I investigate and discuss the effects of fullerenes and their derivatives on both anaerobic and aerobic microorganisms, the underlying metabolic processes involved, and the relevance this has to primitive terrestrial and extra-terrestrial microorganisms and the habitability of carbon-rich environments.

Chapter 2 provides a discussion of the relevant background information and an in-depth review of the current literature pertaining to the effects of fullerenes and fullerols on microorganisms. This chapter highlights the significance of this work and presents the current knowledge gaps which will subsequently be addressed in this thesis.

Chapter 3 details the materials and methods which are used repeatedly throughout the experimental chapters of this thesis.

Chapter 4 investigates the effects of fullerenes and their fullerol derivatives on a relevant anaerobic microbial community and isolate. Additionally, it provides evidence that exposure to extreme early Earth environmental conditions significantly changes the effects observed and increases the biological accessibility of fullerenes.

Chapter 5 provides a comparison to the results obtained in Chapter 4 by determining the effects of fullerenes and fullerols on three species of aerobic bacteria: one model organism and two environmentally relevant species. This chapter discusses the large discrepancy in microbial fullerene responses observed across anaerobic and aerobic species and provides some critical environmental context to explain these differences.

Chapter 6 details an investigation into the change in the metabolomic profile of a model aerobic microorganism and the anaerobic isolate when exposed to fullerenes and when grown with environmentally relevant breakdown products as a carbon source. This chapter provides the first comprehensive metabolomic study into the degradation of fullerenes as a food source by microorganisms.

Chapter 7 summarises the primary findings of this thesis, provides a concluding discussion with respect to the results from all experimental chapters and details the next steps to further this research.

Chapter 2 Background and literature review

This thesis aims to explore the effects of extra-terrestrial fullerenes and their derivatives on early Earth microorganisms and discuss the implications this may have for our understanding of primitive life and its energy sources. In this chapter, I will present and discuss the relevant background information and literature to contextualise the findings discussed later in this thesis. An overview of extra-terrestrial organics is provided with emphasis on their cosmic formation and incorporation into asteroids and planetary bodies, followed by a discussion of their utilisation by microorganisms. The focus is then refined to a discussion on fullerenes and their water-soluble derivatives, their chemistry and relevance on the early Earth, and their interactions with microorganisms under standard and simulated early Earth conditions.

2.1 Microbes and Meteorites

2.1.1 Meteoritic carbon on the early Earth

Living cells are hypothesised to have assembled between 3.6 and 4 billion years ago from pre-biotic molecules (Trevors, 2010). Such precursors could have been synthesised on the early Earth in a reducing atmosphere or on metal sulphides in deep-sea hydrothermal vents, or they could have been accreted from meteoric material during the Late Heavy Bombardment (Orgel, 1998). The earliest microbial life, like modern-day life, must have had a mechanism by which it could generate cellular energy for vital metabolic processes and proliferation. Many assume the earliest cells must have been autotrophic, acquiring their biological carbon from nonbiological atmospheric CO_2 (Schönheit et al., 2016). If the first microorganisms were autotrophic, then when heterotrophy later evolved it is likely that autotrophs became a source of biologically available carbon (Schönheit et al., 2016). However, it is also possible that the earliest lifeforms were heterotrophic, acquiring their carbon from the fermentation of reduced organic compounds and potentially utilising the plethora of organic molecules delivered to the surface via meteoritic bombardment.

Meteoroids are rocky or metallic bodies originating in the interstellar media that can be classed as iron, stony or stony-iron, with stony-iron being further subdivided into chondrites and achondrites (Botta & Bada, 2002). Most meteoroids originate from objects in the asteroid belt and are formed via the fragmentation of main-belt asteroids (Alexander et al., 2017; Botta & Bada, 2002). Stony meteorites are composed of 3-5% carbon, the bulk of which is incorporated into insoluble macromolecular material known as kerogen, which contains polycyclic aromatic hydrocarbons (Botta & Bada, 2002; Chyba et al., 1990). Almost all biologically relevant molecules are found in carbonaceous chondrites including amino acids, aromatic hydrocarbons and carbohydrates (Kwok, 2019). In fact, over 14,000 compounds, each with isometric structures, have been identified in meteorites that have landed on Earth (Kwok, 2019). In general, for a compound with any given number of carbon atoms, all possible isomers are observed in the organic fraction of meteorites, indicating these are likely synthesised in the interstellar media through random chemical processes before being incorporated into the meteorite (Botta & Bada, 2002).

There are three types of extra-terrestrial organic-rich material that can be accreted; interplanetary dust particles, micrometeorites and meteorites (Alexander et al., 2017). During the Heavy Bombardment period 4.5-3.9 billion years ago, large quantities of extra-terrestrial material were delivered to the surface via meteorites (Ehrenfreund et al., 2011). Although it is thought that organics cannot survive atmospheric entry at velocities greater than 10 km/s, which is slower than the speed of even small bodies (Chyba et al., 1990), the presence of organics in accreted meteorites suggests that at least some of the material remains intact during entry (Kwok, 2019). The early atmosphere evidently had a much higher density of carbon dioxide than the present-day, therefore it is possible that on the early Earth, impacts were slowed down by the denser atmosphere so that the energy from their collisions with the surface was low enough to preserve the majority of extra-terrestrial organic material (Chyba et al., 1990; Pasek & Lauretta, 2008). The significance of this is that material accreted by the early Earth from meteorites could have provided a source of pre-biotic organic matter (Alexander et al., 2017; Flynn, 1996). While there is approximately 10^{21} kg of bulk carbon currently on the Earth (up to 90% of which is located in the planet's core) (Fischer et al., 2020), an estimated 10^{20} kg of cometary organic material has impacted the Earth throughout geological time (Chyba et al., 1990), most of which was collected during the Heavy Bombardment, during which the origin of life is estimated to have occurred. It is possible, therefore, that this high concentration of organics provided a 'kickstart' for early heterotrophic metabolism, forming the primary source of carbon for the growth of primitive microorganisms (Pasek & Lauretta, 2008).

2.1.2 Microbial metabolism of meteorites

It has been observed that meteorites become colonised by terrestrial microorganisms after landing on Earth, leading to a growing interest in what species can utilise this meteoritic material and the cellular mechanisms involved (Tait et al., 2017). After landing in Antarctica, the Allan Hills 84001 Martian meteorite was rapidly colonised by terrestrial filamentous bacteria from the Order *Actinomycetales* (Steele et al., 2000). Similarly, the Tatahouine meteorite was found to have been colonised by a highly diverse microbial community consisting of 11 bacterial divisions when examined 70 years after its fall (Benzerara et al., 2006). A 2017 study of meteorites collected from the Nullarbor Plain, Australia, revealed that these meteorites were riddled with 100 µm diameter channels produced by iron-nickel corrosion, some of which were lined with biofilms (Tait et al., 2017). Particularly thick biofilms were found in magnesium calcite-rich veins, indicating the low pH environment produced in these regions is favourable to some types of iron and sulphur-oxidising bacteria (Tait et al., 2017). This not only provides more evidence for the habitability of meteorites but suggests that such extra-terrestrial accumulation creates niche habitats for a select fraction of environmental microbes. It is worth noting, however, that the extent to which meteorites can be colonised may be limited. A 2012 study found that after incubation with a range of anaerobic growth media, the innermost pieces of the Murchison meteorite showed no signs of microbial contamination (Pikuta & Hoover, 2012). However, these samples had been in storage for approximately 10 years at the time of this study and the experimental setup only accommodated the growth of anaerobic microorganisms, therefore although the results suggest only the outer regions of the Murchison meteorite were colonised, this is probably not a universal observation.

Numerous subsequent studies have sought to characterise the inhabitants of other meteorites, but more recently attention has been focused on the cellular mechanisms by which microorganisms can metabolise meteoritic material. Of particular interest to astrobiologists are the mechanisms by which microorganisms can utilise extra-terrestrial material as energy sources for growth, as this is highly relevant for assessing the potential habitability of extra-terrestrial bodies and the future application of biological mining on comets and asteroids. Experiments carried out in 1990 by Stoker et al demonstrated that a variety of aerobic, anaerobic and facultative anaerobic microorganisms can utilise tholins as their sole carbon and nitrogen source (Stoker et al., 1990). Tholins are a broad class of organic compounds formed when simple carbon compounds are exposed to ultraviolet or cosmic radiation, a process which occurs ubiquitously across the solar system and in various extra-terrestrial bodies, including meteorites (Stoker et al., 1990). Bacterial species from the genera *Clostridium, Pseudomonas, Bacillus, Acinetobacter, Paracoccus, Alcaligenes, Micrococcus, Corynebacterium, Aerobacter, Arthrobacter, Flavobacterium* and *Actinomyces* have all been found to grow on tholin as their sole carbon and nitrogen source (Stoker et al., 1990). Findings like this suggest that because tholin compounds can support life as sole or partial energy sources, early terrestrial life may also have been capable of utilising them as a food source.

Several studies have identified a range of microorganisms capable of utilising meteoritic material as their sole carbon and energy sources. *Leptospirillum ferrooxidans* and *Acidithiobacillus ferrooxidans*, for example, can grow on pieces of the Toluca meteorite as their sole energy source, as these iron-oxidising species can efficiently utilise the nickel-iron alloy for metabolic respiration (González-toril et al., 2005). Biological weathering studies of the Murchison and Cold Bokkeveld carbonaceous chondrites and the York and Casas Grandes iron meteorites reveal that both anaerobic sediment cultures and aerobic *Acidithiobacillus ferrooxidans* can use meteoritic iron for growth (Gronstal et al., 2009). The pathogenic soil species *Pseudomonas aeruginosa, Burkholderia cepacia, Klebsiella pneumoniae* and *Serratia marcescens* can grow solely on several extra-terrestrial carbohydrates containing 3, 4, 5 and 6 carbons, including D-enantiomers, which is interesting as usually only L-enantiomers are used and produced by terrestrial life (Domínguez-Andrés et al., 2020).

An aerobic heterotroph capable of growing on meteorite extracts was discovered in 1997 and accordingly named *Nocardia asteroides* (Mautner, 1997). Results from this study also suggest that the thermophilic species *Thermotoga maritima* and *Thermus aquaticus* can use meteorite extracts as their sole carbon source at 70 ºC and 80 ºC, respectively (Mautner, 1997). To test if these meteorite extracts could be used as a sole carbon and energy source, a modified strain of *Pseudomonas fluorescens* was grown in meteorite extract with no additional carbon source (Mautner et al., 1997). The modifications to this strain result in the production of fluorescence when ATP is synthesised as an indicator of metabolic activity. In this experiment, the positive detection of fluorescence indicated that *P. fluorescens* grew 2.4 times faster with the extracts are is sole carbon source than it did on glucose (Mautner et al., 1997). *N. asteroides* and *Arthrobacter pascens*, the latter isolated from the unsterilised meteorite sample, were also able to utilise meteorite extracts as a sole carbon source, although high concentrations decreased the growth of *A. pascens*, probably due to increased toxicity.

Experiments using samples of the Murchison meteorite have revealed that up to 50% of the organics are released under high temperature and pressure conditions in an aqueous environment (Mautner et al., 1995). Bacteria from an unsterilised sample of meteorite, later identified as *Flavobacterium oryzihabitans* and *Pseudomonas maltophilia,* both grew normally on these meteorite extracts (Mautner et al., 1995). Interestingly, both species were also able to grow on the meteorite powder from which the extracts had been removed, suggesting that either some leftover soluble carbon is leeched into the water at 20 ºC, or these species can utilise some of the insoluble organic fraction. When the microbial cultures were grown with both meteorite extract and powder, they showed similar growth rates as when they were solely grown with extracts. However, meteorite powder that had been heat treated at 200 ºC for 24 hours was toxic (Mautner et al., 1995). In 2022, Waajen et al demonstrated that an anaerobic microbial community from pond sediment, which was dominated by species from *Geobacteraceae, Deltaproteobacteria and Desulfuromonadaceae,* could grow on powdered Cold Bokkeveld meteorite material as the sole nutrient source (Waajen et al., 2022). Interestingly, this study also found that the same material became toxic when pyrolyzed by heat exposure. The combined results from the Mautner (1995) and Waajen (2022) studies therefore suggest that temperature plays a critical role in the biological accessibility of meteoritic carbon. However, high temperature is not the only environmental extreme that seems to affect microbial growth with meteorites.

In a 2020 study by Milojevic et al, the growth of the thermophilic archaean *Metallosphaera sedula* on powdered meteorite at low temperatures was investigated (Milojevic et al., 2020). This species usually requires temperatures of 50-80 ºC to survive, however, it was found living in cooler sediments at 25 ºC. Terrestrial energy sources such as pyrite, chalcopyrite and other inorganic electron donors were unable to sustain its growth; however, it was able to grow on powdered stony meteorite as its sole carbon source at an average of 12 ºC (Milojevic et al., 2020). It was suggested that this organism prefers to utilise the multimetallic material in the meteorite as its electron donor because this can function as a metabolic cofactor that results in a more flexible enzyme structure, facilitating survival at such low temperatures by preserving the enzyme function in otherwise non-functional conditions. While these metals are normally toxic, *M. sedula* is extremely metallophilic and can tolerate exposure to heavy metals, resulting in a unique interaction that allows it to thrive in an otherwise uninhabitable environment. Studying interactions such as these is critical for understanding how microorganisms might survive the extremely cold temperatures of space as deliberate or accidental passengers inside meteorites, or for the application of biological technologies in human activity.

It is clear from the studies discussed that many modern terrestrial microorganisms are capable of utilising material from meteorites for growth, thereby suggesting that meteorites may have provided a food source for microbes on the early Earth. Multiple studies have highlighted the importance of the surrounding environmental conditions for these metabolic processes to occur, as extreme conditions such as high or low temperatures may significantly alter the accessibility of this material as an energy source.

2.2 Fullerenes

2.2.1 Chemical properties

Fullerenes are 3-dimensional analogues of aromatic carbon compounds which form spherical carbon cages (Panina et al., 1997). Closed fullerene cages are stable as long as the strain of curvature is evenly distributed, there is aromaticity, the electronic shell is closed and all pentagon arrangements are isolated as much as possible from each other by the hexagon arrangements in between (Kroto, 1988). Cages in which two or more pentagons are fused are less stable due to increased strain on the bonds, and symmetrical isomers have increased stability as the strain induced by the bond angle is more evenly distributed. Fullerene C_{60}, with a diameter of approximately 1 nm, is the most stable fullerene with a cage made up of 12 pentagon and 20 hexagon arrangements forming a structure with icosahedral symmetry in which every carbon has its valence satisfied (Zhang et al., 1986). Individual C_{60} molecules have in water a solubility of approximately 10^{-12} mg/L, which is very low considered insoluble (Avanasi et al., 2014; Lyon et al., 2006; Ruoff et al., 1993), however on contact with water, C_{60} forms stable colloidal aggregates, known as nC_{60}, which usually range in size between 100 and 600 nm, and in some cases have been measured to be as large as 1000 nm in diameter (Avanasi et al., 2014; Duncan et al., 2008; Lyon et al., 2006).

The reason C_{60} is so stable is because it fulfils of all the requirements listed above; it is the smallest fullerene in which all pentagon arrangements are isolated by hexagons and therefore there is the least amount of strain on its bonds (Kroto, 1988). The next smallest fullerene able to satisfy this condition is C_{70}, while C_{20}, consisting solely of pentagons, is the least stable. Fullerenes in the range of 40-80 carbons are highly resistant to chemical attack by reactive species, while those with fewer than 30 carbons are relatively unstable and have yet to be isolated and purified (Zhang et al., 1986).

Terrestrial sources of fullerenes are limited to lightning strikes, wildfires, coal, meteoritic impact craters, certain rock formations, and any other incomplete combustion of organic material (Chae et al., 2014). Because of the need for a large, localised energetic event to form fullerenes on Earth, they tend to only be created naturally in low concentrations (Buseck, 2002). Fullerenes are generated from graphite during partial combustion. Graphite consists of planar sheets of hexagonal carbon rings, however, carbon can maintain its valency in pentagons when atoms are lost from the edge of the sheet (Buseck, 2002). The bond-angle strain of these pentagon arrangements forces the sheet to curve, forming a bowl shape (Chuvilin et al., 2010). If enough curvature is achieved, the ends eventually ‘zip’ and re-join to form a closed, stable cage (Chuvilin et al., 2010).

Perhaps of more interest to astrobiologists and astronomers is the occurrence of extra-terrestrial fullerenes and their eventual accumulation on planetary surfaces, including Earth. It is now well established that fullerenes are present in the interstellar media (ISM) (Chae et al., 2014; Maier & Campbell, 2017; Tielens, 2013), as spectral identities for both cationic and neutral C_{60} are reliably detected with abundances of 10^{-3} (cationic) and between 10^{-4} and 10^{-3} (neutral) of the total gas-phase carbon (Berné et al., 2017; Campbell et al., 2015). Additionally, both C_{60} and C_{70} have been detected in planetary nebulae emission and infrared spectra (Candian et al., 2019; García-Hernández et al., 2012; Otsuka et al., 2014), making up a few percent of the available cosmic carbon in at least one nebulous region of detection (Cami et al., 2010). Fullerenes, particularly C_{60}, are stable under ultraviolet (UV) irradiation and are therefore highly likely to survive the transition from solar atmospheres to the ISM, where they are naturally incorporated into solid bodies such as meteorites (Sabbah et al., 2022).

Fullerenes C_{60} and C_{70} were detected in the Allende meteorite by Becker et al in 1994. This group continued to detect fullerenes in both the Allende and Murchison meteorites (Becker et al., 1999, 2000; Becker & Bunch, 1997), however these results were never successfully replicated by any other groups (Buseck, 2002). Hammond and Zare were later able to show that the fullerenes detected by the Becker group were not intrinsic to the meteorite samples but were rather generated during the one-step laser desorption ionisation technique used for the analysis of the carbon content (Hammond & Zare, 2008). Although this result seemed to indicate fullerenes may not be as present in meteorites as previously assumed, a more recent study by Sabbah et al has successfully located fullerenes $C_{30\text{-}100}$ in the Almahata Sitta meteorite by utilising a two-step laser ionisation mass spectrometry technique (Sabbah et al., 2022). This technique provides a way of analysing organic molecules by spatially and temporally separating desorption and ionisation with two different lasers, which allows for the detection of fullerenes with negligible amounts of fragmentation (Sabbah et al., 2022). This ultimately resulted in the positive identification of fullerenes ranging in concentrations of 15-28 ppm in the Almahata Sitta meteorite (Sabbah et al., 2022).

2.2.2 Biotoxicity

There is a growing number of applications for fullerenes in the nanotechnology and pharmaceutical industries which has triggered an interest in how these structures affect the environment, as anthropogenic use is likely to result in environmental contamination (Avanasi et al., 2014; Pérez et al., 2009), and very little is known about the fate of fullerenes in the environment (Chae et al., 2014). nC_{60} is the standard notation used to refer to aqueous C_{60} aggregates. nC_{60} is widely reported to be bactericidal to both Gram-positive and -negative bacteria, depending on the concentration and functionalisation (Chae et al., 2014; Duncan et al., 2008; Hancock et al., 2012; Tsao et al., 2002) and nC_{60} in aqueous suspensions has been reported to have toxic effects towards fish, terrestrial and aquatic invertebrates and some human cell types (Avanasi et al., 2014; Duncan et al., 2008). C_{60} is also known to be cytotoxic to many eukaryotes and can cause DNA damage to a range of organisms either directly or indirectly by producing reactive oxygen species under light excitation (Peng et al., 2020).

Microbial assays conducted with both Gram-negative *Escherichia coli* and Gram-positive *Bacillus subtilis* under aerobic and anaerobic conditions demonstrate that concentrations of nC_{60} higher than 0.4 mg/L are inhibitory to bacterial growth (Fortner et al., 2005). Both species in this study did grow under lower concentrations of 0.04 mg/L nC_{60}, however growth was recorded as a binary and therefore any growth, even reduced, was recorded as a positive. This means the cultures may still have been inhibited in comparison to the controls, but a reduction in growth would not have been recognised. In another study that tested the effect of nC_{60} aggregates of varying sizes on the growth of *B. subtilis*, it was found that smaller aggregates have a greater antibacterial effect (Lyon et al., 2006). The presence of salt may also affect the biotoxicity of nC_{60} as high salt media can cause fullerene aggregates to precipitate and fall out of suspension (Lyon et al., 2005).

The bacterial species *Pseudomonas putida* and *B. subtilis* both respond to nC_{60} aggregate exposure by altering their membrane lipid composition, phase transition temperature and fluidity (Fang et al., 2007). Although these species demonstrate different physiological changes under the same exposure, the very fact that these alterations occur suggests that some mechanisms exist by which bacteria can adapt to the oxidative stress caused by environmental fullerenes. It was previously assumed that the antibacterial properties of C_{60} were due to reactive oxygen species (ROS) production, however in 2008 the Lyon group showed that the colorimetric agents used in previous studies to evaluate ROS production in aqueous nC_{60} suspensions can interact with C_{60} to produce false positives, and therefore they propose that nC_{60} actually exerts oxidative stress on bacteria independently of ROS production (Lyon et al., 2008).

C_{60} may also have mutagenic potential, as a 2012 study using the model organism *Salmonella typhimurium* suggests (Hancock et al., 2012). After exposure to nC_{60} concentrations of 0.5 mg/L and above, *S. typhimurium* had an extended lag phase at concentrations higher than 0.1 mg/L, and the mutagenic potential increased with concentration, significantly altering the expression of 271 genes. Most of the upregulated genes identified were involved in energy metabolism, amino acid synthesis, transcription and DNA metabolism, while the genes that were downregulated were mostly involved in protein function. The combined data from this study indicate that C_{60} aggregates interact with the outer bacterial membrane and interfere with transport functions while inducing a stress response, which results in delayed growth and increased mutagenicity (Hancock et al., 2012).

After exposure to nC_{60}, *Pseudomonas fluorescens* was found to have undergone alterations to cellular Amide II, proteins and lipids, and had altered carbohydrates, Amide II and DNA after exposure to fullerene soot (Riding et al., 2012). This bacterium demonstrated slightly inhibited metabolic processes in proportion to increasing concentrations of both C_{60} and fullerene soot, although DNA damage after C_{60} exposure was minimal. Interestingly, most of the biochemical changes that were detected occurred to the outer cell components of

P. fluorescens. This suggests that C_{60} can only directly oxidise cellular components, therefore it can only target components on the exterior of the cell (Riding et al., 2012). Despite its obvious antimicrobial effects on aerobic species, C_{60} does not appear to be inhibitory to anaerobic microorganisms in anoxic environments (Nyberg et al., 2008; Zhao et al., 2018).

2.2.3 Biodegradation

Very little is known about fullerene biodegradation, either in environmental or laboratory settings (Peng et al., 2020). However, there is some evidence that certain mammalian enzymes are capable of degrading C_{60} (Litasova et al., 2016). A recent study that characterised the degradation of C_{60} by the human myeloperoxidase enzyme found that C_{60} is degraded by this enzyme without the formation of detectable hydroxylated compounds (Piotrovskiy et al., 2020). In this case, fullerols were not detected as intermediates and instead, aromatic compounds such as benzaldehyde and benzyl alcohol were formed, suggesting this form of degradation did not involve the action of hydroxyl radicals (Piotrovskiy et al., 2020).

C_{60} is resistant to mineralisation in soil over periods of 1-2 years (Avanasi et al., 2014), while other carbon nanomaterials are reported to be modified in the environment by microorganisms (Hyung et al., 2007). Some experimental evidence suggests that C_{60} can be partially transformed by environmental microbes as it is observed that C_{60} aggregates decrease in size and increase in hydroxylation and photosensitivity when aged in the presence of microbes (Chae et al., 2014). In this experiment, bacteria were observed growing in non-sterile fullerene suspensions ranging in age from a few months to two years old. These bacteria were used to inoculate fresh microcosms containing ^{13}C-C_{60} and it was found that these microcosms had significantly higher levels of ^{13}C-CO_2 in the gas space than the controls, although nonbiological mineralisation cannot be completely ruled out (Chae et al., 2014). In 2007, Tong et al demonstrated that the introduction of C_{60}, either in aqueous or solid granular form, to soil microbial communities had little to no effect on community structure and function (Tong et al., 2016). This group later went on to find that nC_{60} aggregates in aqueous suspension have minimal effects on the microbial biomass and metabolic activity of soil communities (Tong et al., 2016). Interestingly however, although the size of the aggregates had little effect on community composition in soils with high organic matter content, in soil with low organic matter, smaller nC_{60} aggregates had a more negative impact on soil biodiversity (Tong et al., 2016).

Many environments that are most likely to be exposed to accumulated carbon nanomaterials are anoxic, and therefore the effect of fullerenes on anaerobic microorganisms is important. However, this is often only studied from a toxicological perspective, therefore very little is known about specific anaerobe-fullerene interactions and any degradation pathways that may be active. As the first microorganisms on the early Earth were anaerobic, understanding how primitive life might have dealt with extra-terrestrial fullerenes also relies on elucidating metabolic processes involved in fullerene degradation in modern-day anaerobes. Experiments conducted on an anaerobic community from wastewater sludge reveal that exposure to C_{60} over 154 days does not affect the gas production of these microorganisms (Nyberg et al., 2008). This study concluded that C_{60} was not toxic to this community, however, it should be noted that a relatively low concentration of C_{60} was used, and no DNA analysis was carried out to assess if the community composition changed in response to exposure. Another anaerobic study using a community from anaerobic digestion reactors found no change in community methane production after 35 days of C_{60} exposure (Zhao et al., 2018), which supports the previous conclusion that C_{60} has no harmful effect on anaerobic sludge bacteria. In 2017 it was found that anaerobic wastewater microorganisms form spores in response to stress induced by high nC_{60} concentrations of 10 and 100 µg/L (Auwerter et al., 2017). Although there is no concrete evidence that this is a survival response to resist C_{60} toxicity, it is likely triggered by concentrated nC_{60} exposure.

The first known report of a bacterial species capable of utilising C_{60} as its sole carbon source was made in 2020 by Wang et al after successfully growing *Labrys sp*. WJW with C_{60} as the only source of carbon (Wang et al., 2020). After 12 days of growth on nC_{60}, *Labrys* sp. WJW had degraded 60% of the available C_{60}, during which time the bacterial growth curve measured using both optical density and qPCR increased steadily and then stabilised around day 10 with cell density increasing approximately 25-fold. Interestingly, cell viability tests showed that nC_{60} still exerted toxic effects on the bacterial cells gathered on biofilms on the surface of the C_{60} aggregates, probably due to the direct contact they maintained with the C_{60} surface. However, despite this loss in viability, the cells could still aerobically uptake C_{60} and bio-transform it by breaking the cage structure, demonstrated by the absence of the three distinct C_{60} peaks when Raman analysis was performed. The authors of this study propose that the breaking of the cage structure by *Labrys sp.* WJW is achieved via a Fenton-like reaction in which a siderophore is secreted by the cells to form a complex with Fe(III), reducing it to Fe(II), which is oxidised by hydrogen peroxide back to Fe(III), producing hydroxyl radicals in the process (Wang et al., 2020) It is proposed that the hydroxyl radicals generated in this process facilitate the extracellular degradation of the fullerene cage. This theory is further backed up by the presence of a siderophore in the growth medium detected with a positive chrome azurol S (CAS) assay. Siderophores are generally produced in response to an iron-deficient environment, and therefore it is likely that that *Labrys sp.* WJW naturally secretes this siderophore when all available trace iron in the growth media is depleted, rather than having evolved specific C_{60}-targeting mechanisms (Wang et al., 2020).

2.3 Fullerols

2.3.1 Chemical properties

Fullerols are derivatives of fullerenes characterised by the attachment of many hydroxyl functional groups (Semenov et al., 2016). Underivatized fullerene cages are made up of sp^2 hybridised carbons. During functionalisation, two adjacent sp^2 hybridised carbons become the target of attack by radical species, which break the double bond between these carbons to allow the addition of two hydroxyl groups (Guldi & Asmus, 1999). The resulting hydroxyl-bound carbons are sp^3 hybridised and therefore the cage structure becomes slightly weaker with each hydroxyl group addition (Friedrich et al., 2011).

C_{60}-fullerol is highly photosensitive and soluble in water (Semenov et al., 2016), however it still tends to form spherical aggregates in aqueous solutions, although to a lesser extent than native C_{60} (Brant et al., 2007; Guldi & Asmus, 1999; Hotze et al., 2009). The mean diameter of these clusters is 100 nm or more, although cluster size is dynamic and can be affected by environmental factors such as pH and temperature (Brant et al., 2007). In biological systems, fullerols act as oxidising agents due to their efficiency at generating singlet oxygen species (Vileno et al., 2004). Both nC_{60} and C_{60}-fullerol can generate ROS when photoexcited (Kamat et al., 2000), but fullerol is particularly effective at producing singlet oxygen in water (Brunet et al., 2009).

2.3.2 Biotoxicity

Fullerene derivatives appear to have very different effects on microorganisms compared to their native fullerene parent molecules, and these effects appear to vary greatly with factors such as charge and pH. For example, positively charged C_{60} derivatives inhibit the growth of model aerobic microorganisms *E. coli* and *Shewanella oneidensis* in concentrations as low as 10 mg/L, whereas negatively charged derivatives do not seem to affect growth at all (Tang et al., 2007). Experimental data also seems to suggest although positively charged derivatives inflict mechanical stress on the microorganisms by attacking the cell wall or membrane, both *E. coli* and *S. oneidensis* can alleviate the stress by aggregating, indicating that the microbial central metabolism is robust against stress inflicted by fullerene nanoparticles (Tang et al., 2007). Further studies seem to consolidate the observation that anionic fullerene derivatives are significantly less toxic to microorganisms than cationic derivatives like fullerols and suggest this toxicity may be the result of positively charged derivatives forming clusters around bacterial cells (Deryabin et al., 2014).

It is reported that C_{70} derivatives are antimicrobial towards both Gram-positive and Gram-negative bacteria and that this is likely the result of the release of reactive oxygen species from the functionalised C_{70} particles attacking bacterial cell walls (Huang et al., 2014; Huang et al., 2013; Ouyang et al., 2016). However, most of the available literature seems to concur that C_{60}-fullerol does not exhibit antibacterial activity, despite having a higher photochemical activity than its parent C_{60} molecule (Li et al., 2008). For example, soluble C_{60} derivatives are significantly less toxic to human cell lines than nC_{60} in water (Sayes et al., 2004). It appears that when C_{60} is functionalised by the addition of multiple electron-releasing groups, the electronegativity of the resulting derivative decreases, and therefore fullerols have reduced chemical activity and lower biological toxicity than nC_{60} (Chiang et al., 1995). In fact, at certain concentrations, it appears that exposure to C_{60}-fullerol can enhance algae density, fungal growth and daphnia lifespan, probably due to its antioxidant properties (Gao et al., 2011). However, there is some suggestion that cationic C_{60} derivatives become more toxic to bacteria when exposed to light, which should be taken into consideration when assessing the biotoxicity of fullerols (Tegos et al., 2005).

2.3.3 Biodegradation

C_{60}-fullerol is much more bioavailable in soils than its fullerene counterpart and is often readily mineralised to CO_2, albeit at a much slower rate than other highly bioavailable carbon sources such as glucose (Navarro et al., 2015). In 2009, the first report of direct fullerol biodegradation was made following experiments with two species of fungi. *Phlebia tremellosa* and *Trametes versicolor* were both found to oxidise C_{60}-fullerol into carbon dioxide over 32 weeks, and a small amount of fullerol carbon was incorporated into the lipid biomass (Schreiner et al., 2009). A subsequent 2017 study was the first to detect the uptake of C_{60}-fullerol in soil microcosms, where two distinct soil samples were able to aerobically mineralise a significant amount of C_{60}-fullerol (Berry et al., 2017). Over 65 days, bacterial abundance in the soil microcosms increased and between 30 and 56% of the total fullerol carbon was converted into CO_2 while pristine C_{60} under the same conditions was not (Berry et al., 2017). The results of this study indicated that although underivatized C_{60} does not appear to be biologically available, C_{60}-fullerol is readily taken up and utilised as a carbon source in soils.

2.4 Effect of UV on fullerenes and fullerols

When studying the degradation of fullerenes and their derivatives by microbes in the environment, it is important to consider the chemical alterations that may occur to pristine fullerenes and fullerols under natural conditions, as this could impact how microorganisms interact with them. One such environmental factor to consider is light, as this is well known to catalyse the degradation of environmental fullerenes (Lee et al., 2009; Sanchís et al., 2018). On the early Earth, any aqueous nC_{60} would have been in a largely anoxic environment and surface UV radiation levels would have been much stronger with wavelengths down to 200 nm reaching the surface of early Earth (Cnossen et al., 2007; Cockell, 1998). In organic solvents such as benzene, C_{60} is converted to $C_{60}O$ when exposed to UV (Creegan et al., 1992), and in the solid state, C_{60} will cross-link under UV exposure to form polymers (Sun et al., 1995). Aqueous nC_{60} degrades when exposed to either solar-wavelength or UV light at 254 nm, and the resulting photoproducts have increased water stability (Sanchís et al., 2018), and are significantly less antibacterial to aerobic bacteria than unaltered C_{60} (Hou & Jafvert, 2009a; Hou et al., 2010; Lee et al., 2009). When these products are added to a microbial soil community, excess CO_2 containing carbon from C_{60} is respired, indicating that the irradiation of C_{60} enhances its degradation in soil (Berry et al., 2016).

C_{60}-fullerol is highly photosensitive and produces a range of reactive oxygen species such as singlet oxygen and hydroxyl radicals when exposed to UV light (Brunet et al., 2009; Chae et al., 2009; Ma et al., 2020), which has been found to induce lipid and protein oxidation in membranes (Kamat et al., 2000). This indicates that C_{60}-fullerol, conversely to native C_{60}, has higher antimicrobial activity upon exposure to light. The exact nature of the ROS species generated is somewhat debated, as various studies have detected different combinations of singlet oxygen, superoxide and hydroxyl radicals (Hotze et al., 2009; Ma et al., 2020), although singlet oxygen seems to be the most consistently produced and detected species. It has been suggested that when fullerol is irradiated, the first radicals to be produced are singlet oxygen and superoxide, which then leads to the formation of secondary species like hydroxyl radicals and hydrogen peroxide (Pickering & Wiesner, 2005), and it is the hydroxyl and singlet oxygen radicals that are responsible for the degradation of organic material (Ma et al., 2020). Singlet oxygen produced by irradiated fullerol can effectively deactivate bacteriophages (Hotze et al., 2009), and this deactivation only occurs with photosensitised fullerol, confirming that exposure to UV is the cause of its toxicity (Badireddy et al., 2007). Interestingly, in a 2008 study by Hotze et al, fullerol suspensions produced both singlet oxygen and superoxide after 60 minutes of UV irradiation, but nC_{60} did not (Hotze et al., 2008). This is partially explained by the fact that nC_{60} forms a much denser aggregate structure in water compared with C_{60}-fullerol, limiting its ability to generate ROS (Hotze et al., 2008).

Very little is known about how nC_{60} and C_{60}-fullerol behave in anoxic aqueous media when exposed to UV radiation at 254 nm. It is thought that fullerene C_{60} in organic solvents still degrades under UV light when no oxygen is present, albeit to a lesser extent (Taylor et al., 1991). Similarly, aqueous C_{60}-fullerol appears to be mineralised when exposed to solar radiation in nitrogen-saturated water, but the photolysis reaction is two times slower under anoxic conditions than in an oxygen atmosphere (Kong et al., 2009). The half-life of solid-state C_{60} mixed with a quartz matrix and irradiated with UV is approximately 13.1 days in anoxic conditions (Carboni et al., 2017), although the exact mechanism of anoxic degradation is not clear.

Any fullerene degradation products produced under anoxic conditions are likely to be most similar to those that would have been produced on the early Earth, just as any strong antibacterial effects produced by photoactivated fullerol likely represent what may have occurred in early microbial systems. Any effects such intermediate products and reactive oxygen species have on microbial life are therefore likely more representative of what would have occurred on the early Earth.

2.5 Summary

This review highlights the current state of knowledge regarding the effects of fullerenes and their derivatives on microorganisms. Multiple studies have assessed the effects of fullerenes and fullerols on both aerobic and anaerobic microorganisms, however large discrepancies in methodology have resulted in conflicting conclusions. While some studies find fullerenes to be inhibitory to bacterial species, others find them to have no adverse effects. While C_{60} appears highly resistant to degradation in the environment, at least one study has identified an aerobic microorganism capable of utilising it as a carbon source. The soluble derivates of fullerenes, fullerols, appear to be more readily biodegraded, although conflicting studies find them to be highly toxic to certain species. Interestingly, UV-degradation appears to make fullerenes more biologically accessible for degradation by microorganisms, while inducing toxicity in their fullerol counterparts. The fate of fullerenes under early Earth environmental conditions is unknown, but understanding how the chemistry of these compounds changes under these conditions will allow us to better predict the bioaccessibility of fullerene carbon on rocky exoplanets. More conclusive data about the effects of fullerenes and fullerols on anaerobic microorganisms is needed to understand how early terrestrial microbes may have interacted with extra-terrestrial fullerenes. Similarly, comparable studies carried out with aerobic species will allow the determination of whether the environment is solely responsible for the clear differences observed between anaerobic and aerobic species' fullerene responses, or whether the metabolomic response is innately different. Lastly, there is nearly no data available detailing any metabolomic pathways involved in fullerene degradation by microorganisms, which severely limits the current understanding of the microbiological effects of fullerenes and their propensity to be utilised as carbon sources, either on the Earth or elsewhere on other habitable exoplanets.

Chapter 3 Materials and methods

This chapter will detail general methods and practical considerations that are referred to repeatedly throughout this thesis. Protocols and data analyses specific to individual experiments are presented within each results chapter. This chapter therefore only contains methodology that is applicable in more than one of the following chapters and will be subsequently referenced as appropriate.

The synthesis of fullerols described in section 3.1.2 was done by Andrei Gromov, School of Chemistry, University of Edinburgh. The TEM sample preparation in section 3.4 was done by Stephen Mitchell from the Centre Optical Instrumentation Laboratory (COIL), which is supported by a Core Grant (203149) to the Welcome Centre for Cell Biology at the University of Edinburgh. DNA sequencing and data analysis was done by Novogene, UK. All other work is my own.

3.1 Fullerene suspensions

3.1.1 Fullerenes

Powdered fullerene C_{60} (99.5+ % purity, purchased from IOLITECH, Germany) and C_{70} (98+ % purity, purchased from MST, Latvia) were acquired. Aqueous suspensions were prepared by adding powdered fullerene to sterile M9 minimal media in glass bottles and submerging them in a sonicator bath (Elma S 60 H Elmasonic) for 6 hours until large aggregates were visually dispersed. The bath temperature was kept below 45 °C via the addition of ice water every 30 minutes to minimise any risk of thermal alteration.

3.1.2 Fullerols

C_{60}- and C_{70}- fullerol were synthesised by adapting a procedure first described by Kokubo et al (Kokubo et al., 2011). Firstly, 150 mg C_{60} was dissolved in 150 mL toluene. Twenty-five millilitres of H_2O_2 (30%) was then slowly added, followed by 0.8 mL tetrabutylammonium hydroxide ($(C_4H_9)_4NOH$, 40% aqueous solution). The mixture was then stirred at 750-1000 rpm at 60 °C for 10-15 hours until the organic layer became colourless. The organic and aqueous layers were then separated. The remaining water and H_2O_2 were evaporated from the aqueous mixture (at 55-60 °C and <20 mbar) until the remaining residue had a waxy consistency. This residue was then diluted with 30 mL of isopropanol and the $(C_4H_9)_4NOH$ was neutralised by adding 0.125 mL of concentrated HCl. A light-yellow solid began to immediately precipitate and continued for 2-3 hours, after which this solid material was separated by centrifugation and vacuum dried. The amounts of starting products detailed here yielded a total of 149 mg of fullerol material. This material was characterised by FT-IR spectroscopy, mass spectroscopy, solid-state ^{13}C NMR and thermal gravimetric analysis, the details of which can be found in Chapter 4. The synthesised fullerols were found to have the formulae $C_{60}(OH)_{44}(6\text{-}8)H_2O$ and $C_{70}(OH)_{50}(14\text{-}16)H_2O$.

To make fullerol suspensions, synthesised fullerol powder was added to M9 minimal media and dissolved with minimal stirring. C_{60} and C_{60}-fullerol mixes were made by adding fullerol powder to freshly prepared C_{60} suspension in M9. All suspensions were stored in the dark before use.

3.1.3 UV-irradiated suspensions

To produce fullerene and fullerol UV products, suspensions were made, purged with N_2 (for three minutes per mL) and sealed inside airtight quartz Erlenmeyer flasks inside an anaerobic chamber (COY Laboratory Products Inc, vinyl anaerobic chamber with a 2% hydrogen 98% nitrogen atmosphere). Sealed anoxic suspensions were then removed from the chamber and placed 10 cm below a suspended 254 nm UV lamp for two weeks. The UV lamp and sample were contained within a non-airtight black box to limit ambient light to the sample and prevent outside exposure to short-wave UV. The resulting UV products were analysed and are described in Chapter 4.

3.2 Preparation of glassware

Anaerobic culturing was done in 15 mL serum bottles with butyl stoppers and aerobic culturing was done in 100 mL Erlenmeyer flasks. All glassware and stoppers used for culturing experiments, both anaerobic and aerobic, were treated to sterilise and remove residual organic contaminants following a protocol adapted from Eaton & Franson (Eaton & Franson, 2005). Glassware used for culturing was washed with detergent (Decon90, 2% solution), rinsed three times with deionised water and then soaked overnight in 0.1 M HCl (12-16 hours). The glassware was then rinsed another three times with deionised water, air dried, capped with aluminium foil, placed in a furnace at 550 °C for 6 hours and then cooled completely before use. Butyl airtight stoppers for use with serum bottles were similarly cleaned by washing with detergent, boiling three times for five minutes in deionised water and air drying in a laminar flow hood. All stoppers were then stored in sterile containers until use.

3.3 Culturing

3.3.1 Microorganisms

The anaerobic community used in experiments detailed in Chapters 4 and 6 was originally derived from anoxic sediment collected by Annemiek Waajen from Blackford Pond, Edinburgh (Waajen et al., 2022). This was sub-cultured three times with raw meteorite material as the only carbon source to obtain a community composition selected to grow on meteoritic carbon which was dominated by species from the *Geobacteraceae* and *Desulfuromonadaceae* families (Waajen et al., 2022). This meteoritic material contained various organics, meaning that the community had already been selected for growth with recalcitrant macromolecular organics. This made it an appropriate choice for subsequent experiments with fullerenes and it was therefore taken as the starting community for the anaerobic growth experiments in this thesis.

For the aerobic experiments detailed in Chapter 5, the model organism *Escherichia coli* was chosen because as well as being very well-characterised, some background literature about the effect of fullerenes on *E. coli* already existed for comparison. The laboratory strain *Escherichia coli* K-12 MG1655 was chosen because it approximates wild-type *E. coli* and has had minimal genetic manipulation, the main alteration being a frameshift mutation that decreases *pyrE* expression, resulting in the strain growing 10-15% slower than wild-type *E. coli* in pyrimidine-free medium (Blattner et al., 1997). It was also relevant to obtain environmental isolates that showed some starting resistance to fullerenes to ensure some growth would be possible. To achieve this, 50 g samples of non-sterile basalt rock were crushed and mixed with 1 g samples of C_{60} powder. These samples were then placed in glass Duran bottles outside in central Edinburgh with covers suspended 5 cm above the bottle openings to promote free air circulation while limiting the entry of rainwater. These samples were left untouched for approximately 6 months, after which they were returned to the laboratory. One-gram aliquots of the basalt-fullerene mix were then incubated at 22 °C in 50 mL M9 minimal media (KH_2PO_4 (1.2%(w/v)), Na_2HPO_4 (2.8%(w/v)), NH_4Cl (0.4%(w/v)), NaCl (0.2%(w/v))) supplemented with 0.4% (w/v) glucose for 48 hours. Samples of the resulting cultures were then streaked on M9 agar (1.5%) with glucose and kept at 22 °C until microbial colonies were visible. Single, discreet colonies were then streaked on fresh agar a further two times to obtain plates of uniform colonies. After this process, two distinct species with different but consistent colony morphologies were successfully isolated. These species were later characterised and used as the environmental isolates for the aerobic experiments in Chapter 5 (see section 3.5).

3.3.2 Culture media

All microbial culturing was done using M9 minimal media because the nutrient-poor nature of this medium allows for careful control of the carbon source available to the microorganisms, which is particularly relevant for the growth experiments detailed in this thesis. Although the original anaerobic community was cultured by Waajen et al with sodium acetate as the positive control carbon source, for these experiments I chose to replace this with 0.4% (w/v) glucose to prevent the sodium ions from sodium acetate interfering with any mass spectrometry data taken of these cultures in downstream analysis. Additionally, glucose is a highly accessible carbon source that can be utilised for growth by most microorganisms and is very commonly used for laboratory culturing, making it a good universal substrate to use with all species cultured for the experiments in this thesis.

3.3.3 Anaerobic culturing methods

For all anaerobic cultures, microcosm volumes of 5 mL were used. Unless otherwise specified, positive controls were made using M9 media supplemented with glucose and inoculated with the relevant microorganism and negative controls for each experimental condition were made identically to the relevant condition, but not inoculated with bacteria.

Microcosms were initially prepared aerobically under sterile conditions; the relevant media and carbon source were added to sterile and organic-free serum bottles which were then stoppered and sealed with aluminium crimps. Each microcosm was then purged with N_2 (for three minutes per mL) using a 22 µm filter attachment to maintain sterility. Microcosms were then moved into an anaerobic chamber (COY Laboratory Products Inc, vinyl anaerobic chamber 2% hydrogen 98% nitrogen) where all subsequent anaerobic culturing was done. For cell counting (detailed in Chapter 4), 50-100 µL aliquots were taken from each microcosm in 1.5 mL Eppendorf tubes and removed from the anaerobic chamber to count using a microscope. This was done so that all microcosms remained inside the chamber but could still be analysed at regular time points using equipment outside of the chamber. Unless otherwise specified, anaerobic cultures were grown for 28 days for end-point analysis as this was found to be the average length for a community growth cycle.

It should be noted that before developing the cell counting method detailed in Chapter 4, I first attempted to quantify the anaerobic community's growth by plating on solid agar and counting the colony-forming units (CFUs). This did not prove to be a successful method of measuring growth over time as the number of colonies formed was very inconsistent over serial dilutions and between triplicates. This is likely because not all the species present in the community can grow on solid agar and therefore any growth data obtained by counting CFUs is not representative of actual whole-community growth.

3.3.4 Aerobic culturing methods

All *E. coli* cultures were incubated in a static (for plates) or shaking (for liquid cultures) incubator at the optimum temperature of 37 °C unless otherwise specified. All *E. coli* growth experiments were started using inoculum from a 25 mL overnight culture (M9 media with 0.4% (w/v) glucose) that was grown for 18-24 hours from a single colony.

The aerobic environmental isolates were always incubated at 22 °C and shaken when in liquid culture. This was to maintain consistency as all incubation during the isolation process was done at 22 °C, and constant shaking at 150 rpm prevents cell clumping. Both environmental isolates were grown in 25 mL overnight cultures (M9 media with 0.4% (w/v) glucose) from single colonies for 24 hours as the inoculum in aerobic growth experiments.

For all aerobic growth experiments, the optical density at 600 nm (OD_{600}) was used as a metric for quantifying culture growth and cell density over time. Experiments were carried out in 96-well plates with culture volumes of 200 µm unless otherwise specified. Unless otherwise specified, growth experiments were carried out in ambient lab light under Osram L 70 W/840 fluorescent bulbs.

3.4 Transmission electron microscopy

Ten-millilitre microbial cultures were prepared following the standard protocols detailed for each species in sections 3.3.3 and 3.3.4. After the specified incubation time, each sample was centrifuged at 5000 rpm for 10 minutes. The cell pellets were then aspirated and washed three times with sterile 1x phosphate-buffered saline (PBS). Each sample was then immediately fixed by suspending in 3% glutaraldehyde in 0.1 M sodium cacodylate buffer at pH 7.3 for two hours. The samples were then washed three times for 10 minutes with 0.1 M sodium cacodylate, and then post-fixed by suspending in 1% osmium tetroxide in 0.1 M sodium cacodylate for 45 mins. Each sample was then washed a further 3 times for 10 mins with 0.1 M sodium cacodylate and then progressively dehydrated with 50%, 70%, 90% and 100% ethanol for 15 minutes each, and then two times with propylene oxide for 10 minutes.

After the fixing process, samples were embedded in TAAB 812 resin and 1 µm thin sections were cut using an ultramicrotome (Leica Ultracut) and then stained with toluidine blue. Each section was viewed under a light microscope to identify suitable areas for investigation. These areas were further cut into 60 nm ultrathin sections and stained with uranyl acetate and lead citrate. Samples were viewed using a JEOL JEM-1400 Plus TEM and images were taken with a GATAN OneView camera.

3.5 DNA extraction and sequencing

Ten-millilitre cultures of each microbial species or community were grown in M9 minimal media supplemented with glucose following the same procedures outlined in sections 3.3.3 and 3.3.4. The aerobic isolates were incubated overnight at 22 °C and the anaerobic community and isolates were incubated in the anaerobic chamber for 28 days before extraction. DNA from each microbial culture was extracted using an extraction kit

(DNeasy PowerSoil Pro, QIAGEN) per the manufacturer's instructions. DNA samples were quantified with a Qubit 3 fluorometer (Invitrogen) and sent to Novogene, UK, for 16S rDNA and bioinformatics analysis. The primers CCTAYGGGRBGCASCAG and GGACTACNNGGGTATCTAAT were used for PCR amplification of the 16SV3-4 genomic regions, and the resulting amplicons were sequenced on an Illumina NovaSeq 6000 paired-end platform, generating 250 bp reads. Raw amplicon data was cleaned using DADA2 software to remove duplications. QIIME2 software was used to annotate each resulting amplicon sequence variant based on the Silva 138.1 database. If applicable, species abundance tables were generated at the taxonomic Family level to assess diversity within community samples. For single isolates, a chao1 index was used to estimate species richness. A value of 0.995 or higher was considered to be a pure species to allow for small amounts of contamination.

Chapter 4 The effect of fullerenes and fullerols on anaerobic microorganisms under early-Earth conditions

The work detailed in this chapter is also included in a first-author paper which is currently under submission to Frontiers in Microbiology. Only the results that I contributed to this paper are included in this chapter. All work presented is my own.

4.1 Introduction

This first experimental chapter aims to assess the effects of fullerenes and their environmentally relevant derivatives on anaerobic microorganisms. To assess if fullerenes could have provided a carbon source for early Earth microbes, a biological sample analogous to primitive microorganisms was selected, and its response to fullerene exposure was assessed. For this, I chose an anaerobic microbial community derived from an environmental sample that had been previously selected to grow on raw meteorite material as an energy source. This chapter will detail a series of growth experiments in which this community was exposed to fullerenes C_{60} and C_{70}, as well as C_{60}- and C_{70}-fullerol to assess not only the effect each fullerene had on growth, but also to determine if fullerenes or fullerols can be utilised as carbon sources by these anaerobic microbes.

Following these initial results, it was important to consider which, if any, environmental factors present on the early Earth may have altered the chemistry of fullerenes on the planet's surface, thereby influencing the way they interact with microorganisms. As well as being anoxic, the early Earth's surface would have been exposed to high levels of UV radiation due to a lack of ozone protection. Exposing fullerenes to these conditions in a laboratory setting produces UV-degradation products that are more representative of the fullerene derivatives likely to be found on the early Earth. These UV-products have very different chemistries to pristine fullerenes and therefore their effect on anaerobic microorganisms is significantly different.

Extra-terrestrial fullerenes as a food source for microorganisms on the early Earth

In this chapter, I explore the effects of pristine and UV-degraded fullerenes and fullerols on both an anaerobic community and a single isolate from this community to assess the effect that extra-terrestrial fullerenes on the early Earth may have had on primitive microorganisms.

4.2 Materials and methods

For details on fullerene and fullerol suspensions, preparation of glassware, standard culturing methods, TEM and DNA extraction and sequencing, see sections 3.1-3.5 in Chapter 3.

4.2.1 Cell counting

For each anaerobic microcosm, 100 µL aliquots were taken at regular intervals over the 28-day growth period for direct cell counting, beginning on day 0, which began immediately after inoculation. Each aliquot was stained by incubating 45 µL of sample with 5 µL SYBR gold nucleic acid stain (Invitrogen, 10,000x concentrate in DMSO) working solution (diluted 1:1000 in sterile deionised water) for five minutes in the dark at room temperature. The stained samples were then serially diluted in sterile deionised water and 10 µL of the appropriate dilution was pipetted into the chamber of a haemocytometer (Blaubrand Neubauer Bright-Line 0.100 mm × 0.0025 mm^2). Cell numbers were counted in all four haemocytometer corners and averaged for each sample. The dilution which gave between 10 and 100 cells per corner was used. This was done under a 20 times magnification microscope lens with a fluorescent light source (Leica DM 4000 B, Leica Kübler CODIX) and cell density was calculated from the known dilution factor.

4.2.2 Microbial growth analysis

The final cell density of each microcosm counted on day 28 was converted to a percentage increase relative to the starting cell density on day 0. This was done to account for discrepancies in initial cell numbers so that cell density values of samples from different conditions could be directly compared. All subsequent analysis is performed on the percentage increase values rather than the raw cell counts and all figures represent cell density as percentage increases values. The cell density in each experimental condition was statistically compared to both the positive control and corresponding negative controls. F-tests were performed to test if the variances between groups were equal or unequal, the result of which was used to identify the correct T-test (assuming equal or unequal variance). T-tests were performed assuming a significance level of $\alpha=0.05$. Error bars on all figures represent the standard error of the mean for each individual experimental group.

4.2.3 Transmission electron microscopy

Transmission electron microscopy images were taken of the anaerobic community after growth with C_{60} (100 mg/L), either as the sole carbon source or with additional glucose (0.4% (w/v)). Ten-millilitre cultures were prepared as described in Chapter 3, section 3.3.3 and inoculated with 100 µL of the anaerobic community from a starting subculture. The same was done for positive controls consisting of M9 media and glucose. All cultures were grown for 28 days as described in Chapter 3, section 3.3.3. TEM sample fixation and imaging methods are detailed in Chapter 3, section 3.4.

4.2.4 Single anaerobic species isolation

To isolate a single species from the anaerobic community, a community subculture grown in M9 minimal media with 100mg/L C_{60} was streaked on M9 agar plates supplemented with glucose. The agar plates were incubated at room temperature inside the anaerobic chamber until visible colonies appeared (approximately four weeks). A single colony was used to inoculate 5 mL of M9 media supplemented with 0.4% (w/v) glucose. This was allowed to grow for three weeks until significant cell growth was confirmed under a microscope, and then was subcultured twice more in identical culture conditions (with a three-week growth period between subcultures). The isolated species was used in further anaerobic isolate experiments detailed within this thesis.

4.3 Results

4.3.1 Anaerobic community growth with fullerenes

The anaerobic community was grown for 28 days with fullerenes C_{60} and C_{70} at two different concentrations- 100 mg/L or 500 mg/L, either with the specified fullerene as the sole carbon source or with additional glucose. These concentrations were chosen to encompass the large range of concentration used in previous studies. The resulting cell densities on day 28 are given in Figure 4.1.

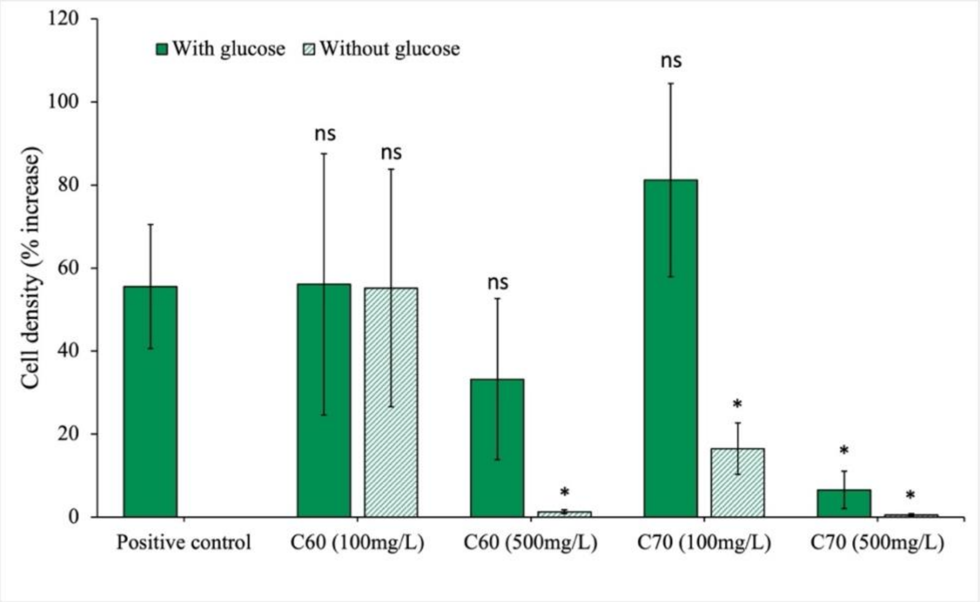

Figure 4.1: Growth of the anaerobic community with 100 mg/L or 500 mg/L of C_{60} or C_{70}, with and without additional glucose. The positive control is growth on glucose only. An asterisk (*) indicates significantly different growth from the positive control while 'ns' denotes no significance.

The cell density for each condition was compared to the positive control using an appropriate T-test and the resulting P-values are listed in Table 4.1.

Table 4.1: Significance of the effects of C_{60} and C_{70} at 100 mg/L or 500 mg/L, with and without glucose, on anaerobic community growth compared with the positive control.

Condition	P-value
C_{60} (100 mg/L) with glucose	0.99
C_{60} (100 mg/L) without glucose	0.99

C_{60} (500 mg/L) with glucose	0.41
C_{60} (500 mg/L) without glucose	0.03
C_{70} (100 mg/L) with glucose	0.42
C_{70} (100 mg/L) without glucose	0.04
C_{70} (500 mg/L) with glucose	0.04
C_{70} (500 mg/L) without glucose	0.03

The results of this initial experiment indicate that at a concentration of 100 mg/L, the presence of C_{60} does not significantly change the growth of the anaerobic community compared to the positive control when glucose is also available as a carbon source. This also appears to be the case when no glucose is available, as there is no significant difference between either of the C_{60} cultures at 100 mg/L ($P=0.094$). This suggests that when glucose is absent, C_{60} alone can be used as a carbon source. In this experiment, the community grew to the same density regardless of the carbon source.

At the higher concentration of 500 mg/L, there is no significant decrease in community growth compared to the positive control if additional glucose is present, but there is a negligible amount of growth is no glucose is available. This indicates that while C_{60} is not inhibitory at 500 mg/L, it is no longer being utilised as a carbon source.

When the community is grown with C_{70} at 100 mg/L and additional glucose, the final cell density is not significantly different from the positive control, indicating there is no inhibition if glucose is present. However, if no glucose is available, there is no growth with C_{70} at this concentration. The cell density value recorded for this condition is the same as in the corresponding negative control, which is probably a result of unavoidable contamination, therefore the small amount of growth recorded is not an indication that C_{70} is being utilised as a carbon source. At 500 mg/L, community growth with C_{70} is significantly reduced both with and without additional glucose, indicating that at the higher concentration, C_{70} is inhibitory even when glucose is available.

I next sought to compare the growth of the community on C_{60} with a more complex fullerene mixture, fullerene soot (25% C_{60}, 53% C_{70}, 22% higher fullerenes) to determine whether the complexity of the latter would influence growth. The anaerobic community was incubated with 100 mg/L of either C_{60} or fullerene soot (FS) as the sole carbon source and the results are given in Figure 4.2.

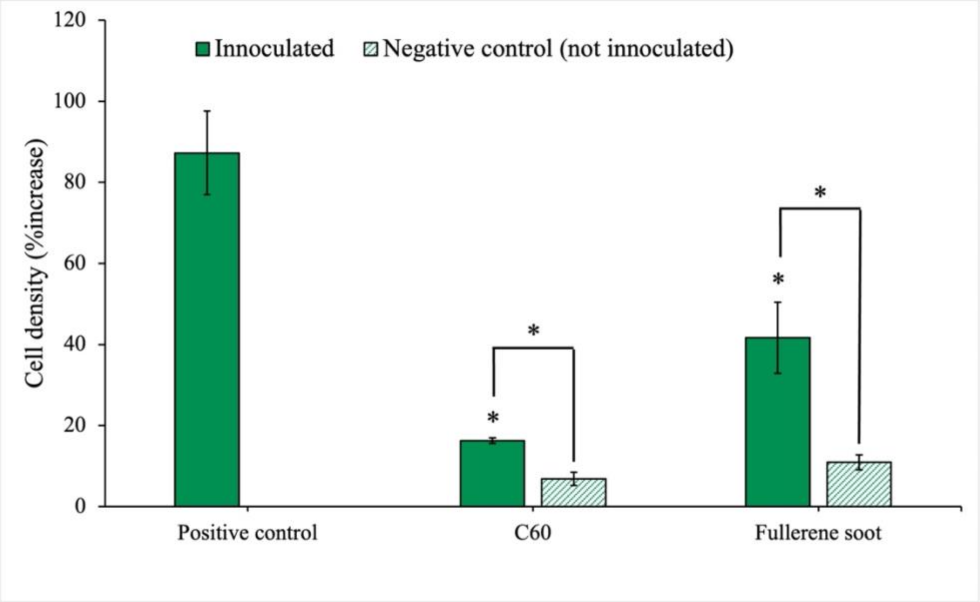

Figure 4.2: Growth of the anaerobic community with 100 mg/L of C_{60} or fullerene soot as the sole carbon source. An asterisk (*) indicates significantly different growth from the positive control while ‘ns’ denotes no significance.

Both the C_{60} and FS conditions have significantly lower final cell densities compared to the positive control ($P=0.021$ and 0.037, respectively). A non-zero cell density was counted in both of the negative control conditions (which are not inoculated), probably because the powdered fullerene material is not sterile. However, because all the cultures were made using the same starting material, any difference in growth between the experimental cultures, which were inoculated with the community, and the negative controls must be due to the presence of the anaerobic community, not baseline contamination. Therefore, the C_{60} culture cell density is indeed statistically higher than the corresponding negative control ($P=0.0054$). Although this is reduced compared to the positive control, there is still a significant amount of growth with C_{60} as a sole carbon source. Similarly, for the FS, there is significantly more growth than in the corresponding negative control ($P=0.031$). Although there is growth with both C_{60} and FS as the sole carbon source, the FS cell density is significantly higher than that in the C_{60} condition ($P=0.042$). This suggests that both C_{60} and FS can be used as a sole carbon source, albeit to a lesser degree than glucose, and that FS is slightly more accessible to the community than C_{60}.

After analysing the results of the experiments presented in Figures 4.1 and 4.2, I noticed a discrepancy in the anaerobic community's response to C_{60} where the degree to which the C_{60} was utilised appeared to vary significantly. Following this, I sought to test the reproducibility of the result where the community appears to be capable of utilising C_{60} as a carbon source. I achieved this by conducting an additional four growth experiments where the community was cultured with C_{60} (100 mg/L) as a sole carbon source. The results are summarised in Figure 4.3.

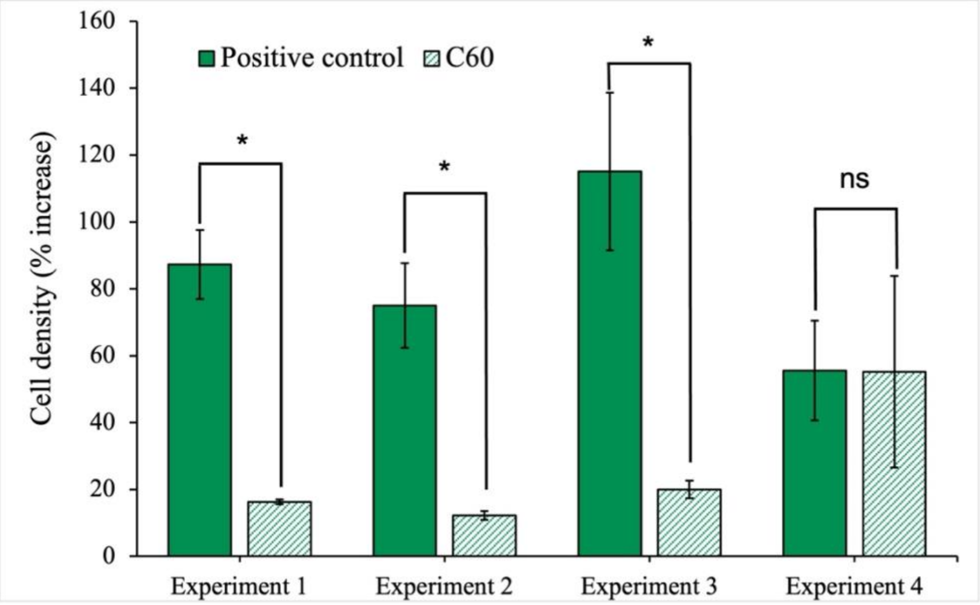

Figure 4.3: Growth of the anaerobic community with 100 mg/L of C_{60} as the sole carbon source across four independent experiments. An asterisk (*) indicates significantly different growth from the positive control while 'ns' denotes no significance. Negative controls are not shown as cell density in all is close to zero.

For each experiment, the cell density of the C_{60} condition on day 28 is compared to the corresponding positive control. The negative controls are not shown as growth in all is close to zero. In experiments 1, 2 and 3, growth with C_{60} as a sole carbon source is significantly lower than the corresponding positive control (P=0.021, 0.02 and 0.05 for experiments 1, 2 and 3, respectively). Additionally, in experiments 1, 2 and 3, growth with C_{60} is significantly higher than the corresponding negative controls (P=0.042, 0.0074 and 0.0086 respectively), which suggests that although growth is reduced compared with the positive control, there is at least some C_{60} utilisation occurring. Conversely, in experiment 4, there is no significant difference in cell density between the C_{60} condition and its positive control (P=0.99), indicating growth was very similar with C_{60} as a carbon source compared with the glucose in the positive control.

Figure 4.4 summarises all the data from experiments in which the community was cultured with C_{60} (100 mg/L) as a sole carbon source or with additional glucose. The box and whisker style plot gives an indication of how the final cell densities of each condition overlap as well as allowing for comparison of the mean and average spread of the data.

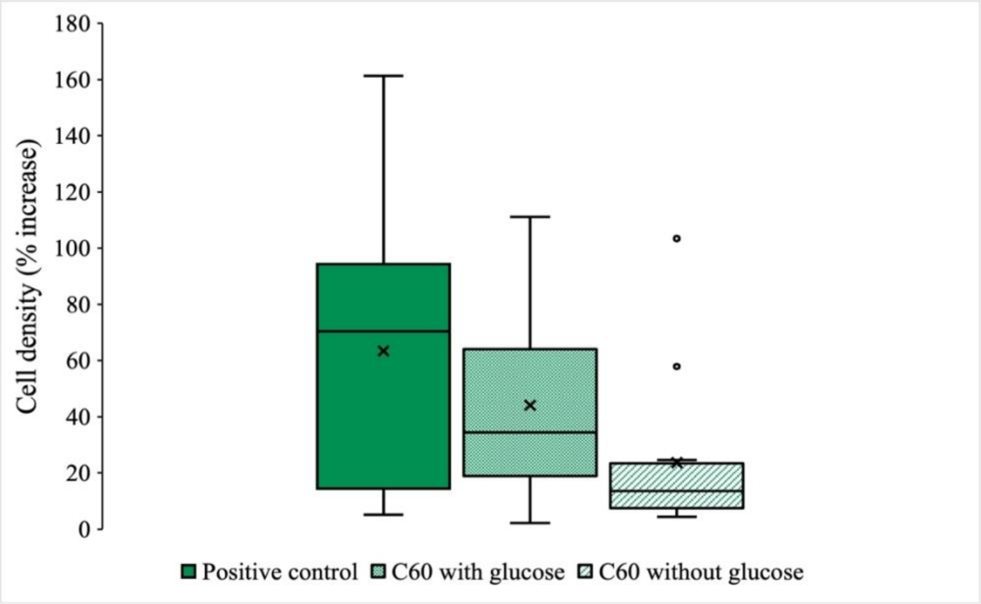

Figure 4.4: Box and whisker plot summarising the cell density data from all experiments in which the anaerobic community was grown with C_{60}. Plot whiskers show the range of data points for each condition, the outer bounds of the solid boxes represent the lower and upper quartiles, the middle line is the median and X markers represent the mean. Outliers are displayed as open circles.

The range of maximum culture growth achieved by the community grown with C_{60} and glucose seems to consistently overlap with the range of growth in the positive control. This indicates that the cell density of the community after growth with C_{60} tends to be very similar to the positive control, provided glucose is available. Growth with C_{60} as a sole carbon source tends to be reduced compared to the positive control, except for two outliers in which the final cell densities were high. However, some growth is always still observed in the C_{60} without glucose, which suggests it can be used as a sole carbon source.

The anaerobic community was cultured with 100 mg/L C_{60} with or without additional glucose and TEM images were obtained of these cultures on day 28 of growth (Figure 4.5) to give more information about the physical interaction between the community cells and the fullerene aggregates. Figure 4.5A shows images of the community grown with C_{60} as a sole carbon source, where the aggregated material is confirmed by Raman spectroscopy to be C_{60} (as detailed in Bethune et al., in preprint).

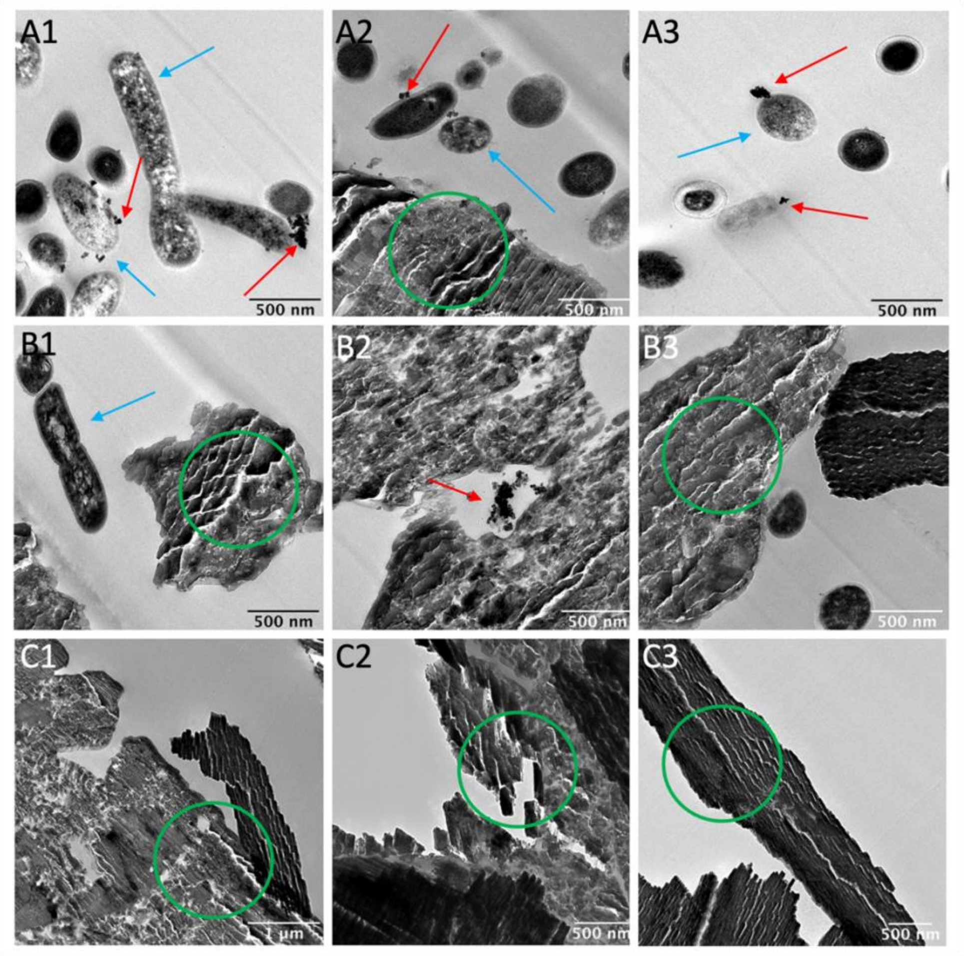

Figure 4.5: TEM images of anaerobic community cultures grown with C_{60} (100 mg/L) as a sole carbon source or with glucose. A: Community grown with C_{60} (100 mg/L) as a sole carbon source, B: community grown with C_{60} (100 mg/L) with additional glucose, C: C_{60} (100 mg/L) negative controls (not inoculated). Red arrows highlight black deposits, blue arrows highlight bacterial cells and green circles highlight C_{60} aggregates.

In the TEM images of the community grown with C_{60}, small black deposits are visible on the surface of some of the bacterial cells (highlighted with red arrows). Figure 4.5B shows the community grown with C_{60} and additional glucose. The aggregated material (highlighted with green circles) is almost certainly C_{60} because these aggregates are not present in the positive control (not pictured). In these images, aggregated C_{60} is observed but the small black cell surface deposits are not, suggesting these only occur in cultures where C_{60} is the sole carbon source. Images of the negative controls (100 mg/L C_{60} with no bacteria) are shown in Figure 4.5C, where aggregated C_{60} is observed, and no bacterial cells are present.

DNA was extracted from the anaerobic community and the 16S rRNA gene was amplified and sequenced to obtain the relative abundances of each taxon present after incubation with C_{60} as the sole carbon source. Figure 4.6 gives the relative abundances of each taxonomic family detected. The majority of the species present belong to the *Enterobacteriaceae* family (82%).

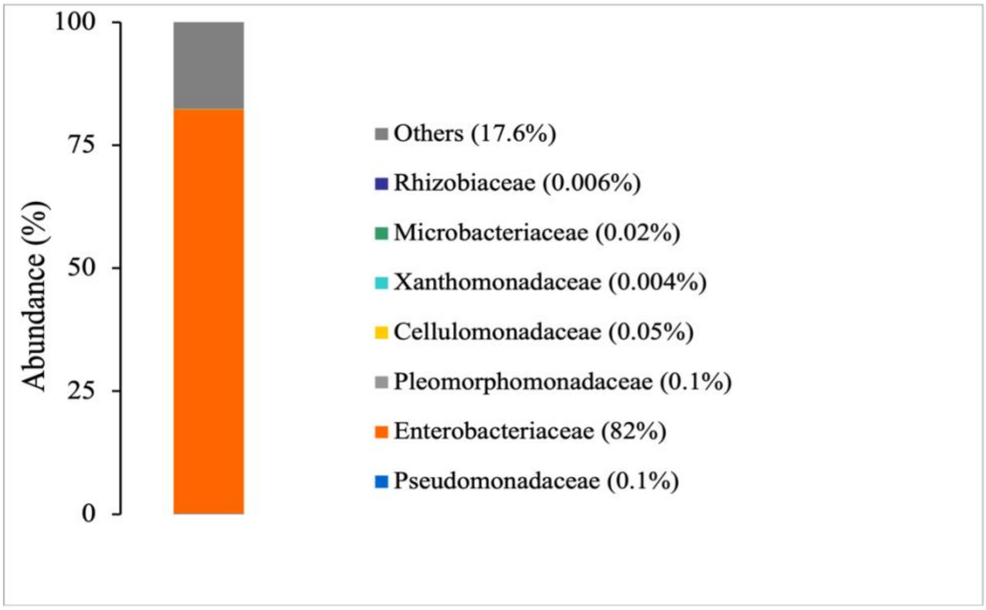

Figure 4.6: Microbial community composition after 28 days incubation with C_{60}. The bar graph and legend show the abundance (as percentages) of each taxon present at the family level. Taxonomic classifications are derived from the Qiime2 database.

4.3.2 Anaerobic community growth with fullerols

In addition to C_{60}, I sought to investigate the effects of soluble fullerene derivatives on the anaerobic community. The community was first cultured with 100 mg/L of C_{60}-fullerol, with and without additional glucose (Figure 4.7).

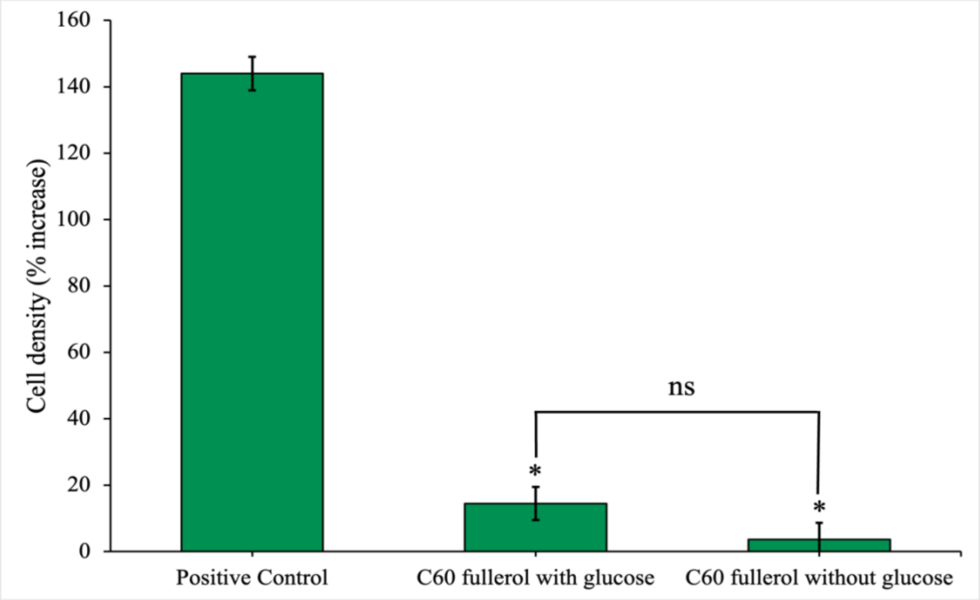

Figure 4.7: Growth of the anaerobic community with 100 mg/L C_{60}-fullerol, with and without additional glucose. An asterisk (*) indicates significantly different growth from the positive control while ‘ns’ denotes no significance.

Community cell density with C_{60}-fullerol is significantly reduced compared with the positive control on day 28, both with and without glucose (P=0.046 and 0.042). Additionally, there is no significant difference between the C_{60}-fullerol conditions with or without glucose (P=0.092). This indicates that not only is C_{60}-fullerol at 100 mg/L inhibitory to the community under ambient conditions, but this inhibitory effect is not altered by the presence of glucose.

C_{60}-fullerol at a concentration of 100 mg/L was exposed to 254 nm UV light for two weeks before inoculating with the anaerobic community. The community cultures were incubated for 28 days with C_{60}-fullerol, both irradiated and non-irradiated, under ambient lab light conditions as well as in the dark. The resulting cell densities are presented in Figure 4.8.

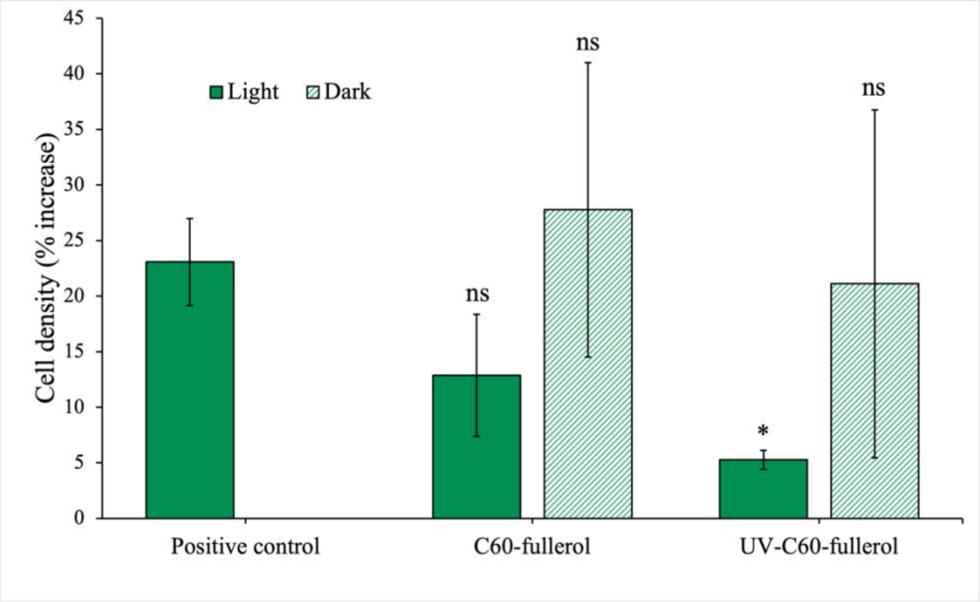

Figure 4.8: Growth of the anaerobic community with 100 mg/L C_{60}-fullerol, either unaltered or after UV-irradiation and then incubated in ambient light or dark conditions. An asterisk (*) indicates significantly different growth from the positive control while 'ns' denotes no significance.

After 28 days, neither of the non-irradiated C_{60}-fullerol conditions have significantly different cell densities from the positive control. This is the case for both the light and the dark conditions, with P-values of 0.17 and 0.75, respectively. Similarly, there is no significant difference between the cultures incubated in the dark with UV-irradiated C_{60}-fullerol and the positive control (P=0.59). However, when the UV-C_{60}-fullerol cultures are grown in ambient light, the growth is significantly reduced compared to the positive control (P=0.005). C_{60}-fullerol therefore appears to be most toxic to the community when it has been irradiated with UV and is then subject to continued ambient light exposure after inoculation.

4.3.3 Effect of fullerenes on an anaerobic isolate

The next step in this study was to repeat a subset of the anaerobic experiments using a single anaerobic species. With this set of experiments, I aimed to simplify any growth data obtained by eliminating the unavoidable complications of such a complex community and to test if the ability to utilise C_{60} as a carbon source is achievable for a single species, or if it is reliant on the complexity of a community structure. To this end, a single isolate was derived from the anaerobic community after it had been growing on C_{60} as the sole carbon source. The DNA sequencing results indicate that this isolate is from the family *Enterobacteriaceae*, but a more specific classification could not be determined due to a lack of matches in the available database.

The anaerobic isolate was incubated for 28 days with 100 mg/L of C_{60} or C_{70}, either unaltered or UV-irradiated, with and without additional glucose. The results of this experiment are presented in Figure 4.9.

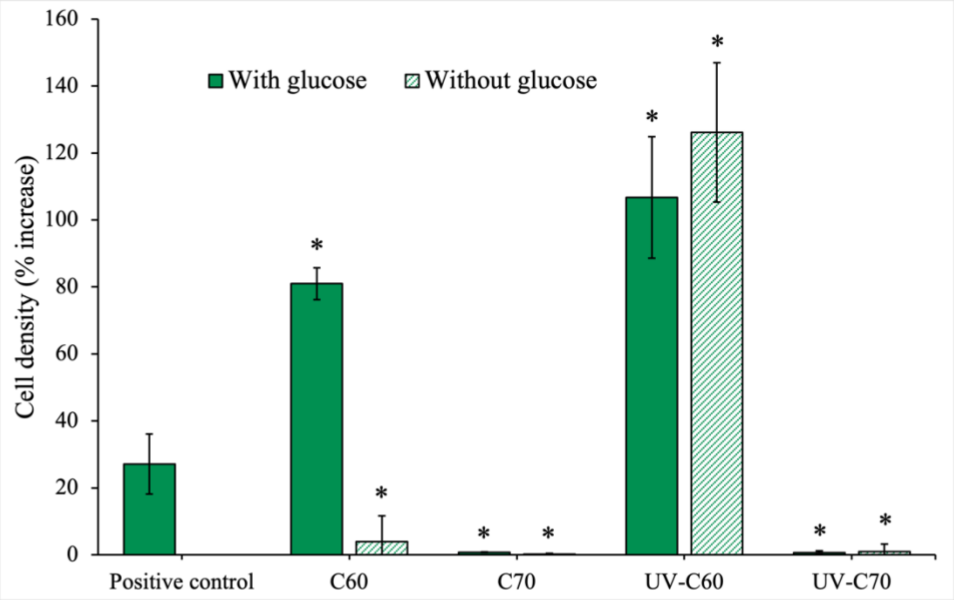

Figure 4.9: Effects of irradiated and non-irradiated fullerenes on growth of anaerobic isolate. The anaerobic isolate was cultured with C_{60} and C_{70} either in the native form or after UV irradiation, with and without additional glucose.

T-tests were performed to compare the day 28 cell density of each condition to the positive control, the results of which are summarised in Table 4.2.

Table 4.2: Significance of anaerobic isolate growth with C_{60}, C_{70} and their UV-degradation products, with and without additional glucose.

Condition	**P-value**
C_{60} with glucose	0.0003
C_{60} without glucose	0.04
C_{70} with glucose	0.03
C_{70} without glucose	0.01

UV-C_{60} with glucose	0.01
UV-C_{60} without glucose	0.01
UV-C_{70} with glucose	0.01
UV-C_{70} without glucose	0.01

From Figure 4.9, it appears the isolate grows well with C_{60} provided glucose is also present. Growth in this condition is significantly higher than the positive control, which could indicate the C_{60} is being utilised in addition to the glucose for increased growth. However, when the glucose is removed, there is no growth as the cell density is not significantly different from the negative control ($P=0.42$), which indicates that C_{60} is not being utilised as a sole carbon source. Conversely, in the cultures grown with UV-C_{60} as the sole carbon source, significant growth is observed. This indicates that the isolate can use the C_{60} UV-degradation products as a carbon source for growth.

No growth is observed in the isolate cultures with C_{70}, either with or without additional glucose. This indicates that C_{70} is not used as a carbon source and exerts an inhibitory effect on the isolate, preventing it from growing. Similarly, isolate growth is inhibited in both UV-C_{70} conditions, showing that the C_{70} UV-degradation products are also highly toxic to this isolate.

The isolate was cultured for 28 days with 100 mg/L C_{60}-fullerol either in ambient light or in the dark. Growth in these conditions was compared to growth with C_{60} (100 mg/L) and an equal mixture of C_{60} fullerene and fullerol (in a total concentration of 100 mg/L). All cultures were grown with additional glucose. The results are presented in Figure 4.10.

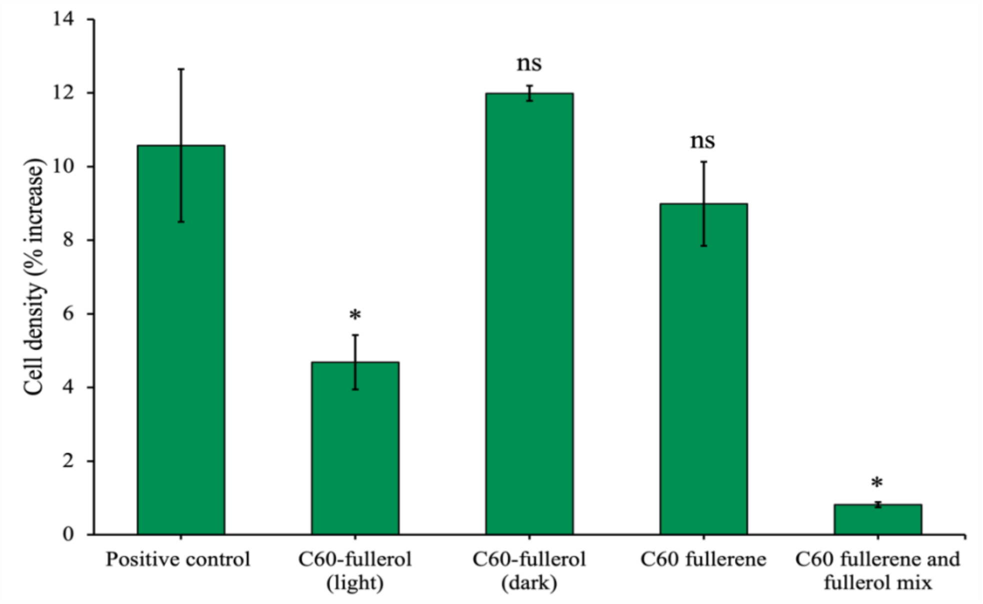

Figure 4.10: Effects of fullerols and fullerene/fullerol mixture on the growth of anaerobic isolate after 28 days incubation with either C_{60}-fullerol (100 mg/L) in the light or dark, C_{60} fullerene (100 mg/L) or a 100 mg/L equal mix of C_{60} fullerene and fullerol. All conditions were supplemented with glucose.

When the isolate is grown with C_{60}-fullerol in ambient light, growth is significantly reduced compared to the positive control (P=0.043). However, when it is grown in the dark, there is no significant difference from the positive control (P=0.47). This suggests that C_{60}-fullerol is more toxic to the isolate when it is exposed to light.

When the isolate is grown with both C_{60} fullerene and fullerol, this mixture is highly inhibitory, significantly reducing growth compared to the positive control (P=0.0095). The cultures grown with just fullerene C_{60} are not significantly different to the positive control (P=0.68), therefore it is likely the presence of the C_{60}-fullerol which causes the mixture to be inhibitory.

The isolate was next grown with C_{60}-fullerol which had been exposed to 254 nm UV to investigate how UV exposure affects fullerol toxicity. The isolate was incubated with UV-C_{60}-fullerol in either ambient light or dark conditions, with and without additional glucose. The results are given in Figure 4.11.

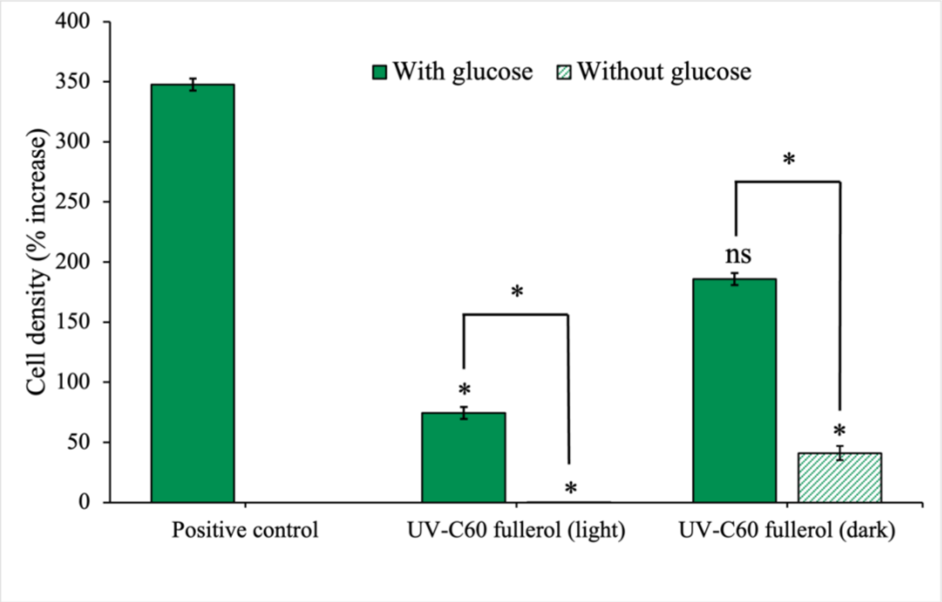

Figure 4.11: Effects of irradiated C_{60}-fullerol on the growth of the anaerobic isolate. Cell density after 28 days of growth with UV-irradiated C_{60}-fullerol in light or dark growth conditions, with and without supplementary glucose is shown.

When the isolate is grown with UV-C_{60}-fullerol without glucose in ambient light, there is no growth. When glucose is available, some growth is observed but is still significantly reduced compared to the positive control (P=0.04). This indicates that C_{60}-fullerol is inhibitory after UV irradiation and with sustained light exposure. However, there is a significant difference between the two UV-C_{60}-fullerol conditions (P=0.073), further indicating that some growth still occurs if there is glucose available.

If glucose is available, the isolate growth with UV-C_{60}-fullerol in the dark is not significantly different to the positive control (P=0.1). However, growth is significantly reduced when no glucose is present (P=0.045). This indicates that the toxicity of UV-irradiated C_{60}-fullerol is dependent on prolonged light exposure and therefore no toxicity is observed in the cultures kept in the dark. A small amount of growth is observed in the dark condition when UV-C_{60}-fullerol is the only carbon source, which indicates although it is toxic under ambient light, it is being used as a carbon source to a small extent by the isolate once the light-induced toxicity is no longer a factor.

The isolate was next grown with 100 mg/L C_{70}-fullerol with and without glucose, under ambient light or in the dark. The results of this are given in Figure 4.12. In this experiment, the positive control was also kept either in the light or dark to test if light exposure alone affected the growth of the isolate. However, because there was no significant difference between the positive controls in the light or dark (P=0.55), all statistical comparisons were made against the positive control grown in ambient light.

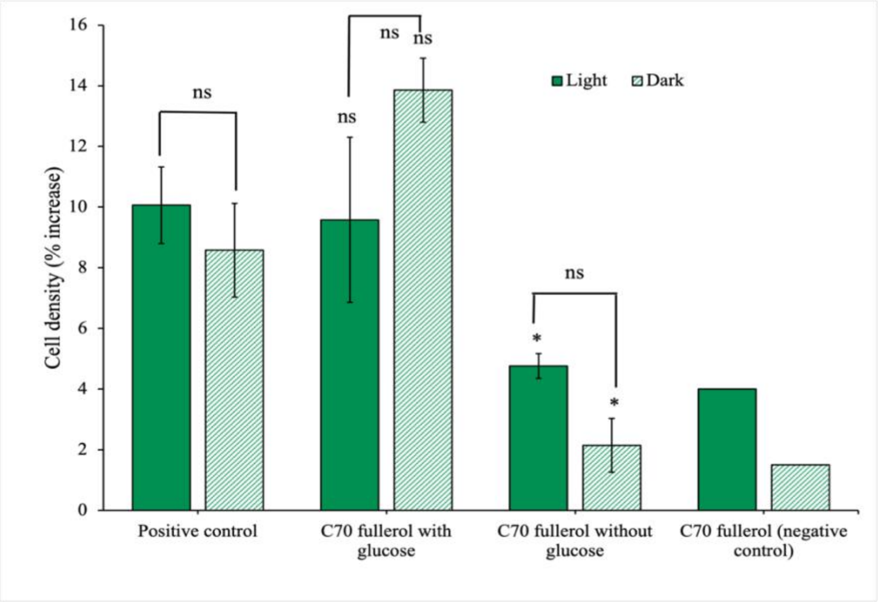

Figure 4.12: Effects of irradiated C_{70} -fullerol on the anaerobic isolate cell density after 28 days incubation with C_{70}-fullerol, with and without glucose under light or dark growth conditions.

There is no significant difference between either of the C_{70}-fullerol conditions with glucose and the positive control (P=0.88 and 0.82 for the light and dark conditions, respectively). Additionally, there is no significant difference between the C_{70}-fullerol conditions with glucose in the light or dark (P=0.22). This indicates that as long as glucose is available, the C_{70}-fullerol is not inhibitory to the isolate. When glucose is not available, growth in both light and dark conditions is significantly reduced compared to the positive control (P=0.029 and 0.0068 for light and dark, respectively). Additionally, neither condition is significantly different from the corresponding negative control (P=0.10 and 0.27 for light and dark, respectively). This indicates that no growth occurs when the C_{70}-fullerol is the sole carbon source. There is no significant difference between the two conditions without glucose (P=0.056), further supporting the conclusion that light exposure does not affect the growth of the isolate with C_{70}-fullerol.

4.4 Discussion

In this chapter, I aimed to examine the effect of fullerenes and their derivatives on anaerobic microorganisms to better understand how these organics may have been used as a food source by early life. This is not only relevant for understanding the appearance and evolution of life on Earth but is also important for understanding how the influx of extra-terrestrial organic material on other rocky planets influences their habitability for microorganisms.

4.4.1 Growth with fullerene C_{60} reduces complexity in the anaerobic community

The initial experiments in this chapter were conducted using an anaerobic community that had already been selected to grow on powdered meteorite containing the relevant organics likely to have been present on the early Earth (Waajen et al., 2022). I chose to conduct the initial anaerobic experiments using this community because of its environmental relevance, as well as its predisposition to dealing with complex organic mixtures. In the original study by Waajen et al, there was a reduction in diversity after the community was grown on powdered meteorite material, which indicated habitat filtering was taking place to produce a more specialised community. Growth with meteorite material created a niche that resulted in the selection of certain species present in the original community. This niche favoured species from the *Deltaproteobacteria, Geobacteraceae* and *Desulfuromonadaceae* families which are known to use sulphur and iron as electron acceptors (Waajen et al., 2022). In my experiments, there was a further decrease in diversity when the community was grown with fullerene C_{60} as the carbon source. This indicates further habitat filtering took place, as by limiting the carbon source to C_{60}, a narrower niche was created which increased habitat selection pressure, resulting in fewer species. Interestingly, most of the species present in the community after growth with C_{60} belong to the *Enterobacteriaceae* family. Although this is a large family consisting of over 30 genera such as *Escherichia*, *Klebsiella* and *Shigella*, most are only facultative anaerobes. Other families present in the C_{60}-adapted community are from the taxonomic families *Pleomorphomonadaceae, Cellulomonadaceae, Xanthomonadaceae, Microbacteriacea* and *Rhizobiaceae*, all of which are made up primarily of species found in soils.

4.4.2 Fullerene C_{60} can be used as a carbon source by the anaerobic community

The anaerobic community can utilise fullerene C_{60} as its sole carbon source as after incubation with 100 mg/L C_{60}, the community growth is comparable to growth with glucose. The community's ability to grow in the absence of glucose indicates it must be utilising carbon from C_{60}. However, the lack of increased growth when both glucose and C_{60} are available suggests that the community reaches a maximum density or growth rate that does not increase with excess carbon, therefore a similar cell density is achieved regardless of the carbon source. At a higher concentration of 500 mg/L, the community's growth results are different: although growth is identical to the positive control with supplementary glucose, there is a significant decrease in cell density without this additional carbon source. This aligns with previous studies showing that C_{60} can inhibit the growth of *Pseudomonas fluorescens* proportionally to its concentration (Riding et al., 2012). While higher C_{60} concentrations appear less accessible, there is no inhibition observed at 100 mg/L with additional glucose.

To further understand the community's behaviour when grown on C_{60}, I conducted four non-simultaneous growth experiments using 100 mg/L C_{60} as the sole carbon source. Each experiment had its own controls and was inoculated from a different starting subculture. The degree to which the community grew on C_{60} varied between experiments, there was consistently at least some significant growth with C_{60} as the sole carbon source. The only varying factor between the four experiments was time and the community inoculation source, therefore the variability observed between experiment repeats is almost certainly due to an inevitable shift in community composition over time arising from its complex microbial architecture.

Limited studies on C_{60}'s effect on anaerobic microorganisms support the finding that nC_{60} is not inhibitory to anaerobic microorganisms. It has previously been found that nC_{60} does not negatively affect the growth, gas production or composition of microbial wastewater communities, although the exact microorganisms present in these communities are not specified (Nyberg et al., 2008; Zhao et al., 2018). However, other studies have shown nC_{60} at 2.5 mg/L or higher to be inhibitory to both *E. coli* and *B. subtilis* when grown both aerobically and anaerobically (Fortner et al., 2005). This concentration is significantly lower than that used in my experiments, and yet there is still no evidence for it being toxic to the anaerobic community at 100 mg/L. One explanation for this is that Fortner et al. conducted these experiments with two species in pure cultures and therefore any toxic effects would have had a significant impact on the growth of these cultures. In a community, however, the diversity of species allows for some redundancy. In other words, even if some species are susceptible to C_{60} toxicity, others are better adapted to withstand it and will therefore become more dominant and able to grow, which may explain why no inhibition is observed when the anaerobic community is grown with C_{60}. A 2017 study in which another anaerobic community was grown with C_{60} found that while higher concentrations of nC_{60} initially reduced the cell density, prolonged exposure led to the selection of resistant species (Auwerter et al., 2017). This is consistent with the proposal that microbial communities possess redundancy that makes them better able to resist fullerene biotoxicity. Similarly, certain species in the community used in this chapter may be better equipped to utilise nC_{60} and therefore when these species become more dominant through compositional shift, the community as a whole is observed to be growing on C_{60} as a sole carbon source.

TEM images of the anaerobic community grown with C_{60} as the sole carbon source revealed flake-like structures formed by C_{60} in M9 media due to salt-induced aggregation, confirmed by Raman spectroscopy. Some nC_{60} remained as smaller aggregates which appear similar to those seen by Lyon et al. (2006). A notable feature in these TEM images is the small black spherical clusters present on the bacterial cell surfaces after growing on C_{60}. Similar clusters have been previously observed under atomic force microscopy of *E. coli* with water-soluble fullerene derivatives (Deryabin et al., 2014), suggesting membrane penetration of C_{60} clusters may play a role in the community's ability to metabolise nC_{60}.

4.4.3 An anaerobic isolate cannot utilise C_{60} when cultured outside of the community

The anaerobic isolate, unlike the community, does not seem to be able to utilise C_{60} as a sole carbon source, although it is not inhibited if glucose is available. The anaerobic community was able to use C_{60} as a carbon source, but when the isolate is removed and cultured alone it does not demonstrate this ability. There are two possible reasons for this; firstly, the community may only be capable of degrading C_{60} by combining different biodegradation processes from multiple different metabolically diverse species. Secondly, and perhaps more convincingly, it may be that only a few species present in the community can use C_{60} carbon and that the single species that was isolated and cultured independently is not able to do this. This is consistent with the hypothesis that the complexity of the microbial community results in a certain degree of redundancy that proves to be essential for the degradation of complex organics such as fullerenes.

4.4.4 The anaerobic isolate can utilise UV-degraded C_{60} as a carbon source

nC_{60} aggregates in water degrade readily when exposed to UV light, and the degradation products are less aggregated and have increased water stability (Hou & Jafvert, 2009; Hou et al., 2010; Lee et al., 2009; Sanchís et al., 2018). Additionally, C_{60} will degrade in the absence of oxygen under UV in the solid state (Carboni et al., 2017) and when dissolved in organic solvents (Taylor et al., 1991), so it is highly likely it also degrades under UV in water when no oxygen is present. In my experiments, aqueous, anoxic C_{60} suspensions were exposed to UV for two weeks, as the half-life of anoxic solid state C_{60} under UV is 13.1 days (Carboni et al., 2017). After these two weeks, I observed a distinct colour change which indicated degradation had occurred. The anaerobic isolate was cultured with these degradation products, both with and without glucose, and the resulting cell densities were statistically comparable to the positive control in both cases. This indicates that not only are UV-C_{60} degradation products utilised by the isolate as a sole carbon source, but they also appear to be equally as accessible as glucose. This does seem to be consistent with results from previous studies; it is known that the combination of photodegradation and biodegradation significantly increases the rate of C_{60} mineralisation in soils (Peng et al., 2020), and this enhanced degradation of UV-irradiated C_{60} has been observed in soil microcosms (Berry et al., 2016). To the best of my knowledge at the time of writing this thesis, this demonstrates the first anaerobic biodegradation of UV-irradiated C_{60} in aqueous microcosms.

4.4.5 Fullerene C_{70} is not accessible as a carbon source

The effect of C_{70} on both the community and the isolate deviates from what was observed with C_{60}. The community, while able to utilise C_{60}, does not utilise C_{70} as a carbon source in any amount, as no growth occurs when C_{70} is the sole carbon source. If glucose is available, then the community is still able to grow normally with C_{70} at 100 mg/L, but at the higher concentration of 500 mg/L, it becomes significantly inhibitory, even with glucose. This seems to indicate that fullerene toxicity may increase with molecular weight, with larger fullerenes like C_{70} becoming more inhibitory than smaller species. Interestingly, the fullerene soot, containing large amounts of both C_{60} and C_{70}, can support the growth of the community, albeit to a much lesser extent than glucose. The total concentration of FS in these microcosms was 100 mg/L, so the total concentration of C_{70} is lower. When the community was grown with 100 mg/L C_{70} and additional glucose, no inhibition was observed, so it is likely that the C_{70} present in the FS is not in a high enough concentration to exert any toxic effects. The community growth with FS was significantly higher than growth with C_{60} as the sole carbon source, therefore other fullerene species present in the mixture may have provided accessible carbon sources alongside the available C_{60}. Although C_{70} is inhibitory to the community, we still observe some degree of growth, especially at lower concentrations. The isolate, however, does not grow in any discernible amount with C_{70}, with or without glucose. As already discussed, this increase in susceptibility to C_{70} toxicity when the isolate is removed from the community environment could be indicative of the species redundancy in the community, as although the C_{70} is still exerting the same toxic effects, some species in the community may be better adapted to resist complete inhibition, while the isolate is evidently not.

There is almost no literature available which assesses the effect of C_{70} on microorganisms. However, it is known that the toxicity of nC_{60} aggregates is size-dependent, with smaller aggregates being more toxic (Lyon et al., 2006; Tong et al., 2016). C_{70}, although it is a larger fullerene, tends to form smaller aggregates than C_{60} in water (Kyzyma et al., 2019) and therefore a possible explanation for its increased inhibitory effects is due to smaller aggregate size.

4.4.6 The effect of fullerols on anaerobic microorganisms

The soluble fullerol derivatives of C_{60} and C_{70} exhibit significantly different effects on the anaerobic microbes in this study compared to their fullerene parent molecules. While C_{60} is a biologically accessible carbon course for the anaerobic community, C_{60}-fullerol inhibits growth under identical conditions, even with supplementary glucose. Additionally, C_{60}-fullerol inhibition seems to be linked to light exposure, as this inhibition is reduced when cultures are grown in the dark. This trend is also observed with the anaerobic isolate, which is significantly inhibited by C_{60}-fullerol in ambient light but not in the dark. When C_{60}-fullerol suspensions are exposed to UV under an anoxic atmosphere, they become significantly more inhibitory to both the community and the isolate, but only if the cultures are kept under prolonged ambient light exposure. Interestingly, while C_{70} fullerene is inhibitory to both the community and isolate to varying degrees, C_{70}-fullerol has no effect on the growth of either, provided additional glucose is available. However, the lack of available literature on the effects of C_{70} and its fullerol derivative makes it difficult to form any consensus on the reproducibility of this observation. The difference between light and dark conditions for both C_{60}- and C_{70}-fullerol indicates that photoactivity plays a key role in their toxicity.

Several previous studies have found that C_{60}-fullerol does not exhibit antibacterial activity despite being photoactive (Chiang et al., 1995; Li et al., 2008), and is even used by soil microbes as a carbon source (Berry et al., 2017). This is contradictory to the results presented in this chapter. However, a major difference is that these previous studies were conducted aerobically, whereas in this chapter experiments were done with anaerobic species in an anoxic environment. Reactive oxygen species (ROS) are generated intracellularly as a product of aerobic metabolism, and therefore aerobic bacteria have evolved mechanisms to counteract the effects of oxidation and can tolerate low levels of ROS (Nasim & Hamblin, 2017). Obligate anaerobes, on the other hand, escape exposure to oxidative damage because they grow in anoxic habitats, therefore they have not evolved any mechanisms to mitigate the damage of reactive oxygen (Seixas et al., 2022). It is therefore possible that the aerobic species from previous studies are less susceptible to fullerol biotoxicity than the anaerobes used in my experiments as they are better equipped to deal with the oxidative stress fullerols exert.

C_{60}-fullerol produces ROS when exposed to both UV and visible light (Pickering & Wiesner, 2005). ROS are generated at a much higher rate under UV (Pickering & Wiesner, 2005), which may explain why the largest biotoxic effect is observed when cultures are grown with irradiated C_{60}-fullerol under prolonged visible light exposure, as this condition likely produces the highest ROS concentration. Additionally, ROS tend to be short-lived due to their high reactivity, therefore those produced under UV are likely neutralised quickly within the suspension and therefore do not have a chance to exert oxidative effects on the microbes when incubated in the dark. When under constant visible light exposure, however, this supply of ROS may be continuously generated, leading to the greater antibacterial activity observed in the cultures kept in ambient light. This effect is interesting from an early Earth perspective as constant UV exposure would presumably increase the biotoxicity of any fullerols in the environment.

If ROS production is indeed the cause of fullerol biotoxicity towards anaerobic microorganisms, then we might expect to see the same inhibition of growth with native C_{60}, as previous studies claim to have detected ROS production in photosensitised nC_{60} suspensions (Kamat et al., 2000). However, Lyon et al (2008) did not observe any ROS-mediated inhibition to the growth of *E. coli* or *B. subtilis* after exposure to C_{60}, and neither did they detect any ROS production in the suspensions (Lyon et al., 2008). After further investigation, these authors concluded that C_{60} itself reacts with the dyes in the ROS colourimetric assays used to detect ROS production, giving false positive results, and that in actuality fullerene suspensions do not produce ROS in any detectable amount (Lyon et al., 2008). Hotze et al similarly went on to explain the absence of ROS in UV-irradiated nC_{60} suspensions by comparing the density of fullerene aggregates to their fullerol derivatives. More densely aggregated nC_{60} is less likely to produce singlet oxygen than the more loosely packed fullerol derivative (Hotze et al., 2008). The less densely-packed fullerols have a larger fullerol-water interface, which facilitates ROS production, as well as a longer-lived triplet state which leads to a higher generation of singlet oxygen (Hotze et al., 2008).

The accessibility of UV-degraded C_{60} for anaerobic microorganisms is consistent with the hypothesis that early life on Earth could have use extra-terrestrial fullerenes as a carbon source, but the toxicity of their soluble derivatives may counteract this to some extent. Before speculating on the significance of fullerol toxicity on the early Earth, it is important to consider whether or not fullerols would even have been present in this environment. A recent study by Sanchís et al (2018) concluded that fullerols are not produced from UV exposure in fullerene water suspensions, and so if this is the case, it is possible that fullerols might not have been present on the early Earth in high enough quantities that their antimicrobial properties significantly altered the growth of primitive microorganisms. It is possible, therefore, that the light-induced toxicity of fullerols demonstrated in this thesis, although very relevant for modern microorganisms, may not apply to primitive microorganisms on the early Earth.

4.5 Conclusions

In this chapter, I aimed to investigate the effect of fullerenes and fullerols on anaerobic microorganisms by growing an anaerobic community and single isolate with C_{60}, C_{70} and their fullerol derivatives, to establish whether extra-terrestrial fullerenes could have been used as carbon sources on the early Earth. The main findings of these experiments are summarised in Table 4.3.

Table 4.3: Summary of the anaerobic community and isolate responses to C_{60}, C_{70} and C_{60}-fullerol

Anaerobic community	**Anaerobic isolate**
Can utilise pristine C_{60} as a sole carbon source	Cannot utilise C_{60} unless it has been degraded with UV light
Cannot utilise C_{70}	Inhibited by C_{70}
Cannot utilise C_{60}-fullerol (is inhibitory, particularly when exposed to light)	Cannot utilise C_{60}-fullerol (is inhibitory, particularly when exposed to light)

In this Chapter, I show that an anaerobic community is able to grow on fullerene C_{60} as a sole carbon source, but that the larger fullerene C_{70} is not biologically accessible. C_{60}-fullerol is inhibitory to the anaerobic community, particularly when exposed to UV or visible light, suggesting that exposure to light on the early Earth may have increased the toxicity of soluble fullerene derivatives.

When a single isolate is removed from the community and cultured independently, it is not able to utilise C_{60} as a carbon source, suggesting that the community's ability to use C_{60} carbon is either due to collaborative metabolic processes or that only select species can degrade C_{60}, and the isolate is not one of them. When C_{60} is exposed to simulated early Earth conditions, the resulting UV-degradation products provide a highly accessible carbon source for the anaerobic isolate. These results suggest that fullerenes on the early Earth, having been exposed to environmental extremes such as short-wave UV radiation, may have provided a source of carbon and energy for the growth of primitive microorganisms.

Previous studies investigating the effects of C_{60} on microorganisms give some conflicting results, particularly when the effect of fullerenes on aerobic microorganisms is studied. To provide some clarity on the actual effect of fullerenes on microorganisms, and to compare the response of anaerobic and aerobic microbes to fullerenes, the next stage of this research is to investigate how relevant aerobic species respond to fullerene exposure to test if the accessibility of native and UV-degraded fullerenes is universal, or unique to specific anaerobic species.

Chapter 5 The effect of fullerenes and fullerols on aerobic growth of *E. coli* and *Pseudomonas sp.*

5.1 Introduction

Chapter 4 examined the effect of fullerenes and fullerols on anaerobic microorganisms and presents evidence that early terrestrial microbes may have been capable of metabolising extra-terrestrial fullerenes as an energy source. The next step in this research is to use relevant aerobic species to provide a comparison in the microbial response. In other words, adapting the protocols used in Chapter 4 to test the effects of fullerenes and fullerols on aerobic microorganisms allows us to assess if the microbial response observed in Chapter 4 is universal, or only observed in anaerobic species, thereby suggesting that fullerene utilisation is a conserved process uniquely relevant to anaerobic environments. As discussed in Chapter 2, most previous studies assessing the effect of fullerenes on microbes are done using aerobic species, and the only known reports of biodegradation are from aerobic studies (Berry et al., 2016, 2017; Peng et al., 2020; Wang et al., 2020).

This chapter will examine the effect of C_{60}, C_{70} and their fullerol derivatives on select aerobic microorganisms to compare to the results obtained in Chapter 4, as well as provide a better understanding of the effect fullerenes have on a range of microorganisms. *E. coli* is a well-characterised model organism used in previous studies assessing the toxicity of fullerenes and fullerols (Deryabin et al., 2014; Fortner et al., 2005; Lee et al., 2009; Lyon et al., 2005). Here, it is again exposed to a range of fullerenes and fullerols to provide a response comparison both to previous studies and to additional results obtained within the scope of this thesis. In addition to *E. coli*, two environmental microorganisms isolated from a basalt-C_{60} mixture, identified as two distinct species of *Pseudomonas*, are tested as a representative sample of naturally occurring and abundant environmental aerobes to provide better clarity on the effect fullerenes have on aerobic microorganisms.

5.2 Materials and Methods

For details on fullerene and fullerol suspensions, preparation of glassware, standard culturing methods and DNA extraction and sequencing, see sections 3.1-3.5 in Chapter 3: Materials and Methods.

5.2.1 Microorganisms

Escherichia coli K-12 MG1655 was cultivated from laboratory glycerol stocks on Luria Broth agar plates (1.5% agar) and subsequently grown in liquid M9 minimal media with 0.4% (w/v) glucose.

Two environmental isolates were derived from a C_{60}-basalt mixture that was left outside for six months to allow microbial colonisation to take place (see Chapter 3, section 3.3.1). The two isolates were sequenced (see section 3.5) and identified as two distinct species in the *Pseudomonas* genus. These are subsequently referred to as *P. sp1* and *P. sp2* in this thesis.

5.2.2 Culturing

Overnight cultures were prepared by inoculating 25 mL of M9 media (with 0.4% (w/v) glucose) with a single colony of the appropriate species growing on agar. Unless otherwise specified, all *E. coli* cultures were incubated at 37 °C and all *P. sp1* and *P. sp2* cultures were incubated at 22 °C (room temperature) in accordance with the culturing technique detailed in Chapter 3 Materials and Methods. Cultures which are specified to have been grown under ambient lab light were grown under constant illumination from Osram L 70W/840 cool white fluorescent bulbs.

Liquid cultures containing 5 mL of fullerene, fullerol, or fullerene UV irradiation products in M9 minimal media were prepared, either with or without 0.4% (w/v) glucose added. Each experimental culture was inoculated with 100 μL of overnight culture of the appropriate species.

For growth experiments conducted in a microplate reader, 200 μL was pipetted into each well of a 96-well plate (a minimum of 3 wells was used for each condition and control).

Positive control conditions consisted of M9 minimal media with glucose. Negative controls were made in parallel to all inoculated conditions but were not inoculated. The 96-well plates were placed into a plate reader (SPECTROstar Nano, BMG Labtech) set to either 37 or 22 °C (depending on organism type) and the OD_{600} of each well was read every 10 minutes for 24 hours.

For growth experiments in which the colony forming units (CFUs) were counted, experimental cultures and controls were prepared as described above, in triplicate. Cultures were grown at the optimal conditions for 24 hours and then serially diluted 10 times. Dilutions of 10^7-10^{10} were plated on M9 agar plates supplemented with glucose (10 µL plated onto a quarter of each plate). Plates were incubated at the optimal growth temperature for each species until visible colonies formed (1-3 days), and CFUs were counted manually for whichever dilution contained 50-200 discreet colonies for each replicate.

5.2.3 Growth analysis

For the microplate growth experiments, each datapoint for each individual well was corrected against the blank value for the corresponding timepoint. The raw growth curves for each well of each condition were graphed and the Y-axis OD_{600} values were converted to the natural logarithm scale ($\ln(OD_{600})$). From these curves, the start and end timepoints for the exponential phase were manually identified and the corresponding OD_{600} values were selected from the dataset. The maximum OD_{600} value in each well was also extracted. These values were used to calculate the growth rate and maximum cell density (in OD units) for each well to produce an average for each condition. Growth rate during the exponential phase (µ) was calculated using the following formula:

$$\mu = \frac{\ln{(OD_2)} - \ln{(OD_1)}}{t_2 - t_1}$$

Where $OD_1 =$ OD_{600} at the start of the exponential phase

$OD_2 =$ OD_{600} at the end of the exponential phase

And $t_2 - t_1 =$ length of exponential phase (hrs)

To compare µ and maximum OD_{600} between each condition and the positive control, F-tests were first performed to assess if the data had equal or unequal variances. The results of this were used to determine the appropriate T-test, assuming equal or unequal variance, which was performed with a significance level of $\alpha=0.05$.

For the CFU growth experiments, the number of CFUs per mL was calculated using the following formula:

$$CFU/mL = \frac{(number\ of\ colonies\ \times\ dilution\ factor)}{volume\ of\ plated\ culture}$$

The CFUs/mL for each condition were averaged and compared using T-tests as described above.

5.2.4 Transmission electron microscopy

Transmission electron microscopy images were taken of the *P. sp1* and *P. sp2* after growth with C_{60}. Ten-millilitre volumes of C_{60} (100 mg/L) supplemented with glucose (0.4% (w/v)) were inoculated with 100 µL of either *P. sp1* or *P. sp2* from overnight cultures. The same was done for positive controls consisting of M9 media and glucose. All cultures were incubated at 22 °C for 24 hours. TEM sample fixation and imaging methods are detailed in Chapter 3, section 3.4.

5.3 Results

5.3.1 Effects of fullerenes and fullerols growth of *E. coli*

E. coli was grown under optimal conditions (aerobically at 37 °C) in M9 minimal media with glucose (positive control), C_{60} (100 mg/L) with and without glucose or C_{70} (100 mg/L) with and without glucose. The OD_{600} growth curves were measured over 20 hours (Figure 5.1). Growth curves are shown in both the normal scale and natural logarithm scale for comparison. The logarithmic scale curves were used to identify the exponential phase timepoints during analysis but all other calculations were done using the OD_{600} values (see section 5.2.3).

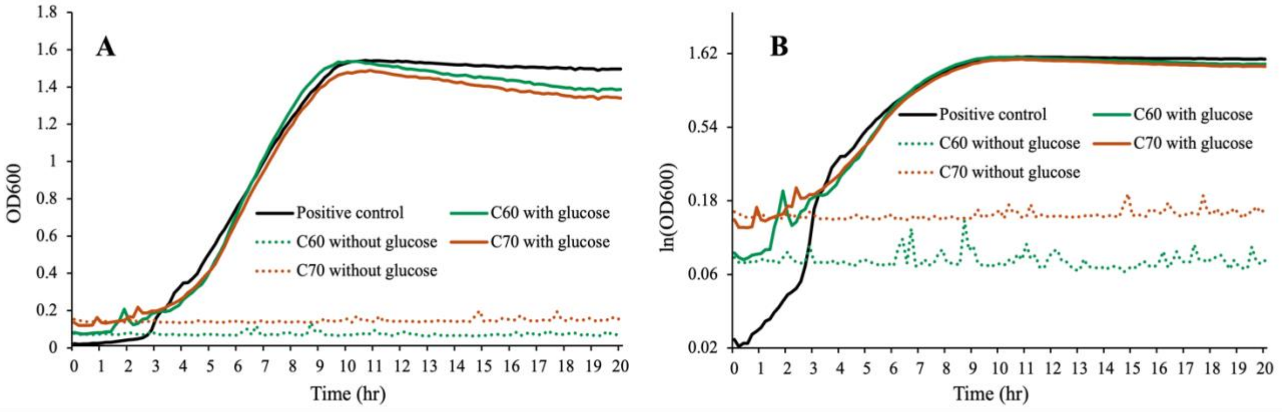

Figure 5.1: *E. coli* growth curves over 20 hours with fullerenes C_{60} and C_{70}, with and without additional glucose. A: original scale, B: Y-axis scaled to the natural logarithm of original OD_{600}

When C_{60} or C_{70} are the only carbon source, there is no growth, and therefore neither fullerene is being used as a carbon source. The spike-like features observed particularly in the first few hours of growth are likely due to cell clumping resulting is occasionally high OD_{600} readings in some populated wells and are therefore ignored. The average growth rate during the exponential phase (μ) and the maximum OD_{600} reached over the 24-hour growth period are summarised in Table 5.1.

Table 5.1: Exponential phase growth rate and maximum culture density values for *E. coli* after growth with C_{60} and C_{70}, with and without glucose.

Condition:	**Growth rate (μ):**	**Max OD_{600}:**
Positive control	0.50	1.55
C_{60} with glucose	0.37	1.54
C_{70} with glucose	0.31	1.49
C_{60} without glucose	NA	NA
C_{70} without glucose	NA	NA

Both the C_{60} and C_{70} conditions with glucose have a significantly reduced growth rate compared to the positive control (P=0.00046 and 0.00098, respectively), however, neither fullerene has any effect on the maximum OD_{600} (P=0.77 and 0.19). This suggests that the fullerenes have a small deleterious effect on the growth of *E. coli*, resulting in reduced growth rate, but do not ultimately affect the amount of growth achieved.

E. coli was grown under identical conditions with 100 mg/L of either C_{60}- or C_{70}-fullerol, with and without additional glucose, the results of which are shown in Figure 5.2.

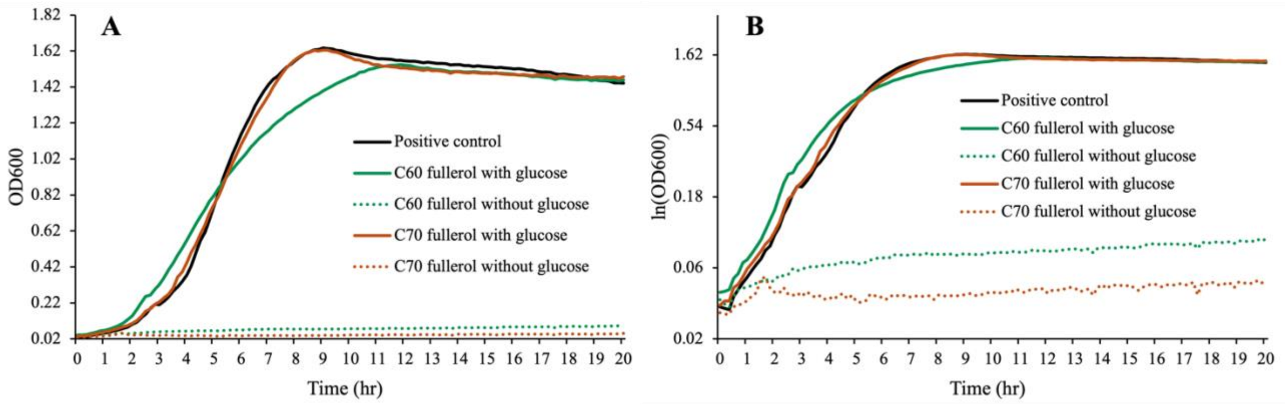

Figure 5.2: *E. coli* growth curves over 20 hours with C_{60}- and C_{70}-fullerol, with and without additional glucose. A: original scale, B: Y-axis scaled to the natural logarithm of original OD_{600}

On the logarithmic scale, the C_{60}- and C_{70}-fullerol conditions without glucose appear to increase slightly, however this increase is non-significant when the starting OD_{600} values are compared to the final values with a T test ($P<<0.01$). Therefore, as with the underivatized fullerenes, when no glucose is available, there is no growth, therefore neither fullerol is being utilised as a sole carbon source. The average exponential growth rates and maximum OD_{600} for each condition are summarised in Table 5.2.

Table 5.2: Exponential phase growth rate and maximum culture density values for *E. coli* with C_{60}- and C_{70}-fullerol, with and without glucose.

Condition:	**Growth rate (µ):**	**Max OD_{600}:**
Positive control	0.61	1.60
C_{60} fullerol with glucose	0.58	1.59
C_{70} fullerol with glucose	0.58	1.58
C_{60} fullerol without glucose	NA	NA
C_{70} fullerol without glucose	NA	NA

Both C_{60}- and C_{70}-fullerol reduce the growth rate compared to the positive control when glucose is available ($P=0.039$ and $P=0.034$, respectfully), however, the maximum OD values achieved in both conditions are not significantly different from the positive control ($P=0.80$ and 0.88, respectfully). Therefore, as with the underivatized fullerenes, C_{60}- and C_{70}-fullerol reduce the growth rate of *E. coli* but do not ultimately change the amount of growth achieved.

To test if light exposure effects these results, *E. coli* was grown again with C_{60}- or C_{70}-fullerol with and without additional glucose, but in this experiment half of the cultures were kept in ambient lab light and half were kept in the dark. As the inside of the 96-well plate reader is mostly dark with short bursts of light at 600 nm every 10 minutes, cultures were grown in 96-well plates on a shaker outside of the plate reader. All cultures were incubated at 22 °C as incubation at 37 °C would have required a dark incubator and therefore light exposure would not be possible. These conditions meant that only the endpoint growth values were measured and compared. After 20 hours of growth, the OD_{600} of each culture was measured, the results of which are presented in Figure 5.3.

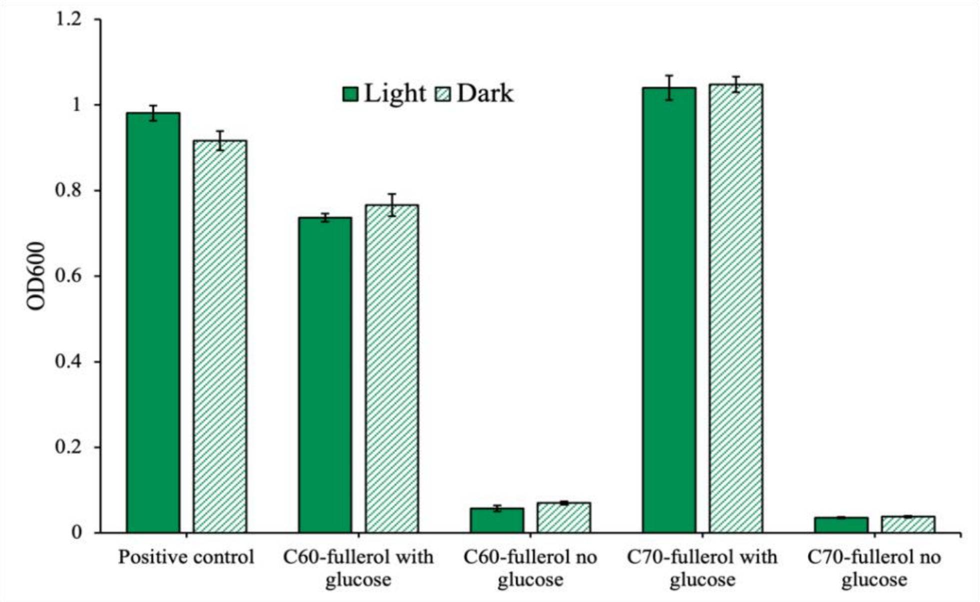

Figure 5.3: Comparison of *E. coli* culture density after 20 hours growth with C_{60}- or C_{70}-fullerol at 22 °C in either ambient light (solid green) or the dark (stripes).

Student's T tests were carried out to compare the light and dark measurements of each condition, the results of which are summarised in Table 5.3.

Table 5.3: Significance of the effects of incubation in light or dark conditions with C_{60}- and C_{70}-fullerol on the growth of *E. coli*.

Condition:	**P-value:**	**Significance:**
Positive control	0.058	ns
C_{60} fullerol with glucose	0.33	ns
C_{60} fullerol without glucose	0.16	ns
C_{70} fullerol with glucose	0.82	ns
C_{70} fullerol without glucose	0.49	ns

There is no significant difference between the light and dark cultures of any condition, which indicates that incubation in the light has no effect on the final growth measurement for cultures with either C_{60}- or C_{70}-fullerol at this temperature.

The next step in this series of experiments was to test if the response of *E. coli* to fullerenes and fullerols changes when it is growing under anaerobic conditions as this changes the primary respiratory pathway. To achieve this, *E. coli* was grown again with C_{60}, C_{70}, C_{60}-fullerol and C_{70}-fullerol, all with and without glucose. Two identical experiments were carried out, one aerobic and one anaerobic. The anaerobic cultures were kept at 22 °C inside an anaerobic chamber (see Chapter 3 Materials and Methods for anaerobic culturing details) and OD_{600} was measured after 20 hours of growth. The aerobic cultures were kept under identical growth conditions (22 °C with no shaking) outside of the chamber. The final OD_{600} measurements are compared in Figure 5.4.

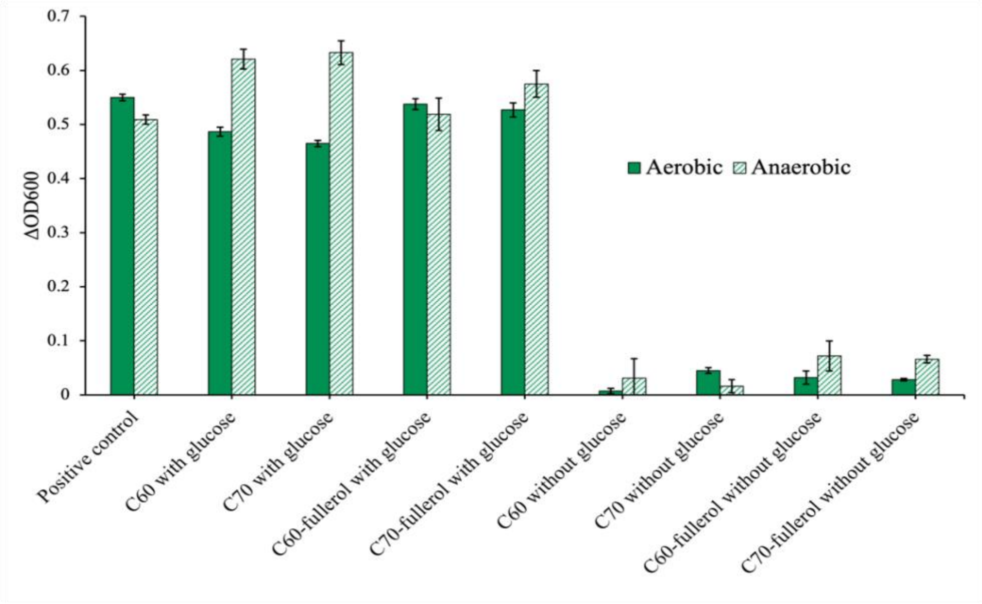

Figure 5.4: Effect of aerobic or anaerobic conditions on the growth of *E. coli* with fullerenes and fullerols.

Figure 5.4 shows that there is variation in the maximum OD_{600} between the aerobic and anaerobic cultures. However, this cannot be treated as significant or compared directly between growth conditions as although these experiments were run in parallel, the different locations and inevitable delay between inoculation and measurements mean they must be treated as two different experiments. The difference between the two is therefore not treated as significant and the relative growth across different conditions is intended for reference only to show that there is no obvious difference in *E. coli* response to fullerenes and fullerols when it is grown anaerobically.

5.3.2 The effect of UV-degraded C_{60} on *E. coli*

After establishing the effect of pristine fullerenes on *E. coli* under various growth conditions, I sought to compare how *E. coli* responded to UV-degraded C_{60}. In Chapter 4 I found that the anaerobic isolate, while not able to grow on C_{60} as a sole carbon source, could utilise UV-degraded C_{60} effectively. Establishing if *E. coli* is also able to utilise UV-C_{60} therefore provides some clarity on whether UV-C_{60} is universally accessible, or whether this is unique to certain bacterial species. To test this, *E. coli* was grown with UV-C_{60} with and without additional glucose under optimal growth conditions (Figure 5.5).

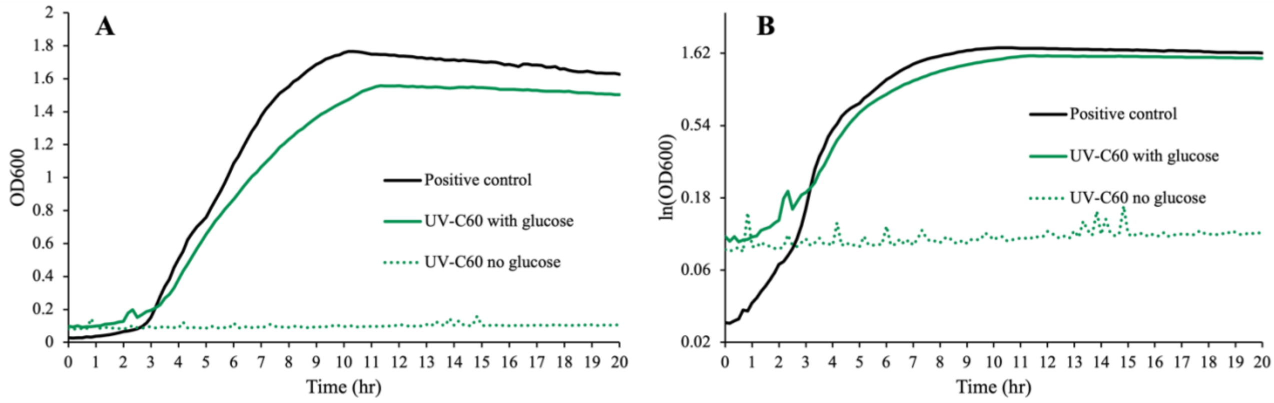

Figure 5.5: *E. coli* growth curves over 20 hours with UV-C_{60}, with and without additional glucose. A: original scale, B: Y-axis scaled to the natural logarithm of original OD_{600}.

Without additional glucose, no increase in growth is observed, indicating the UV-C_{60} cannot be used as a carbon source by *E. coli.* The average exponential growth rate and maximum OD_{600} values for each condition are summarised in Table 5.4.

Table 5.4: Exponential phase growth rate and maximum culture density values for *E. coli* grown with UV-C_{60}.

Condition:	**Growth rate (μ):**	**Max OD_{600}:**
Positive control	0.60	1.77
UV-C_{60} with glucose	0.34	1.56
UV-C_{60} without glucose	NA	NA

When glucose is available, the growth rate with UV-C_{60} is decreased compared to the positive control ($P=8.8x10^{-6}$), however the maximum OD_{600} was not significantly different (P=0.15), which indicates that although *E. coli* growth is slower with the UV-C_{60}, the amount of growth is not ultimately limited, following the same trend already observed in the *E. coli* response to C_{60} and C_{70} fullerenes and fullerols.

E. coli was grown again with UV-C_{60} with and without glucose, at either 37 °C or 22 °C (Figure 5.6). This experiment was done to assess if the different response to UV-C_{60} by *E. coli* compared with the anaerobic isolate in Chapter 4 was related to the difference in growth temperature.

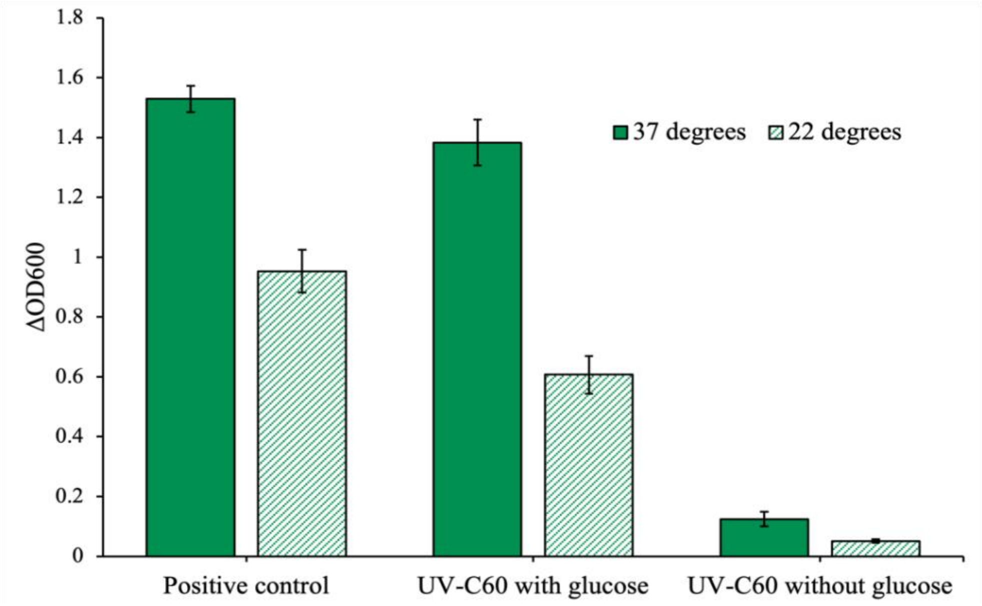

Figure 5.6: Effect of temperature on the growth of *E. coli* with UV-C_{60}, with and without glucose.

T-tests were carried out to compare each combination of conditions, the results of which are summarised in Table 5.5.

Table 5.5: Significance of temperature on the growth of *E. coli* with UV-C_{60}. P-values indicate the significance of the comparison between the maximum culture density of two conditions.

Condition 1:	**Condition 2:**	**P value:**	**Significance:**
Positive control (37 °C)	UV-C_{60} with glucose (37 °C)	0.13	ns
Positive control (37 °C)	UV-C_{60} without glucose (37 °C)	7.80E-11	*
Positive control (22 °C)	UV-C_{60} with glucose (22 °C)	0.0047	*
Positive control (22 °C)	UV-C_{60} without glucose (22 °C)	0.000058	*
Positive control (37 °C)	Positive control (22 °C)	0.000045	*
UV-C_{60} with glucose (37 °C)	UV-C_{60} with glucose (22 °C)	0.000014	*
UV-C_{60} without glucose (37 °C)	UV-C_{60} without glucose (22 °C)	0.027	* (consider not significant) **

** The results of the T-test comparing the UV-C_{60} without glucose (37 °C) condition to its corresponding negative control are non-significant (P=0.063), so we can consider the 'significant' difference between the 37 °C and 22 °C conditions to be negligible.

Growth at 22 °C appears to reduce the maximum OD_{600} at 20 hours evenly across all conditions, which is to be expected as this is below the optimal incubation temperature. The lower temperature does not, however, appear to alter the trend between conditions; UV-C_{60} still does not support growth as a sole carbon source and slightly reduces growth even when glucose is available. The different response to UV-C_{60} between *E. coli* and the anaerobic isolate is therefore likely down to species differences, not growth conditions.

5.3.3 The effect of fullerenes on *P. sp1* and *P. sp2*

Two aerobic *Pseudomonas* species were isolated from a basalt-fullerene mixture that was deliberately contaminated with environmental microorganisms. This exposure experiment was done to obtain naturally-occurring environmental species which presumably already had some resistance to C_{60} expsure due to their successful colonisation of the contaminated basalt. The isolates, *P. sp1* and *P. sp2* were exposed to similar experimental conditions as *E. coli* to investigate how the response of environmental species to fullerenes differs from that of a lab-engineered model organism.

The aerobic isolate *P. sp1* was grown with fullerene C_{60} and C_{70}, with and without additional glucose and compared to growth on just glucose (positive control). Both the normal and natural logarithm scale growth curves for this experiment are presented in Figure 5.7.

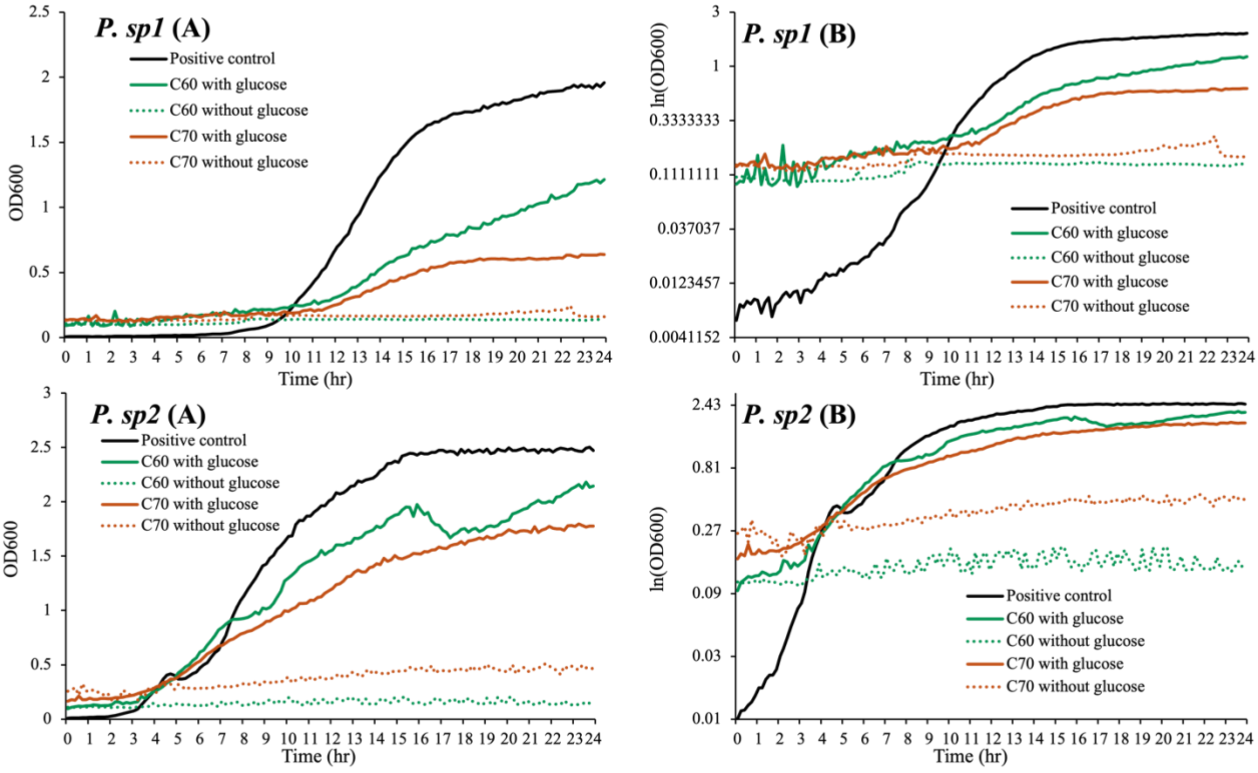

Figure 5.7: *P. sp1* and *P. sp2* 24-hour growth curves with fullerenes C_{60} and C_{70}, with and without additional glucose. *P. sp1* and *P. sp2* (A): original scale, *P. sp1* and *P. sp2* (B): Y-axis scaled to the natural logarithm of original OD_{600}.

The average exponential growth rate and maximum OD_{600} for each *P. sp1* condition are summarised in Table 5.6.

Table 5.6: Exponential phase growth rate and maximum culture density values for *P. sp1* grown with C_{60} and C_{70}, with and without glucose.

Condition:	**Growth rate (μ):**	**Max OD_{600}:**
Positive control	0.53	1.98
C_{60} with glucose	0.19	1.21
C_{70} with glucose	0.19	0.66
C_{60} without glucose	NA	NA
C_{70} without glucose	NA	NA

The slight increase in growth with *P. sp1* is incubated with either C_{60} or C_{70} as the sole carbon source is nonsignificant ($P<<0.01$ when starting and final OD_{600} values are compared with a T test). Therefore, *P. sp1* is not observed to utilise either fullerene as a carbon source for growth. C_{60} and C_{70} both reduce the growth rate compared with the positive control ($P=0.000031$ and 0.000013), and both reduce the maximum OD_{600} ($P=0.00086$ and 0.000013 for C_{60} and C_{70} respectively). Although it is clear from the growth curves in Figure 5.7 that some growth does still occur with C_{60} and C_{70}, it is significantly reduced even with additional glucose, suggesting both fullerenes are inhibitory to *P. sp1* to some degree.

The aerobic isolate *P. sp2* was grown under identical conditions to *P. sp1* with C_{60} and C_{70} as sole carbon sources or with additional glucose (Figure 5.7). The growth rate and maximum OD_{600} values are presented in Table 5.7.

Table 5.7: Exponential phase growth rate and maximum culture density values for *P. sp2* grown with C_{60} and C_{70}, with and without glucose.

Condition:	**Growth rate (μ):**	**Max OD_{600}:**
Positive control	0.51	2.51
C_{60} with glucose	0.28	2.19
C_{70} with glucose	0.19	1.81
C_{60} without glucose	NA	NA
C_{70} without glucose	NA	NA

Again, there is no significant growth in the C_{60} and C_{70} cultures without glucose, indicating *P. sp2* is also unable to utilise either fullerene as a carbon source. C_{60} and C_{70} both significantly reduce the growth rate compared to the positive control ($P=0.00028$ and $7.3x10^{-5}$ for C_{60} and C_{70}, respectfully). C_{70} also significantly reduces the maximum OD_{600} reached over the 24-hour growth period ($P=4.9x10^{-8}$), indicating C_{70} does have an inhibitory effect on *P. sp2*. C_{60}, however, does not significantly reduce the maximum OD_{600} ($P=0.13$). This would seem to suggest that despite reducing the growth rate, C_{60} does not ultimately change the amount of growth achieved. However, because the growth rate and the curve shape are more similar between the C_{60} and C_{70} conditions than with the positive control, it is a reasonable assumption that *P. sp2* is similarly inhibited by both C_{60} and C_{70}.

TEM images were taken of *P. sp1* and *P. sp2* after 24 hours growth with C_{60} (100 mg/L) to identify any morphological changes or evidence of direct association of C_{60}

aggregates with the bacterial membranes. The resulting images are presented in Figures 5.8 and 5.9.

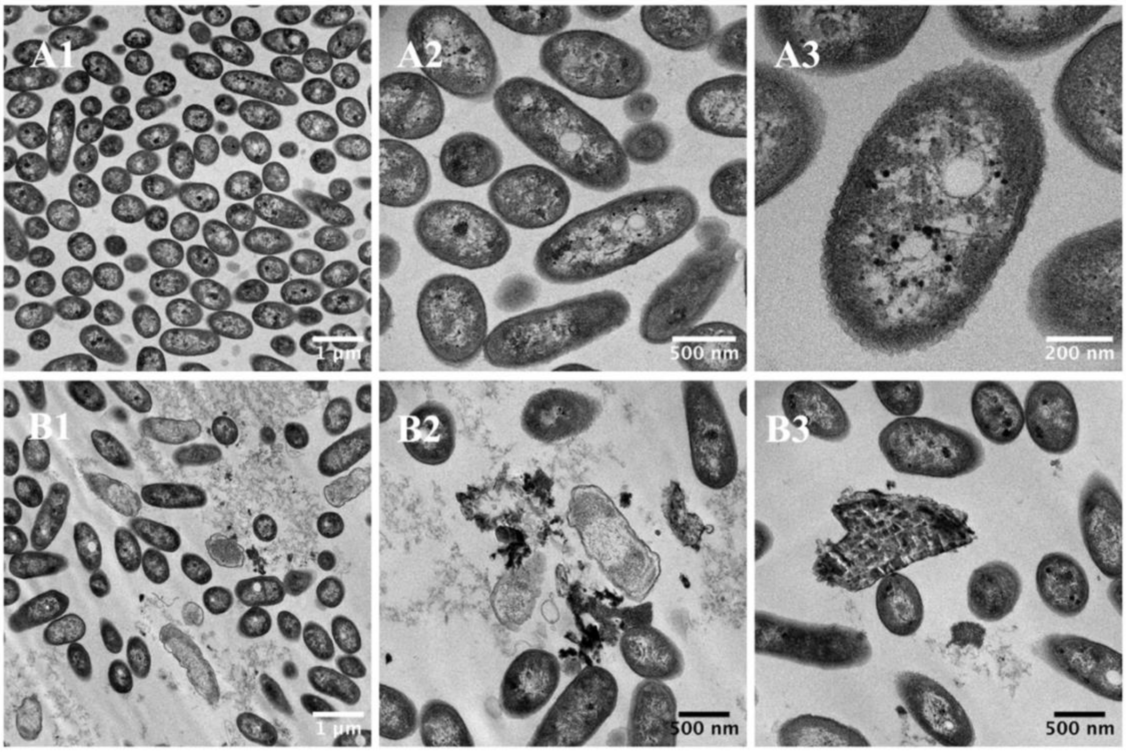

Figure 5.8: TEM images of *P. sp1* after 24 hours growth with (A): glucose only (positive control), (B): glucose and 100 mg/L C_{60}.

The *P. sp1* positive control (Figure 5.8A) was grown only on glucose. The cells in this culture are ovaloid rod-shaped and many contain large vacuoles. *P. sp1* grown with C_{60} (Figure 5.8B) have very similar morphology, including visible vacuoles in many of the cells, however there is a much higher number of dead and lysed cells easily visible (Figure 5.8B2-B3), with an abundance of cellular material in the media, particularly in areas surrounding C_{60} aggregates.

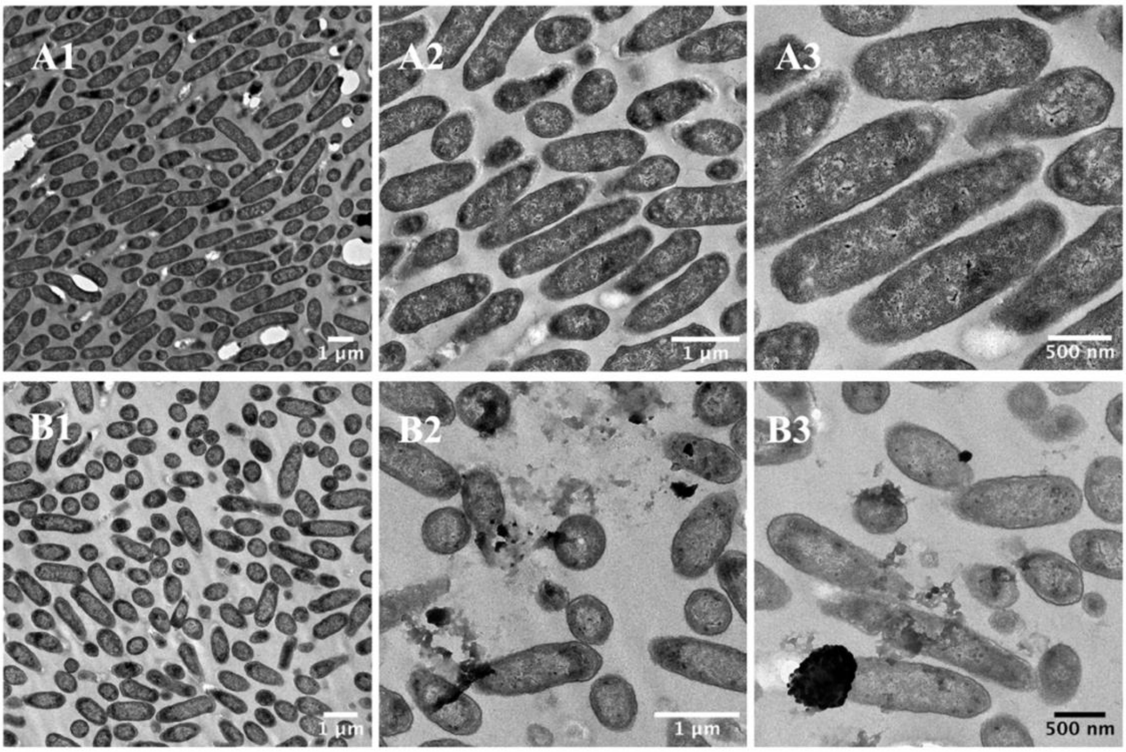

Figure 5.9: TEM images of *P. sp2* after 24 hours growth with (A): glucose only (positive control), (B): glucose and 100 mg/L C_{60}.

The *P. sp2* positive control appears slightly different to the *P. sp1* cells, forming longer, more elongated rod shapes that appear to roughly align to point in the same direction (Figure 5.9(A)). Unlike *P. sp1,* there are no visible vacuoles in the *P. sp2* cells. When *P. sp2* is grown with C_{60}, there appears to be a higher proportion of smaller, more ovaloid cells compared with the longer rod shapes seen in the positive control (Figure 5.9B). There do not appear to be as many easily visible lysed cells in the *P. sp2* C_{60} condition as there are in the *P. sp1* images, however, in areas where there are visible C_{60} aggregates, there does appear to be some cellular membrane damage occurring (Figure 5.7B2-B3) and the background debris resembles cellular debris.

5.3.4 Effect of UV-degraded fullerenes on *P. sp1* and *P. sp2*

The isolate *P. sp1* was grown with UV-C_{60} and UV-C_{70}, with and without additional glucose and the resulting growth curves are presented in Figure 5.10 in both the normal and natural logarithm scale.

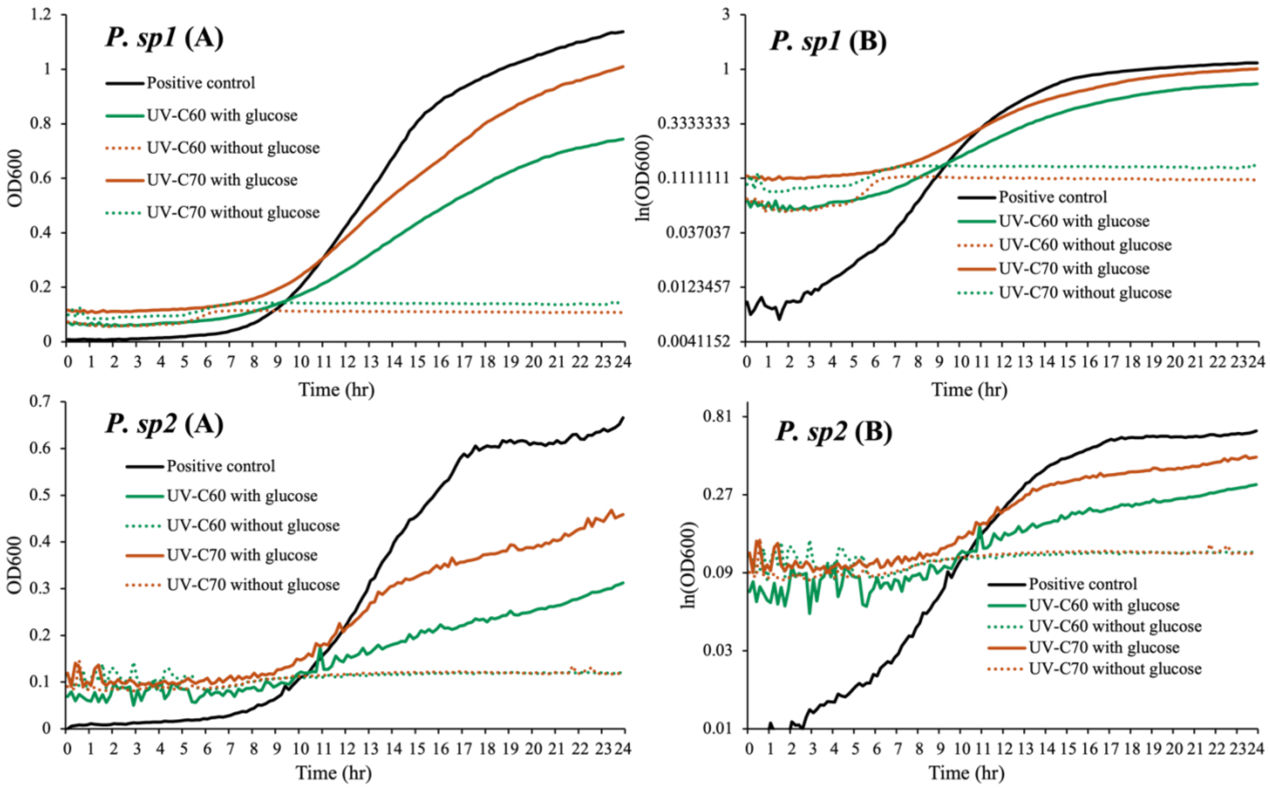

Figure 5.10: *P. sp1* and *P. sp2* 24-hour growth curves with fullerene C_{60} and C_{70} UV-degradation products, with and without additional glucose. A: original scale, B: Y-axis scaled to the natural logarithm of original OD_{600}.

The growth rate and maximum OD_{600} values for *P. sp1* with UV-fullerenes are summarised in Table 5.8.

Table 5.8: Exponential phase growth rate and maximum culture density values for *P. sp1* grown with UV-C_{60}, with and without glucose

Condition:	**Growth rate (μ):**	**Max OD_{600}:**
Positive control	0.38	1.14
UV-C_{60} with glucose	0.17	0.74
UV-C_{70} with glucose	0.17	1.01
UV-C_{60} without glucose	NA	NA
UV-C_{70} without glucose	NA	NA

Neither the UV-C_{60} nor UV-C_{70} are utilised as sole carbon sources by *P. sp1*, as no significant growth is observed in these cultures. UV-C_{60} and UV-C_{70} with additional glucose both reduce the growth rate compared with the positive control (P=0.0002 and 0.00016 for UV-C_{60} and UV-C_{70}, respectfully). Similarly, both UV-treated fullerenes reduced the maximum OD_{600} value obtained in the 24-hour growth period (P=0.0045 and 0.012 for UV-

C_{60} and UV-C_{70}, respectively). This indicates that both fullerenes become inhibitory to *P. sp1* when UV-degraded, and it is clear from the growth curves that UV-C_{60} has a greater inhibitory effect than UV-C_{70}.

P. sp2 was grown with UV-C_{60} and UV-C_{70} (Figure 5.10) under identical conditions to *P. sp1*. The same trend is observed with *P. sp2* as was seen with *P. sp1*; there is no growth with UV-C_{60} or UV-C_{70} as the sole carbon source, and both UV-C_{60} and UV-C_{70} decrease the growth rate compared with the positive control (P=0.014 and 0.000019) and both fullerenes reduce the maximum OD_{600} (P=0.037 and 0.000036), detailed in Table 5.9. This suggests both UV-degraded fullerenes are inhibitory to *P. sp2*, but C_{60} appears to be more so.

Table 5.9: Exponential phase growth rate and maximum culture density values for *P. sp2* grown with UV-C_{60}, with and without glucose.

Condition:	**Growth rate (µ):**	**Max OD_{600}:**
Positive control	0.35	0.67
UV-C_{60} with glucose	0.12	0.31
UV-C_{70} with glucose	0.16	0.48
UV-C_{60} without glucose	NA	NA
UV-C_{70} without glucose	NA	NA

5.3.5 Effect of fullerols on *P. sp1* and *P. sp2*

The isolate *P. sp1* was grown with C_{60}- and C_{70}- fullerol, with and without glucose, the growth curves of which are presented in Figure 5.11 in both the normal and natural logarithm scales.

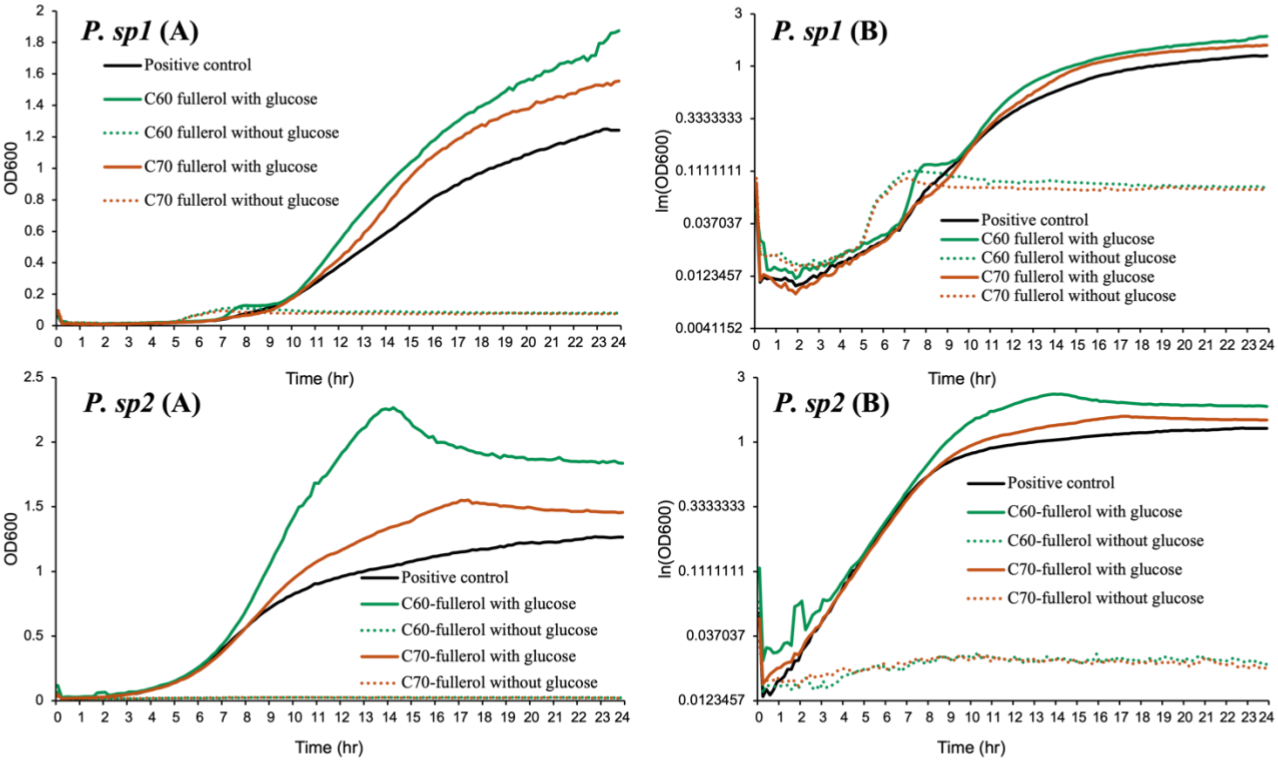

Figure 5.11: *P. sp1* and *P. sp2* 24-hour growth curves with C_{60}- or C_{70}-fullerol, with and without additional glucose. A: original scale, B: Y-axis scaled to the natural logarithm of original OD_{600}.

The growth rates and maximum OD_{600} are presented in Table 5.10.

Table 5.10: Exponential phase growth rate and maximum culture density values for *P. sp1* grown with C_{60}- and C_{70}-fullerol, with and without glucose

Condition:	**Growth rate (μ):**	**Max OD_{600}:**
Positive control	0.32	1.26
C_{60}-fullerol with glucose	0.33	1.87
C_{70}-fullerol with glucose	0.35	1.54
C_{60}-fullerol without glucose	NA	NA
C_{70}-fullerol without glucose	NA	NA

Interestingly, while neither C_{60}- nor C_{70}-fullerol affected the growth rate compared with the positive control (P=0.25 and 0.24 for C_{60}- and C_{70}-fullerol, respectfully), the maximum OD_{600} in both conditions was significantly higher ($P=8.1\times10^{-6}$ and 0.00024). On the normal scale, there is no growth with either C_{60}- or C_{70}-fullerol without glucose. However, on the logarithmic scale, these two conditions do seem to increase slightly with a short exponential increase followed by a plateau which is significantly below the maximum growth achieved when glucose is present. This would seem to suggest there is a small amount of growth even without glucose, however when the initial and final OD_{600} values for these conditions are compared with a T test, the result is nonsignificant ($P=0.91$ and $P=0.19$ for C_{60}-fullerol without glucose and C_{70}-fullerol without glucose, respectfully). Therefore, there is no evidence that *P. sp1* can utilise either fullerol without additional glucose.

P. sp2 was also grown with C_{60}- and C_{70}-fullerol with and without glucose (Figure 5.11), and the growth rate and maximum OD_{600} values for each condition are summarised in Table 5.11.

Table 5.11: Exponential phase growth rate and maximum culture density values for *P. sp2* grown with C_{60}- and C_{70}-fullerol, with and without glucose.

Condition:	**Growth rate (μ):**	**Max OD_{600}:**
Positive control	0.43	1.28
C_{60}-fullerol with glucose	0.42	2.30
C_{70}-fullerol with glucose	0.41	1.56
C_{60}-fullerol without glucose	NA	NA
C_{70}-fullerol without glucose	NA	NA

Again, neither C_{60}- nor C_{70}-fullerol effect the growth rate compared to the positive control ($P=0.77$ and 0.33 for C_{60}- and C_{70}-fullerol, respectfully), while the maximum OD_{600} for both conditions is higher ($P=0.036$ and 0.0051). However, there is no growth when the fullerols are the sole carbon source. These results suggest that either both fullerols act to increase the cell density of *P. sp1* and *P. sp2*, without actually being utilised as an extra source of carbon, or other another effect is taking place which increases the absorbance at 600 nm proportionally to cell density.

After observing the effects of C_{60}-fullerol on *P. sp1* and *P. sp2*, I conducted a further growth experiment under identical conditions in which both species were grown again with C_{60}-fullerol (100 mg/L), a C_{60} fullerene/fullerol mix where both compounds were present at 100 mg/L, and a C_{60} fullerene/fullerol mix where both were at 50 mg/L (Figure 5.12).

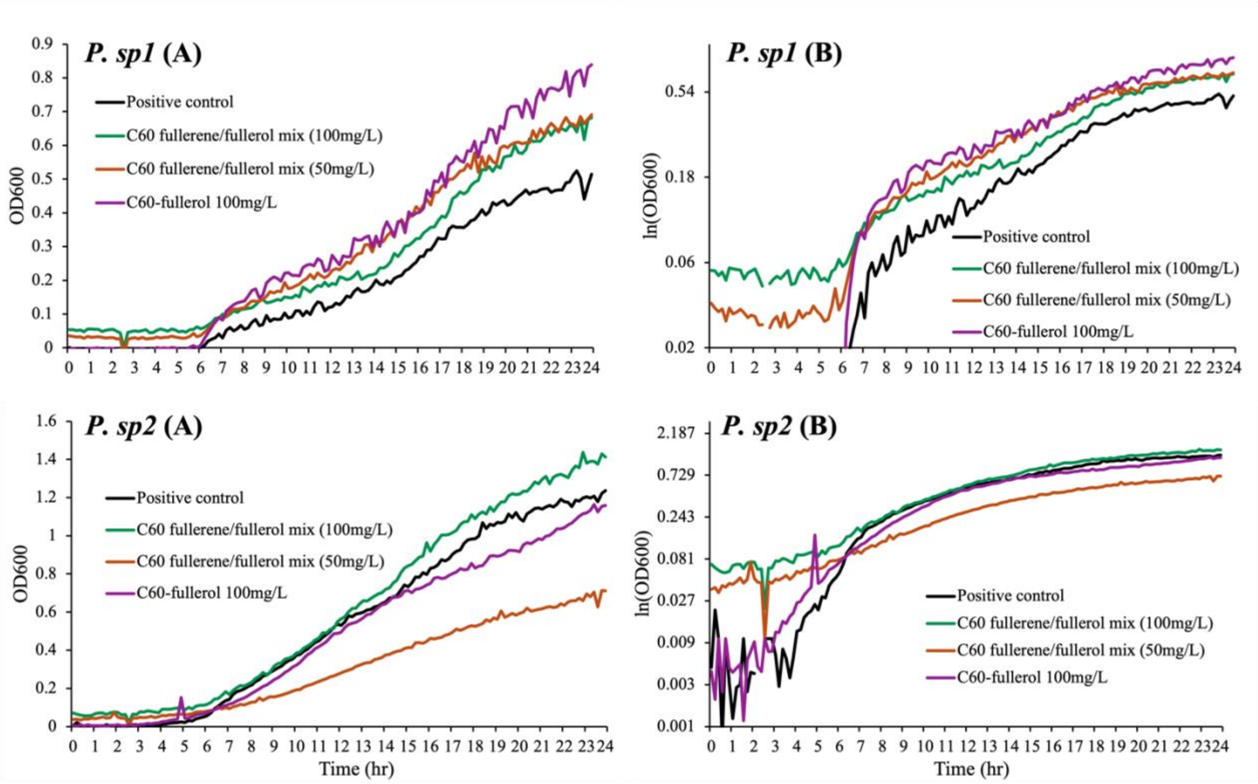

Figure 5.12: *P. sp1* and *P. sp2* 24-hour growth curves with C_{60}-fullerol (100 mg/L) and a C_{60} fullerene/fullerol mix at either 50 or 100 mg/L. A: original scale, B: Y-axis scaled to the natural logarithm of original OD_{600}.

The resulting growth curves for *P. sp1* (Figure 5.12) show that in this experiment, there was no significant difference between the growth rates of any of the three fullerol conditions (C_{60}-fullerol (100 mg/L), C_{60} fullerene/fullerol mix at 100 mg/L, and C_{60} fullerene/fullerol mix at 50 mg/L) and the positive control (P=0.64, 0.66 and 0.72). Similarly, there is no significant difference between the maximum OD_{600} achieved by each of the three conditions compared with that of the positive control (P= 0.11, 0.38 and 0.35). The growth rate and maximum OD_{600} values for each *P. sp1* condition are summarised in Table 5.12.

Table 5.12: Exponential phase growth rate and maximum culture density values for *P. sp1* grown with C_{60}-fullerol a C_{60}-fullerol/fullerene mix.

Condition:	**Growth rate (μ):**	**Max OD_{600}:**
Positive control	0.21	0.54
C_{60} fullerene/fullerol mix (100 mg/L)	0.17	0.69
C_{60} fullerene/fullerol mix (50 mg/L)	0.25	0.71
C_{60}-fullerol (100 mg/L)	0.26	0.85

All three fullerol conditions (C_{60}-fullerol (100 mg/L), C_{60} fullerene/fullerol mix at 100 mg/L, and C_{60} fullerene/fullerol mix at 50 mg/L) had a reduction in growth rate compared to the positive control (P=0.032, 0.011 and 0.0026. The C_{60} fullerene/fullerol mix at 50 mg/L also had a significantly lower maximum OD_{600} compared to the positive control (P=0.0026), while the 100 mg/L mix and the C_{60}-fullerol did not (P=0.08 and 0.12). The values for growth rate and maximum OD_{600} of *P. sp2* are presented in Table 5.13 and the growth curves are shown in Figure 5.12).

Table 5.13: Exponential phase growth rate and maximum culture density values for *P. sp2* grown with C_{60}-fullerol a C_{60}-fullerol/fullerene mix.

Condition:	**Growth rate (μ):**	**Max OD_{600}:**
Positive control	0.44	1.25
C_{60} fullerene/fullerol mix (100 mg/L)	0.22	1.47
C_{60} fullerene/fullerol mix (50 mg/L)	0.19	0.72
C_{60}-fullerol (100 mg/L)	0.34	1.08

After analysing the results of the experiments shown in Figures 5.11 and 5.12, I sought to confirm whether the differences in growth observed when *P. sp1* and *P. sp2* were grown with C_{60}-fullerol and C_{60} fullerene/fullerol mixes were true reflections of how much each culture grew, or whether something else was occurring in the fullerol media that increased the OD_{600} without enhancing culture growth. To achieve this, I repeated the experiment described in Figure 5.12 but plated each culture after 24 hours of incubation with each condition to count the CFUs that grew on solid agar. The results of the *P. sp1* experiment are shown in Figure 5.13. In this experiment, the positive control, C_{60} and C_{60} fullerene/fullerol mix (50 mg/L) conditions were counted and are represented accurately in Figure 5.13. However, the C_{60}-fullerol and C_{60} fullerene/fullerol mix (100 mg/L) conditions grew significantly more on the agar plates and produced such a large number of colonies that these could not be discreetly counted. Visually, the density of these plates appeared to be about double that of the positive control plates, and therefore an approximation of the CFUs/mL for these conditions is represented in Figure 5.13.

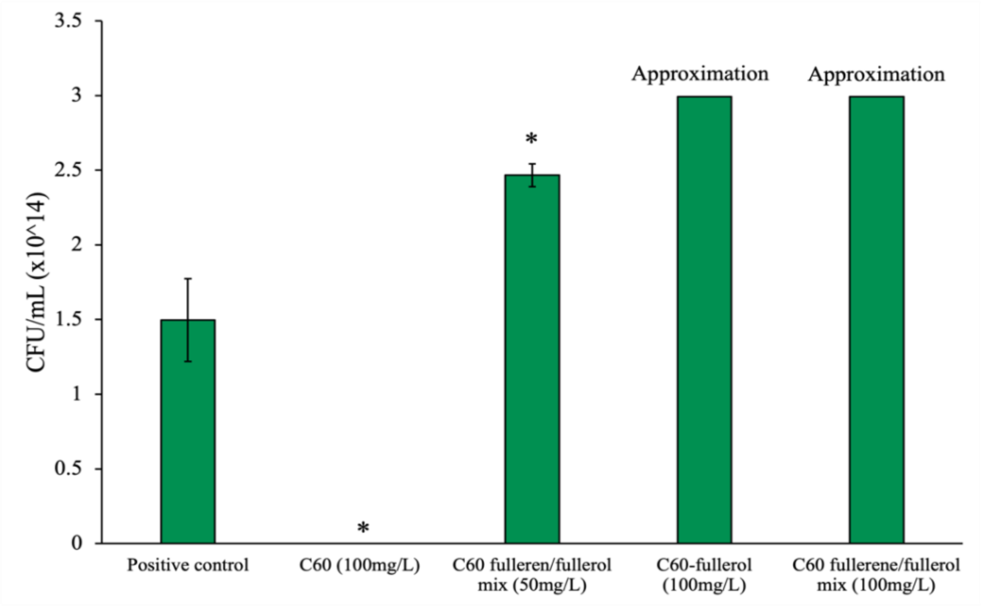

Figure 5.13: Effect of C_{60}-fullerene/fullerol mixtures on growth of *P. sp1*. CFUs/mL after 24 hours growth with C_{60} (100 mg/L), C_{60} fullerene/fullerol mix (50 mg/L), or C_{60} fullerene/fullerol mix (100 mg/L). The positive control, C_{60} and C_{60} fullerene/fullerol mix (50 mg/L) show exact amounts, while the C_{60}-fullerol and C_{60} fullerene/fullerol mix (100 mg/L) are approximated to give a rough comparison.

The same experiment was done with *P. sp2*, however, on all except the C_{60} plate, growth was too dense to count discrete CFUs. Photographs taken of each plate are shown in Figure 5.14 to demonstrate the density of growth and allow for visual comparison between conditions.

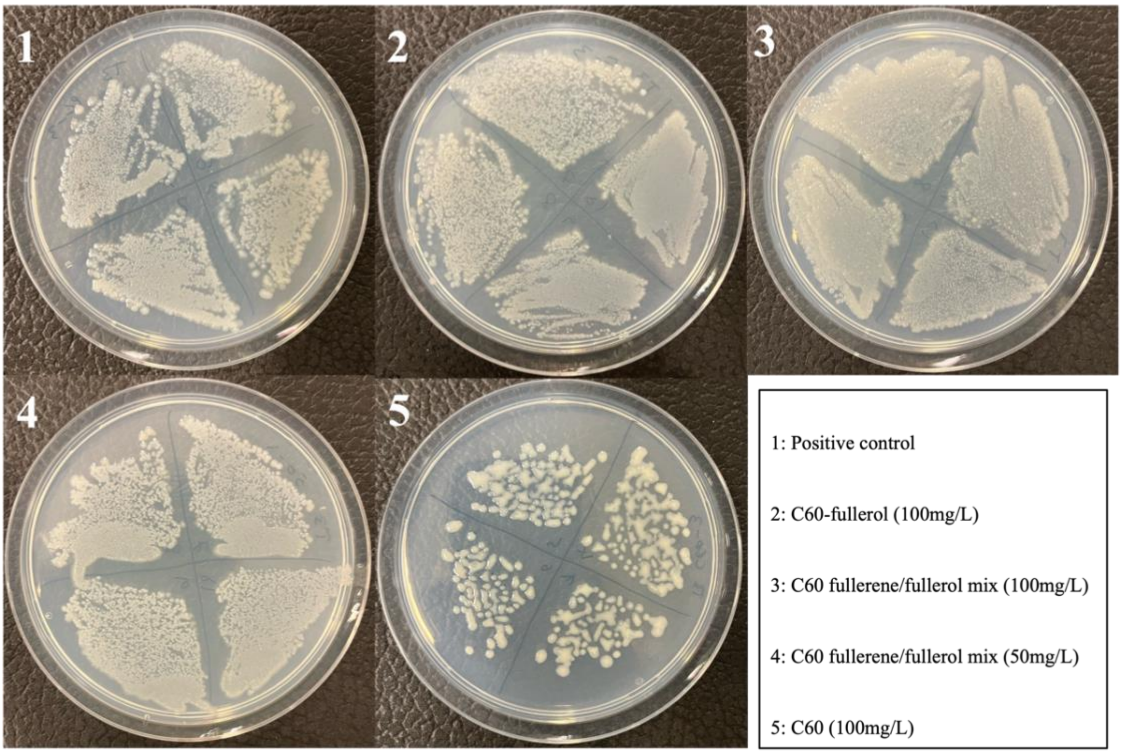

Figure 5.14: Photographs of *P. sp2* (dilutions 10^7-10^{10}) plated after 24 hours of growth with glucose (positive control), C_{60} (100 mg/L), C_{60}-fullerol (100 mg/L), C_{60} fullerene/fullerol mix (100 mg/L) or C_{60} fullerene/fullerol mix (50 mg/L).

From these photographs, it is clear that the C_{60} condition has fewer colonies and less growth than all the other conditions, including the positive control. It is also apparent that there is no visually discernible difference between any of the fullerol conditions and the positive control. It is not possible to say with any certainty that one condition grew significantly more than the others, however, it is reasonable, based on the photographs, to assume that all the fullerol conditions grew at least as much as the positive control.

5.4 Discussion

In this Chapter, I sought to explore the response of model and environmental aerobic microorganisms to fullerenes for comparison to my previous work with anaerobic species. The responses observed in Chapter 4 highlight the impact fullerenes may have had on primitive microorganisms on the early Earth. By replicating these experimental conditions with both the well-characterised model species *Escherichia coli* and two environmentally relevant species, I can ascertain which, if any, of these responses are innate to all microorganisms, and which are relevant only in an anaerobic environment. Additionally, the impact that fullerenes and their derivatives have on aerobic environmental species is more relevant for assessing the effect of fullerenes on modern-day Earth as potential anthropogenic environmental pollutants.

5.4.1 C_{60} and C_{70} are not inhibitory to aerobic growth of *E. coli*

E. coli was initially grown in M9 media under optimal growth conditions (aerobic at 37 °C) with 100 mg/L of either C_{60} or C_{70}, with and without additional glucose. In the absence of glucose, *E. coli* did not grow with C_{60} or C_{70}, indicating it is unable to use either fullerene as a carbon source. This is not unexpected, as to the best of my knowledge there is no evidence of *E. coli* being able to utilise fullerenes in the existing literature, despite several studies using *E. coli* for fullerene microbial growth experiments (Fortner et al., 2005; Lee et al., 2009; Lyon et al., 2005). When *E. coli* was grown with glucose as the carbon source, the presence of fullerenes did not have any significant impact on its growth rate or magnitude of growth. This indicates that neither C_{60} nor C_{70} had any inhibitory effect on the growth of *E. coli*, and these results did not change regardless of whether the cultures were grown aerobically or anaerobically. This result is important because it contradicts the available literature which assesses fullerene toxicity using *E. coli*. For example, a 2005 study found aqueous nC_{60} to be highly inhibitory to *E. coli*, even at concentrations much lower than those used in my experiments (Fortner et al., 2005). One of the differences between the experimental method in this study and that detailed in this chapter is the protocol used to prepare the aqueous fullerene suspensions; while I prepared my suspensions via sonication in M9, the Fortner et al group prepared nC_{60} by dissolving C_{60} in an organic solvent and forcing it to enter an aqueous layer with a mixture of physical agitation and vacuum-driven evaporation of the organic layer (Fortner et al., 2005), which almost certainly resulted in different in aggregate sizes. However, it is not likely that the difference in toxicity to *E. coli* observed in the Fortner et al study and in my experiments is due to the suspension preparation method, as it was shown in 2006 that C_{60} suspensions made using four different methods were all equally as antibacterial (Lyon et al., 2006).

A particularly interesting aspect of the 2005 Fortner et al study relates to how the toxicity of aqueous nC_{60} changes with increased media salt content. In their study, when *E. coli* was grown with C_{60} in a low salt (minimal Davis) media, there was no detectable growth, however when it was grown in high salt (LB) media under identical conditions, *E. coli* was able to grow with 2.5 mg/L nC_{60} (Fortner et al., 2005). This observation that C_{60} was less toxic to *E. coli* in higher salt media is further supported by another 2005 study which assessed the antimicrobial properties of nC_{60} in either high (LB) or low (MD) salt media, where it was found that high salt content reduced the toxicity of nC_{60} towards both *E. coli* and *Bacillus subtilis* (Lyon et al., 2005). It was shown in this study that C_{60} aggregates in lower-salt media directly associated with the bacterial cell membrane of *E. coli* and *B. subtilis*, and this membrane contact was probably instrumental in the C_{60} having an inhibitory effect (Lyon et al., 2005). In media with higher salt content, the C_{60} formed much larger aggregates which caused it to fall out of the suspension more quickly, therefore limiting the amount left in suspension to come in contact with the bacterial cell membranes and significantly reducing the toxicity (Lyon et al., 2005). In all growth experiments detailed within this chapter, cultures were grown in M9 minimal media, which has a high salt concentration, therefore it is likely that the nC_{60} aggregates behaved similarly to that in the high salt media in the Lyon et al study, forming large clusters that fell out of suspension and therefore did not have a chance to exert any toxic effects on the growing *E. coli*.

5.4.3 ***Pseudomonas sp1.*** **and** ***sp2.*** **are partially inhibited by C_{60} and C_{70}**

The environmental *Pseudomonas* species, *P. sp1* and *P. sp2*, used in this study were originally derived from a basalt-fullerene mixture which was left unsealed outside to deliberately contaminate it with microorganisms. I initially hypothesised that any species isolated from this mixture would therefore be fullerene-tolerant, having survived colonisation of a fullerene-rich basalt media. Interestingly, however, C_{60} and C_{70} exposure reduces the growth of both *P. sp1* and *P. sp2* compared with their positive controls, indicating that although they are still able to grow, they are at least partially inhibited by both fullerenes. This is consistent with multiple previous studies which have consistently found nC_{60} to be inhibitory to a variety of aerobic species (Fang et al., 2007; Riding et al., 2012). In 2007, Fang et al showed that nC_{60}, as well as being bacteriostatic, significantly altered the membrane composition of the environmental soil species *Pseudomonas putida* (Fang et al., 2007). This was further corroborated in 2012 by Riding et al who found that all of the inhibitory effects of nC_{60} were associated with the outer bacterial cell membrane, probably because nC_{60} is not able to penetrate the membrane to alter the internal architecture of the cell (Riding et al., 2012). Aqueous nC_{60} has been shown to associate directly with cell membranes in aerobic cultures with the aggregates visibly adhering to the bacterial cell surfaces under TEM imaging (Lyon et al., 2005, 2006). Both studies showing this also observed nC_{60}-induced inhibition of the bacterial cultures. In this chapter, although I do observe nC_{60} to have an inhibitory effect on *P. sp1* and *P. sp2*, the TEM images of these cultures do not show any conclusive evidence of nC_{60} aggregates adhering to the bacterial cell surfaces. There is, however, a higher number of dead cells and lysed cell debris visible in the images of both species after incubation with nC_{60}, and this does seem to occur more in areas with a larger amount of nC_{60} clustering. Although this is a qualitative observation and not quantifiable within the scope of these experiments, it does provide further evidence that factors associated with the presence of nC_{60} aggregates causes cell death within these cultures, and the lack of direct membrane association might be due to a difference in TEM sample preparation rather than definitive proof it is not occurring.

5.4.4 UV-degraded C_{60} negatively affects the growth of *E. coli*

In Chapter 4, I showed that the anaerobic isolate can use UV-degraded C_{60} as a sole carbon source, and these UV-degradation products are just as accessible to this anaerobe as glucose. I therefore adapted the protocols described in Chapter 4 to carry out a series of experiments with aerobic species to ascertain if UV-C_{60} is ubiquitously accessible as a carbon source, or if this is unique to anaerobic metabolism.

In this chapter I show that *E. coli* incubated with 100 mg/L UV-C_{60} does not grow without an additional carbon source, indicating that the UV degradation products are not accessible to the *E. coli*. Additionally, when glucose was provided as an alternate carbon source, the presence of UV-C_{60} significantly reduced the growth rate. Although the maximum culture density achieved by the *E. coli* exposed to UV-C_{60} was not ultimately reduced, the decrease in growth rate indicates that the UV-degradation products were inhibitory to some degree. The aerobic isolates *P. sp1* and *P. sp2* were similarly inhibited by UV-C_{60}, to an even greater degree than *E. coli* as both the growth rate and maximum culture density were significantly reduced for both species. Interestingly, this contradicts the results of a previous study which found nC_{60} to be significantly less antibacterial after UV degradation (Lee et al., 2009). In this chapter, however, I find that UV exposure increases nC_{60} toxicity towards *E. coli* and has no discernible change in the level of inhibition towards *P. sp1* and *P. sp2*.

Another study assessing the effects of UV-irradiated C_{60} on soil microorganisms found that not only was the UV-degraded C_{60} nontoxic, it was readily degraded by microbes in soil microcosms (Berry et al., 2016). It is not surprising that a different response to UV-C_{60} is observed with *E. coli*, as a laboratory *E. coli* strain incubated in liquid culture is only comparable to a mixed community in a soil-based microcosm to a limited degree. The two species of *Pseudomonas*, however, were derived directly from environmental samples and are therefore more similar to other soil species, so we might expect them to have a similar response to UV-C_{60} as the soil microbes in the Berry et al study. However, the Berry et al microcosm experiments were done using UV-irradiated C_{60} which was mixed with granular soil, whereas the experiments in this chapter were all done in liquid cultures, therefore the chemistry of the UV-C_{60} was almost certainly affected by the aqueous state of the suspension and may be responsible for the resulting toxicity.

5.4.5 C_{60}- and C_{70}-fullerol are not inhibitory to *E. coli*

E. coli was grown with 100 mg/L of either C_{60}- or C_{70}-fullerol under identical growth conditions to those employed in the fullerene growth experiments. A nearly identical response to the fullerols as to fullerenes was observed; neither fullerol was utilised by the *E. coli* as a sole carbon source, however normal growth was observed in the presence of both fullerols when glucose was available, indicating that neither C_{60} nor C_{70} was inhibitory. These results are consistent with previous studies assessing aerobic microbial response to fullerols; for example, it has previously been shown that negatively charged fullerene derivatives, including fullerols, have no effect on aerobic microorganisms (Tang et al., 2007), which is line with what I observe in this chapter. However, multiple studies also show that fullerol is readily degraded by microbes in soils, even in cases where pristine C_{60} is not (Berry et al., 2017; Navarro et al., 2015), whereas with *E. coli* there is no evidence of this.

The results presented in Chapter 4 showed that C_{60}-fullerol was inhibitory to the anaerobic microorganisms. In this chapter I repeated the experiment under both aerobic and anaerobic conditions to assess if this discrepancy in fullerol-sensitivity was due to the fullerol interacting with oxygen in the environment. However, there was no difference in the *E. coli* response to either C_{60}- or C_{70}-fullerol under anaerobic growth conditions, indicating that *E.*

coli's resistance to fullerol toxicity must be due to a difference in species biology, not the growth or oxygen environment. One such biological difference that could result in increased fullerol-tolerance may come from mechanisms possessed by aerobic microorganisms which facilitate resistance to oxidative stress and low levels of reactive oxygen species (ROS) (Seixas et al., 2022). The explanation for the discrepancy may therefore be as simple as the fact that aerobic microbes have evolved to cope with the consequences of being constantly exposed to a reactive, oxygen-rich environment, whereas obligate anaerobes are not as well equipped and therefore are more susceptible to fullerol toxicity.

5.4.6 C_{60}- and C_{70}-fullerol increase growth of *Pseudomonas sp1* and *sp2*

When the two environmental species *P. sp1* and *P. sp2* are grown with C_{60}- and C_{70}-fullerol, they demonstrate a more complex response than that observed with *E. coli*. In the presence of glucose, neither fullerol significantly increased the growth rate, however they did seem to increase the amount of growth achieved over 24 hours compared to the positive controls, for both species. If the fullerols were being used as carbon sources, this increase in growth could be explained relatively easily as the fullerols could be providing extra carbon. However, when there is no additional glucose, neither *P. sp1* nor *P. sp2* show any significant growth, which indicates the fullerols are not being utilised as carbon sources in the absence of glucose. The results of this first fullerol growth experiment alone would therefore suggest that the fullerols are somehow enhancing the growth of *P. sp1* and *P. sp2*, increasing the cell density, without being used as a carbon source. A subsequent growth experiment was conducted to test if C_{60}-fullerol would have the same growth-enhancing effect on *P. sp1* and *P. sp2* if C_{60}, which was previously inhibitory to both species, was also present. To test this, both species were incubated with equal mixes of C_{60} fullerene and fullerol, as well as supplementary glucose. Two concentrations were tested- a higher one where both C_{60} and C_{60}-fullerol were present at 100 mg/L (to a total concentration of 200 mg/L), and a lower one where both were present at 50 mg/L (to a total of 100 mg/L)- in case the total carbon present changed the observed results. This experiment again indicated that C_{60}-fullerol enhanced the growth of both species and additionally showed that in almost all cases, the presence of fullerol 'cancelled out' the previously observed inhibitory effects of C_{60}, regardless of the mixed concentration. It is unclear, however, whether this is because the fullerol is chemically or biophysically interfering with the C_{60} mechanism of toxicity, or whether the enhancing effect it has on the bacterial growth is great enough that it causes the cultures to overcome the C_{60}-induced reduction in growth rate.

One possibility for the increase in growth rate and maximum culture density observed in *P. sp1* and *P. sp2* cultures with C_{60}-fullerol is that a chemical reaction occurs between fullerol and something in the cultures which increases the absorbance at 600 nm, resulting in higher OD_{600} measurements. To determine if this was the case in the first two fullerol growth experiments, I repeated a growth experiment by incubating both species with C_{60}, C_{60}-fullerol and the C_{60}/fullerol mixes at both 50 and 100 mg/L for 24 hours and plated the resulting cultures on agar to produce CFUs, instead of measuring the OD_{600}. Each CFU results from a viable cell, therefore it was possible to determine if the same growth pattern was observed by counting CFUs, ruling out the possibility that fullerol somehow increases the OD_{600} readings. The *P. sp1* results give the same pattern in the magnitude of growth after 24 hours as in the previous fullerol growth experiments. From the CFU counts, the C_{60} condition produces significantly lower CFUs than the positive control, and the C_{60} fullerene/fullerol mix (50 mg/L) has significantly more than the positive control. The remaining two conditions, the C_{60}-fullerol and C_{60} fullerene/fullerol mix (100 mg/L) grew so much, even in the most diluted conditions, that discreet CFUs could not be counted. Visually, these appeared to be about twice as dense as the positive control plates, so for the purposes of this analysis they are considered to be significantly higher than the positive control. In other words, all the fullerol conditions, both C_{60}-fullerol and the two fullerene/fullerol mixes, increased the growth of *P. sp1* after 24 hours compared to the positive control, while C_{60} on its own decreased it.

The *P. sp2* results are presented slightly differently, as after being plated on solid agar they grew to higher densities than could be counted, even at the highest dilution. Photographs of each plate were taken in order to allow some qualitative comparison for the amount of growth between conditions. In the case of *P. sp2*, the positive control and all the fullerol conditions, C_{60}-fullerol and the two mixes, all appear to have similar amounts of growth, even if discrete CFUs could not be counted. As with the *P. sp1* results, however, the C_{60} conditions had reduced growth compared with the positive control. This experiment is only required to provide a comparison to the previous growth experiments, and therefore although these results are purely qualitative, it is clear that they match the pattern observed in the previous experiments in which the OD_{600} was measured. We can therefore be confident that the increase in growth rate and maximum growth observed when C_{60}-fullerol is present in *P.*

sp1 and *P. sp2* cultures is an accurate reflection of the amount of growth occurring in these cultures, rather than fullerol-induced chemical interference causing a false increase in the OD_{600} measurements.

The results of the CFU experiment confirm that fullerol is indeed enhancing *P. sp1* and *P. sp2* growth in some way. This enhancement is only observed in cultures which have supplementary glucose, while all other conditions are identical, therefore the first thing to consider is whether the glucose itself reacts with the fullerols to increase bacterial growth. Functionalised fullerenes are known to interact with glucose and are used in a variety of glucose biosensors (Akter et al., 2022; Gavalas & Chaniotakis, 2000; Jothi et al., 2018). However, for this interaction to result in increased culture growth, it would need to trigger a chemical change which increases the bioaccessibility of the glucose so that it is used more efficiently as a carbon source. Glucose is already a highly accessible carbon source and the limiting factor for bacterial growth is almost certainly not the cells' ability to quickly degrade glucose. Increasing glucose bioaccessibility is therefore almost certainly not the cause of the fullerol-induced growth enhancement observed. However, it is possible that fullerol somehow facilitates other cellular processes which result in increased culture growth, provided the cells do have a source of carbon- in this case, glucose.

In 2015, a study in which the effect of C_{60}-fullerol on *E. coli* was tested generated very similar results to those in this thesis (An & Jin, 2015). This study reported that exposure to C_{60}-fullerol improved the growth *E. coli* while simultaneously inhibiting all ethanol and lactate production via fermentative respiration (An & Jin, 2015). The authors explained these apparent 'paradoxical' results by suggesting that C_{60}-fullerol can improve cell growth by speeding up aerobic respiration, but that oxidative cell damage also occurs when the fullerol passes over the cell membrane. This theory reconciles the discrepancy found across various literature which claims fullerols are either beneficial for various forms of life (Gao et al., 2011) or highly toxic (Tang et al., 2007; Tegos et al., 2005) and may explain the results obtained in this thesis. If this is the case, then the presence of C_{60}-fullerol does indeed enhance the growth of *P. sp1* and *P. sp2* without being utilised as a carbon source.

5.5 Conclusions

In this chapter I present the results of a series of experiments in which the model organism *E. coli* and two environmentally relevant *Pseudomonas* species were grown aerobically with fullerenes and fullerols. Each species was grown with C_{60}, C_{70}, and their fullerols to determine how the aerobic microbial response differs from that observed with the anaerobic microorganisms in Chapter 4, and whether these differences are linked to environmental factors or innate microbial processes that vary depending on the primary metabolism. The key responses of all three species are summarised in Table 5.14.

Table 5.14: Summary of the *E. coli, P. sp1* and *P. sp2* responses to fullerenes, fullerols and UV-degraded C_{60}

	E. coli	***P. sp1***	***P. sp2***
C_{60}	Not utilised as a carbon source, not inhibitory to growth	Inhibitory to growth (decreases growth rate and culture density)	Inhibitory to growth (decreases growth rate and culture density)
C_{70}	Not utilised as a carbon source, not inhibitory to growth	Inhibitory to growth (decreases growth rate and culture density)	Inhibitory to growth (decreases growth rate and culture density)
C_{60}-fullerol	Not utilised as a carbon source, not inhibitory to growth	May increase cell density	May increase cell density
C_{70}-fullerol	Not utilised as a carbon source, not inhibitory to growth	May increase cell density	May increase cell density
UV-C_{60}	Slightly inhibitory to growth	Inhibitory to growth (decreases growth rate and culture density)	Inhibitory to growth (decreases growth rate and culture density)

Fullerenes C_{60} and C_{70} and their fullerol derivatives were found to have no effect on the growth of *E. coli* under optimal conditions, but their UV-degradation products were inhibitory. These findings contradict some previous studies, however it is evident that aggregate preparation method and media salt content are linked to fullerene toxicity. The toxicity of UV-degraded C_{60} towards *E. coli* demonstrates that despite being an accessible carbon source for the anaerobic isolate, fullerene UV-degradation products are not universally accessible to all microorganisms.

The two aerobic *Pseudomonas* species give very different results to *E. coli*, as both C_{60} and C_{70} fullerenes are inhibitory. Additionally, their fullerol derivates significantly enhance the growth of both *Pseudomonas* species, possibly by increasing the rate of aerobic respiration, thereby increasing the available energy for cell growth. The large variation in response to each fullerene and derivative shows that the microbial response to fullerenes is highly species-specific and is not linked to either the oxygen saturation of the environment or the primary respiratory mechanism utilised by the organism.

To conclude, this chapter provides evidence that the effect of fullerenes and their derivatives on aerobic microorganisms is highly variable and specific to each species. The results detailed throughout this chapter help to reconcile the conflicting and scattered literature pertaining to the effect of fullerenes on *E. coli*, as well as present new data on how environmentally relevant aerobes may react to fullerene exposure. This chapter provides additional context for the results obtained in Chapter 4 as upon conclusion of these aerobic studies, it is evident that the utilisation of fullerenes on the early Earth and similar exoplanets may be unique to certain anaerobic microorganisms which possess highly conserved metabolic pathways. Further work to elucidate the underlying metabolic processes involved in fullerene degradation will therefore provide an important link between the novel findings discussed in this chapter and the previous Chapter 4.

Chapter 6 The metabolomic response of *E. coli* and anaerobic isolate to growth with native and UV-degraded C_{60}

6.1 Introduction

The results presented in the previous two chapters of this thesis provide a comprehensive understanding of how fullerenes and fullerols affect the growth of aerobic and anaerobic microorganisms. Additionally, these experiments provide compelling evidence that fullerenes exposed to early Earth environmental conditions could have provided primitive microorganisms with an accessible carbon source. After establishing how C_{60} and its environmentally relevant UV-degradation products affect the growth of a variety of microorganisms, the next step in this research is to unravel the underlying cellular causes of these different responses. In previous chapters, the model aerobic organism *Escherichia coli* was found to grow normally with C_{60} and additional glucose. However, when C_{60} was degraded with 264 nm UV light in anoxic conditions, the resulting degradation products became toxic for *E. coli* growth. Investigating the exact mechanism of UV-C_{60} toxicity is therefore important for understanding which microbes may be susceptible to fullerene toxicity under light exposure. The anaerobic isolate, contrary to *E. coli*, was found to be capable of using UV-C_{60} as a carbon source, despite not being able to utilise native C_{60} without additional glucose. Elucidating the underlying metabolic pathways which allow this microorganism to grow on UV-C_{60} as a sole carbon source will provide a better understanding of how microbes can degrade fullerenes and how relevant this is to primitive microorganisms.

This chapter focuses on the metabolomic analysis of *E. coli* and the anaerobic isolate from Chapter 4 after growth with both native and UV-degraded C_{60}. Metabolomics is defined as the study and analysis of all metabolites in a biological sample (Clish, 2015), therefore providing a powerful experimental tool for characterising the underlying biological response to fullerene exposure. In this chapter, the anaerobic isolate is grown again with UV-C_{60} as the sole carbon source and all of the metabolites which become differentially expressed are analysed to provide a better understanding of the metabolic pathways which become activated to allow this isolate to degrade UV-C_{60}. Additionally, the metabolomic profile of *E. coli* after growth with C_{60} and UV-C_{60} is analysed to explain the inhibition observed in Chapter 5, as well as provide a comparison to the isolate in the form of a metabolic response that does not involve any active biodegradation pathways. This chapter therefore provides one of the first metabolomic-level explanations for both C_{60} biotoxicity and carbon utilisation.

6.2 Materials and Methods

The mass spectrometry and raw data processing was carried out by the EdinOmics research facility (RRID: SCR_021838) at the University of Edinburgh. I performed all culturing, metabolite extractions and analysis of clean data.

6.2.1 Culture conditions

Both *E. coli* and the anaerobic isolate were grown anaerobically with 100 mg/L C_{60} or UV-C_{60}, with and without additional glucose, before metabolite extraction. For *E. coli*, overnight cultures were made by inoculating 25 mL of anoxic M9 media (supplemented with 0.4% (w/v) glucose) with a single colony from agar. Overnight cultures were grown for 18-24 hours. For the anaerobic isolate, starting subcultures were made by inoculating 10 mL of anoxic M9 media supplemented with 0.4% (w/v) glucose and were allowed to grow for 28 days. Ten-millilitre cultures of C_{60} or UV-C_{60} in M9, both with and without supplementary 0.4% (w/v) glucose, were made in triplicate and inoculated with 100 µL of the pre-prepared starting cultures of either *E. coli* or the anaerobic isolate. All *E. coli* cultures were grown for 24 hours and all anaerobic isolate cultures were grown for 28 days. All cultures were grown at 22 °C inside an anaerobic chamber (COY Laboratory Products Inc, vinyl anaerobic chamber 2% hydrogen 98% nitrogen) without shaking.

Based on results from growth experiments in Chapters 4 and 5, I predicted that no growth would occur in the *E. coli* conditions without glucose, or in the anaerobic isolate culture with C_{60} and no glucose. These predictions were confirmed with negative OD_{600} readings for the *E. coli* cultures and microscopy for the anaerobic cultures, therefore these conditions were not tested any further.

6.2.2 Metabolite extraction

Metabolite extractions were performed after 24 hours of growth for each *E. coli* condition or after 28 days growth for the anaerobic isolate conditions. Culture density measurements were done to ensure a high number of cells were present in the cultures for metabolite extraction. The OD_{600} for all *E. coli* cultures was higher than 1 before extraction and the cell density for all anaerobic isolate cultures was greater than 10^{15} cells/mL (see Chapter 3 Materials and Methods for details the respective cell counting techniques).

The following method was performed for each triplicate of each condition and all samples were kept on ice between each step. Five hundred µL of culture was transferred to a sterile 1.5 mL Eppendorf tube and submerged in a mixture of dry ice and ethanol for three seconds while mixing vigorously. Samples were centrifuged at 1,000 g for 10 minutes, and then at 2,500 g for a further 5 minutes, all at 4 °C. The supernatant was removed, and the pellets were suspended in 250 µL of chloroform/methanol/water (in a volume ratio of 1:3:1) at 4 °C. Samples were vortexed briefly and then incubated at 4 °C on a shaking mixer at 1,200 rpm for 1 hour. After incubation, the samples were vortexed at 4 °C for 5 minutes before centrifuging at 13,000 g for 3 minutes at 4 °C. Aliquots of 200 µL of supernatant were transferred to clean Eppendorf tubes and stored at -80 °C before downstream analysis (maximum of three days storage).

6.2.3 Mass spectrometry of metabolites

Global metabolomics was performed on the extracted metabolite samples according to the method described by Pičmanová et al which uses liquid chromatography (LC) coupled to ion mobility (IM) quadrupole time-of-flight (qTOF) mass spectrometry (MS) (Pičmanová et al., 2022). The instrument used consisted of an Agilent 1290 Infinity II series UHPLC system hyphenated with an Agilent 6560 IM-qTOF with a Dual Agilent Jet Stream Electron Ionisation source. LC separation was performed on an InfinityLab Poroshell 120 HILIC-Z, 2.1 mm × 50 mm, 2.7 µm UHPLC column (Agilent Technologies 689775–924) coupled to an InfinityLab Poroshell 120 HILIC-Z, 3.0 mm × 2.7 µm UHPLC guard column (Agilent Technologies 823750–948). A 3.5-minute gradient was run using an organic buffer (acetonitrile) combined with an aqueous buffer with low pH (10 mM ammonium formate, pH

3) or high pH (10 mM ammonium acetate, pH 9) for positive and negative ionisation modes, respectively. Data acquisition was done with MassHunter Data Acquisition 10.0 software on a 1 µL sample aliquot separated on the column with a flow rate of 800 µL/min. A quality control sample was made by pooling equal volumes of each sample and was injected five times at the beginning of the experiment to condition the column, and again after every five test samples to monitor the instrument throughout data acquisition. The data were acquired in the 50 – 1,700 m/z range and an MS acquisition rate of 0.8 scans/sec.

6.2.4 Raw data processing

Raw data files were processed using the Agilent MassHunter software suite. The PNNL PreProcessor v2020.03.23 function was used to demultiplex the ion multiplex data and calibration files (the default settings for demultiplexing, moving average smoothing, saturation repair and spike removal were applied). Each data file was recalibrated for accurate mass and drift time using the AgtTofReprocessUi and the IM-MS Browser 10.0, respectively. Molecular features were extracted in Mass Profiler 10.0 with a retention time tolerance of ± 0.3 minutes, drift time tolerance of ± 1.5% and accurate mass tolerance of ± (5 ppm + 2 mDa). Features were annotated based on accurate mass and collision cross section (CCS) values using McLean CCS Compendium PCDL library (Picache et al., 2018).

6.2.5 Analysis of clean data

Multivariate statistical analysis was performed using the MetaboAnalyst 6.0 web-based platform (Lu et al., 2023). All input data was normalised by log transformation (base 10) and Pareto-scaling. The results for the total relative abundance data for each species were visualised using principal component analysis (PCA), partial least squares-discriminant analysis (PLS-DA) and variable importance in projection (VIP). Heat maps were generated using group averages of the top 50 significant features (based on ANOVA across the whole dataset with a significance level of $\alpha=0.05$). Volcano plots were generated to combine fold change (FC) and T-test (significance of $\alpha=0.05$) data between two conditions.

6.3 Results

6.3.1 *E. coli* metabolomic analysis

Principle component analysis (PCA) was performed on the cleaned metabolomic data for the *E. coli* samples (Figure 6.1). The PCA plot shows a clear separation between the UV-C_{60} and other groups, although there is a large spread and overlap between the positive control and C_{60} conditions. PLS-DA was performed in parallel to PCA as a supervised analysis in which experimental groups are considered- the results of the PLS-DA show that the three experimental groups have good separation from each other and clustering within each group (Figure 6.1). The PCA analysis shows that while the UV-C_{60} group is separated, there is a larger spread between data points and there is overlap between the C_{60} group and the positive control . The PLS-DA, however, gives good separation and clustering of each group. The PCA and PLS-DA combined show that there are clear differences between the metabolomic profile of *E. coli* with UV-C_{60}, C_{60} and the positive control which warrant further analysis, and that there is great variability between the positive control and the UV-C_{60} group than the C_{60} group.

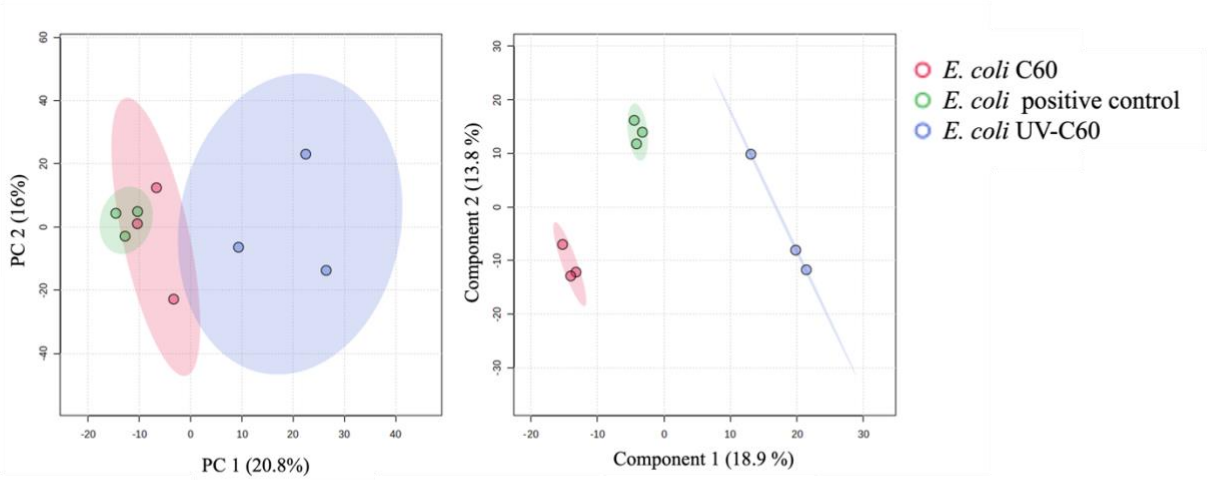

Figure 6.1: PCA (left) and PLS-DA (right) plots of *E. coli* after growth with C_{60} and glucose (red), UV-C_{60} and glucose (purple) and glucose only (green). Each point represents a single triplicate datapoint. Shaded regions around triplicate data points from the same experimental group represent the 95% confidence interval

Figure 6.2 shows a heat map consisting of group averages for the top 40 significant metabolites defined by two-way ANOVA performed over the entire dataset with a significance level of α=0.05. Hierarchical clustering splits metabolites which were detected in the dataset into groups according to their Euclidean distance and the colour scale indicates how under or overexpressed each metabolite is in each condition. In this Figure, all three experimental conditions are compared; to reiterate, the C_{60} condition is from *E. coli* grown with 100 mg/L C_{60} and glucose, the UV-C_{60} condition is from growth with 100 mg/L UV-irradiated C_{60} and glucose, and the positive control is from *E. coli* grown only with glucose. From the heat map, three visually distinct groups can be defined; the first 13 metabolites form the first group, the next 13 form the second group and the remaining 24 form the third group. In the first group, the UV-C_{60} and C_{60} conditions are similar, and all the metabolites in this class for both conditions are downregulated compared to the positive control. In the second group, the C_{60} and positive control conditions are similar, with this class of metabolites being upregulated compared to the UV-irradiated condition. In the third group, the same pattern is observed as in the second, with the C_{60} and positive control conditions being the most similar.

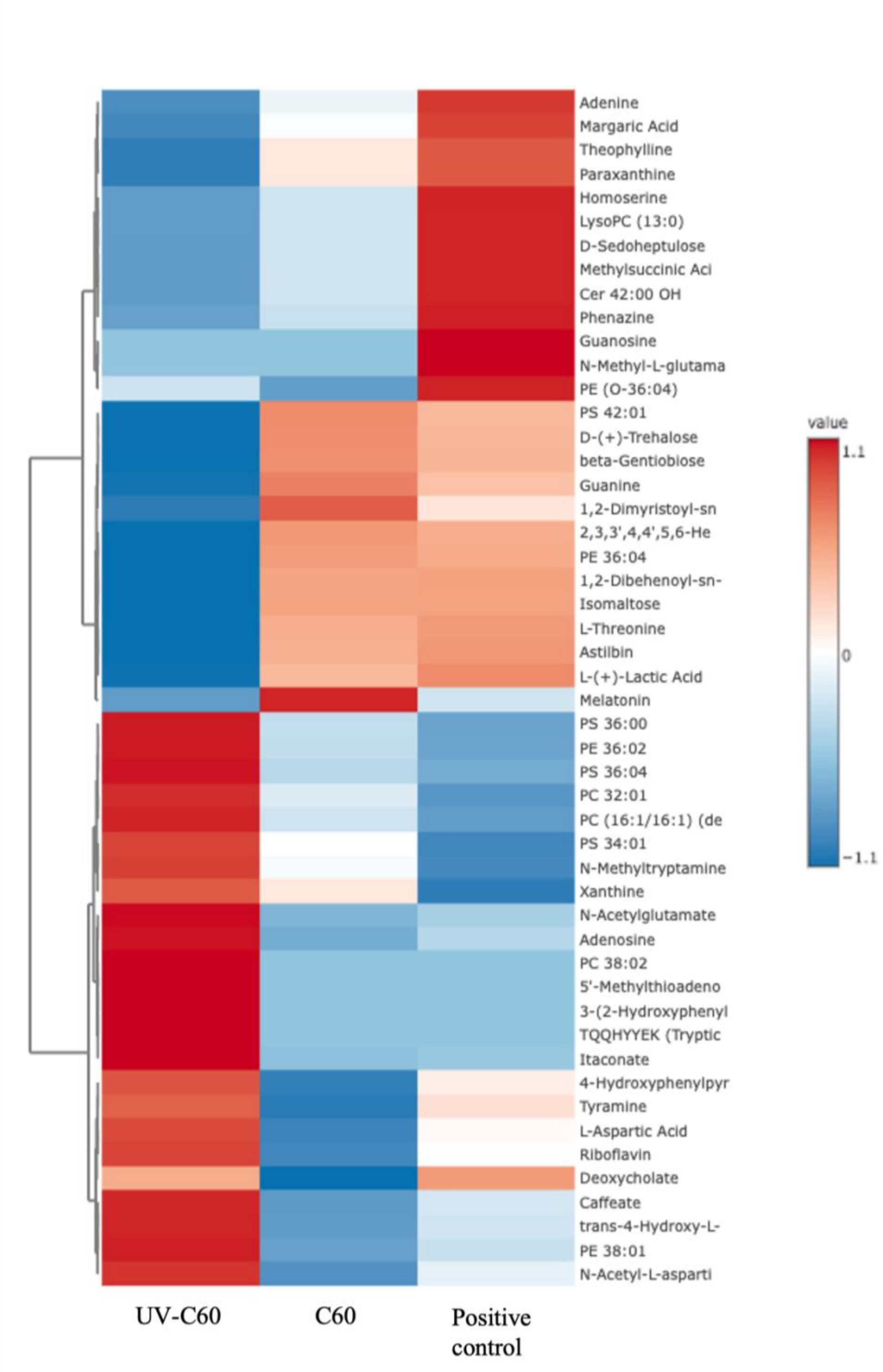

Figure 6.2: Hierarchical clustering heat map of the top 40 significant metabolites across *E. coli* conditions. Rows represent individual metabolites and columns represent the group average for each experimental condition.

Figures 6.1 and 6.2 indicate that there are clear differences between groups in the *E. coli* dataset, however for more in-depth analysis, each of the two experimental conditions, C_{60} and UV-C_{60}, are compared directly to the positive control to identify which individual metabolites are up- or down-regulated in response to each condition. For this analysis, the expression level of each metabolite in the experimental condition is compared to the positive control using a T-test with a significance level of α=0.05. Volcano plots are generated showing all the significantly up- or downregulated metabolites in the condition using the P-value and fold change (FC) of each metabolite. The volcano plot for the *E. coli* UV-C_{60} condition is given in Figure 6.3.

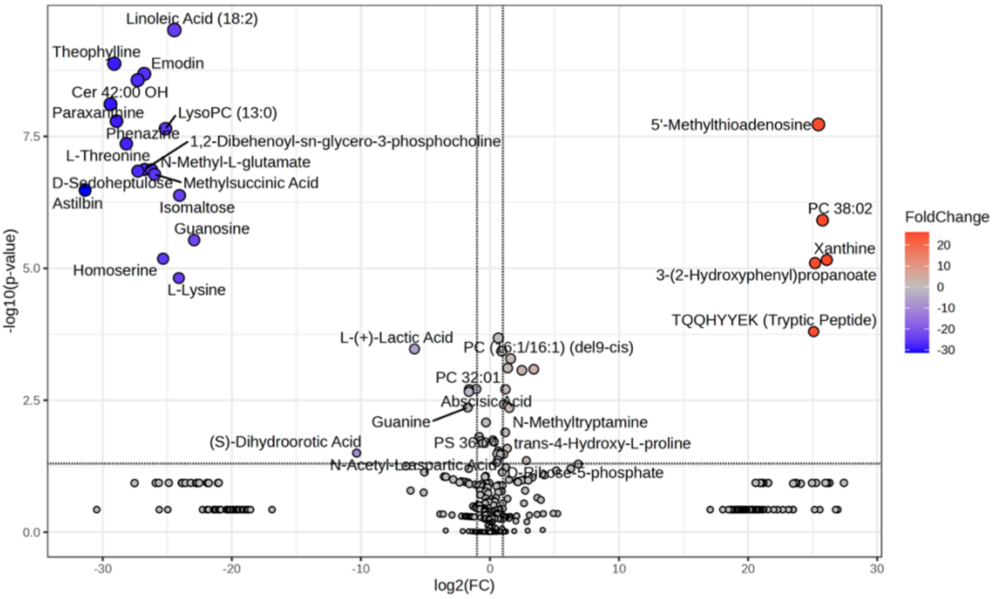

Figure 6.3: Volcano plot of significant features in the *E. coli* UV-C_{60} condition compared to the positive control. The X-axis gives the log-transformed fold change value, and the Y-axis gives the log-transformed P-value (from T-tests) for each significantly up- or down-regulated metabolite. The horizontal and vertical dotted lines represent the minimum significance level for both P-values and FC.

In the *E. coli* UV-C_{60} condition, there are 16 upregulated and 24 downregulated metabolites. Out of the 40 significantly changed metabolites, nine are classed as membrane phospholipids or other membrane-associated components, and 15 are amino acids or amino acid derivatives, nine of which are highly downregulated. Additional metabolites of interest in this dataset include 5-methylthioadenosine (FC=45,623,000 and P-value=1.9×10^{-8}), xanthine (FC=71,790,000 and P-value=7×10^{-6}), dihydroorotic acid (FC=0.000777 and P-value=0.03) and ribose-5-phosphate (FC=7.0735 and P-value=0.044). The significant metabolites expressed in the UV-C_{60} condition, their P-values compared with expression levels in the positive control, description and functional class are summarised and ranked by lowest-highest fold change in Table 6.1.

Table 6.1: Significant metabolites expressed *by E. coli* after growth with UV-C_{60} ordered by lowest-highest fold change compared to expression in the positive control.

Metabolite	**Fold change**	**P-value**	**Description**	**Functional class**
Astilbin	3.6039E-10	3.3273E-07	Flavonoid	Other
1,2-Dibehenoyl-sn-glycero-3-phosphocholine	8.8293E-09	1.339E-07	Glycerophosphocholine phospholipid	Membrane phospholipid
Emodin	8.6188E-09	2.0752E-09	A pigment compound (quinone)	Other
D-Sedoheptulose	6.156E-09	1.4423E-07	Monosaccharide	Other
Cer 42:00 OH	6.0438E-09	2.7244E-09	Ceramide	Membrane associated component
L-Threonine	3.2936E-09	4.3622E-08	Amino acid precursor	Amino acid
Phenazine	1.9487E-09	1.628E-08	Orangic compound	Other
Theophylline	1.7273E-09	1.3255E-09	Derivative of xanthine	Metabolite of interest
Paraxanthine	1.4101E-09	7.76E-09	Derivative of xanthine	Metabolite of interest
Isomaltose	5.741E-08	4.1655E-07	Dissaccharide	Other
L-Lysine	5.539E-08	1.5289E-05	Amino acid	Amino acid
Linoleic Acid (18:2)	4.3515E-08	3.0578E-10	Omega-6 fatty acid	Other
LysoPC (13:0)	2.7043E-08	2.2682E-08	Lysophospholipid	Membrane phospholipid
Homoserine	2.3791E-08	6.5804E-06	Amino acid	Amino acid
Methylsuccinic Acid	1.5075E-08	1.657E-07	Carboxylic acid	Other
N-Methyl-L-glutamate	1.279E-08	1.3631E-07	Amino acid derivative	Amino acid (derivative)
Guanosine	1.2595E-07	2.9193E-06	Amino acid	Amino acid
PE 36:04	0.47531	0.0019421	Phosphatidylethanolamine	Membrane phospholipid
beta-Gentiobiose	0.32538	0.0019608	Dissacharide	Other
D-(+)-Trehalose	0.32317	0.001993	Disscharide	Other
2,3,3',4,4',5,6-Heptabromodiphenyl ether	0.32183	0.0021853	Aromatic organobromine ether	Other
Guanine	0.30262	0.0043308	Purine base	Metabolite of interest
L-(+)-Lactic Acid	0.017372	0.0003378	End product of carbohydrate fermentation	Other

(S)-Dihydroorotic Acid	0.000777	0.031699	An intermediate in pyridine breakdown	Metabolite of interest
N-Acetyl-L-aspartic Acid	2.0881	0.033379	Amino acid	Amino acid
Abscisic Acid	2.1097	0.0037693	Organic compound	Other
PS 36:04	2.2756	0.012874	Phosphatidylserine	Membrane phospholipid
PS 36:00	2.3069	0.0019677	Phosphatidylserine	Membrane phospholipid
trans-4-Hydroxy-L-proline	2.5262	0.025806	Amino acid	Amino acid
PC 32:01	2.5853	0.0007764	Phosphatidylcholine	Membrane phospholipid
N-Methyltryptamine	2.8271	0.0044255	Amino acid	Amino acid
PC (16:1/16:1) (del9-cis)	3.0282	0.0005148	Phosphatidylcholine	Membrane phospholipid
Adenosine	5.544	0.0008559	Amino acid	Amino acid
D-Ribose-5-phosphate	7.0735	0.044015	Intermediate nhe pentose phosphate pathway	Metabolite of interest
Itaconate	10.515	0.0008175	Fatty acid	Other
TQQHYYEK (Tryptic Peptide)	35392000	0.0001578	Product of trypsin digestion	Other
3-(2-Hydroxyphenyl)propanoate	38120000	7.9494E-06	Carboxylic acid	Other
5'-Methylthioadenosine	45623000	1.8841E-08	Derivative of adenosine	Metabolite of interest
PC 38:02	57131000	1.2263E-06	Phosphatidylcholine	Membrane phospholipid
Xanthine	71790000	6.9298E-06	A purine degradation product- created from degradation of guanine	Metabolite of interest

The same analysis described above was performed for the *E. coli* C_{60} condition, where metabolites with statistically significant fold changes were identified by using T-tests to compare to the positive control. These are represented in a volcano plot in Figure 6.4.

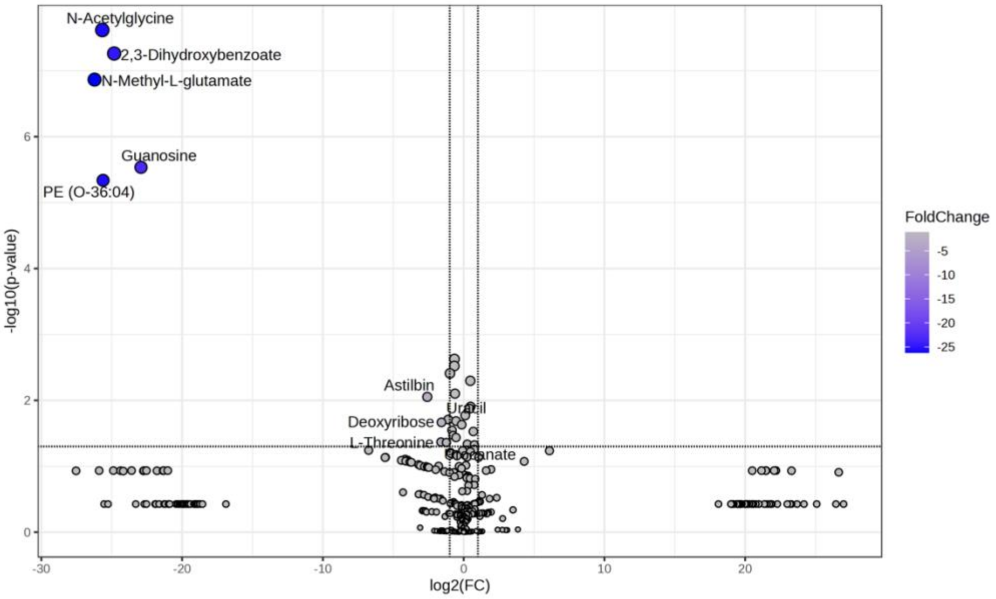

Figure 6.4: Volcano plot of significant features in the *E. coli* C_{60} condition compared to the positive control. The X-axis gives the log-transformed fold change value, and the Y-axis gives the log-transformed P-value (from T-tests) for each significantly up- or down-regulated metabolite. The horizontal and vertical dotted lines represent the minimum significance level for both P-values and FC.

The *E. coli* C_{60} condition has no metabolites which are significantly upregulated compared to the positive control. However, there are 10 significantly downregulated metabolites, including five amino acids or amino acid derivatives, two DNA or RNA componants and one membrane phospholipid. The significant metabolites expressed in the *E. coli* C_{60} condition, their P-values compared with expression levels in the positive control, description and functional class are summarised and ranked by lowest-highest fold change in Table 6.2.

Table 6.2: Significant metabolites expressed by *E. coli* after growth with C_{60} ordered by lowest-highest fold change compared to expression in the positive control.

Metabolite	**Fold change**	**P-value**	**Description**	**Functional class**
2,3-Dihydroxybenzoate	3.3576E-08	5.4782E-08	Organic compound	Other
PE (O-36:04)	1.9473E-08	4.5991E-06	Phosphatidylethanolamine	Membrane phospholipid
N-Acetylglycine	1.8724E-08	2.414E-08	Amino acid derivative	Amino acid
N-Methyl-L-glutamate	1.279E-08	1.3631E-07	Amino acid derivative	Amino acid
Guanosine	1.2595E-07	2.9193E-06	Amino acid	Amino acid
Astilbin	0.16642	0.0088594	Flavonoid	Other

L-Threonine	0.32588	0.042803	Amino acid precursor	Amino acid
Deoxyribose	0.33455	0.021565	DNA backbone	DNA/RNA component
Urocanate	0.42803	0.043527	Amino acid degradation intermediate	Amino acid
Uracil	0.46655	0.019553	RNA nucleotide	DNA/RNA component

6.3.2 Anaerobic isolate metabolomic analysis

The same analytical process was performed on the anaerobic isolate data as for the *E. coli* data. Both PCA and PLS-DA were performed across the entire dataset (Figure 6.5). PCA plots of the first and second principal components show good clustering within each group. There is overlap between the positive control, C_{60} and UV-C_{60}-glucose groups, while the UV-C_{60} group is tightly clustered and completely separated from the other groups and the positive control. PLS-DA plotting of components 1 and 2 shows good separation between each of the three groups and the positive control with no overlap.

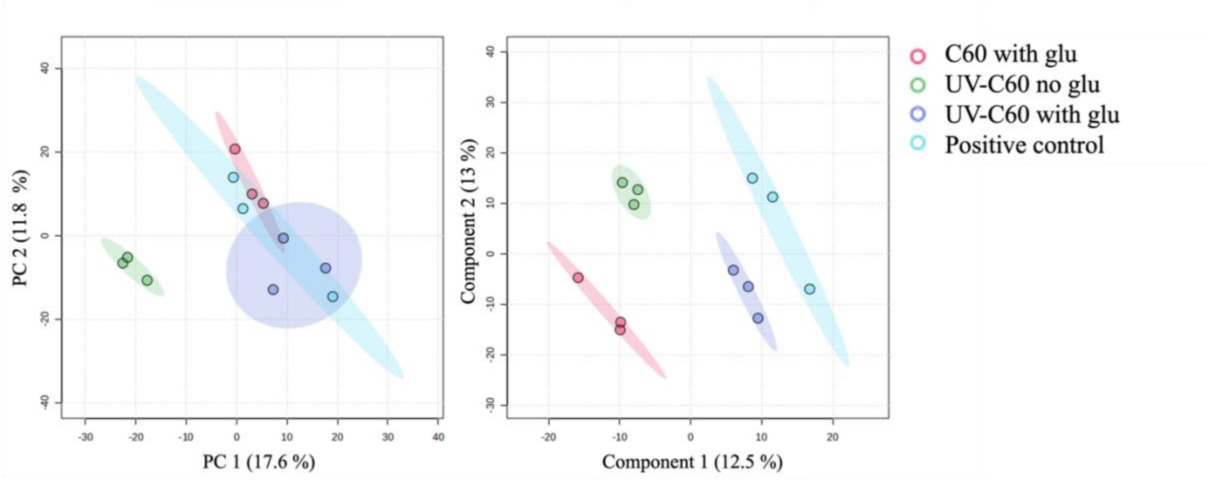

Figure 6.5: PCA (left) and PLS-DA (right) plots of anaerobic isolate after growth with C_{60} and glucose (red), UV-C_{60} with glucose (purple), UV-C_{60} without glucose (green) and glucose only (blue). Each point represents a single triplicate datapoint. Shaded regions around triplicate data points from the same experimental group represent the 95% confidence interval

Figure 6.6 shows a heat map of the top 50 significant metabolites across the anaerobic isolate dataset. In this heat map, the group consisting of the first 14 metabolites has no obvious visual trend between conditions, however, the remaining 36 metabolites constituting the second group are underexpressed in the UV-C_{60} group compared to the other three groups, in which there are similar expression levels. This further indicates that the UV-C_{60} group is more different to the positive control than the C_{60} and UV-C_{60}-glucose groups.

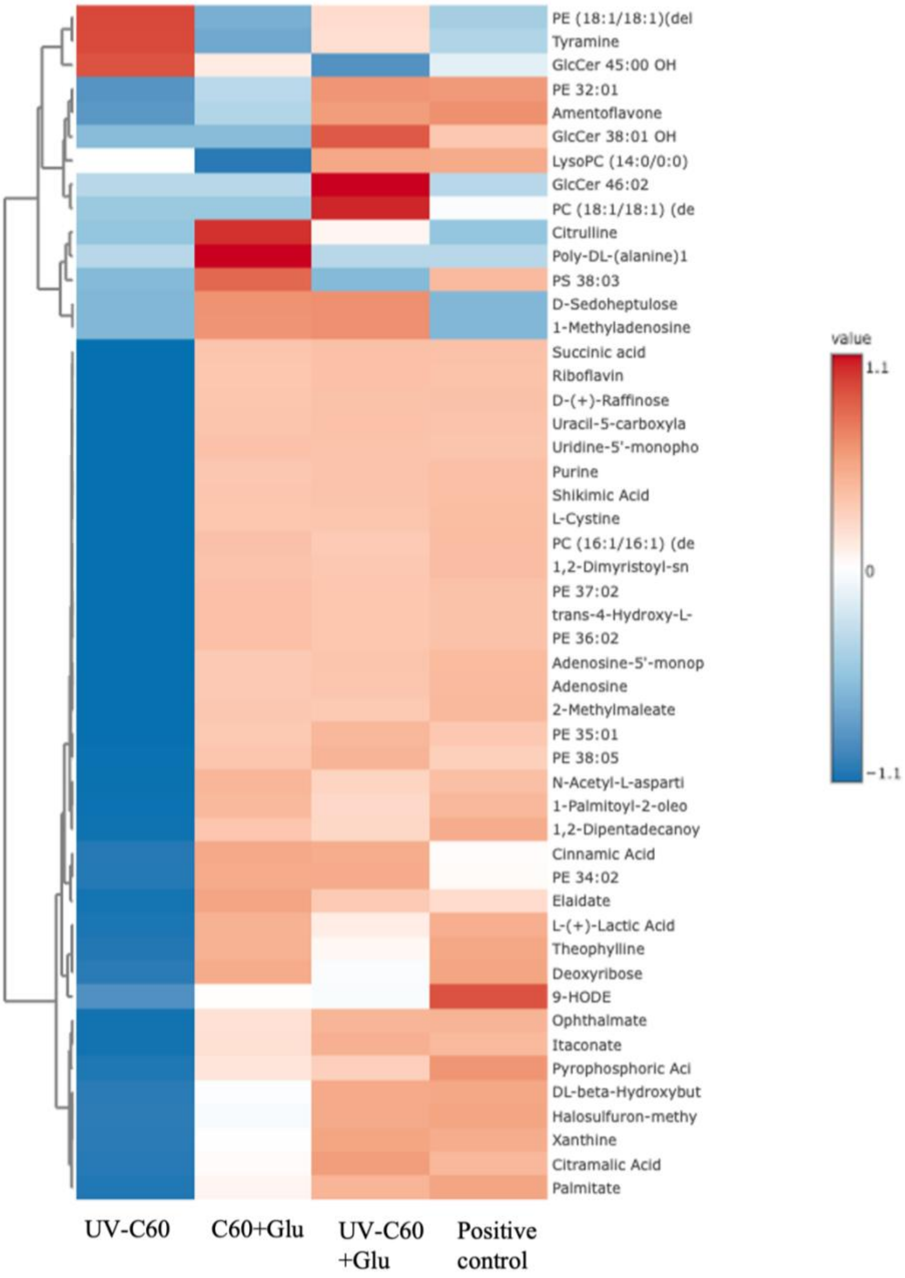

Figure 6.6: Hierarchical clustering heat map of the top 50 significant metabolites across anaerobic isolate conditions. Rows represent individual metabolites and columns represent the group average for each experimental condition.

The main condition of interest in the anaerobic isolate dataset is the UV-C_{60}, as this is the condition in which the anaerobic isolate was grown with UV-C_{60} as a sole carbon source. Figure 6.7 represents the significantly up- or down-regulated metabolites in the UV-C_{60} conditions compared to the positive control in a volcano plot.

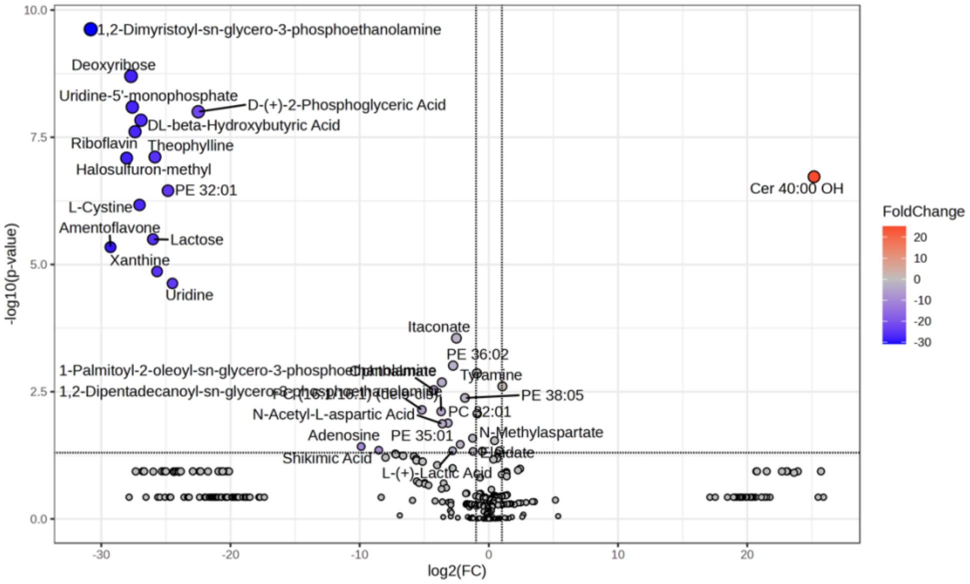

Figure 6.7: Volcano plot of significant features in the anaerobic isolate UV-$C_{60\_}$ condition compared to the positive control. The X-axis gives the log-transformed fold change value, and the Y-axis gives the log-transformed P-value (from T-tests) for each significantly up- or down-regulated metabolite. The horizontal and vertical dotted lines represent the minimum significance level for both P-values and FC.

In this condition, there are a total of 31 metabolites with statistically significant fold changes, 29 of which are downregulated and two of which are upregulated compared to the positive control. Only 1,2-Dimyristoyl-sn-glycero-3-phosphoethanolamine is present in the significant metabolite list of either the C_{60} or UV-C_{60}-glucose conditions with the same fold change direction. Out of the 31 significant metabolites, eight are amino acids or amino acids derivatives, all of which except tyramine are downregulated. There are also eight significantly downregulated membrane phospholipids or other membrane-associated components and one upregulated membrane ceramide. Of particular interest in this condition is also the downregulation of uridine, uridine-5'-monophosphate and deoxyribose. The significant metabolites present in the anaerobic isolate UV-C_{60} condition, their P-values and functional class are ranked by increasing fold change and summarised in Table 6.3.

Table 6.3: Significant metabolites expressed by anaerobic isolate after growth with UV-C_{60} ordered by lowest-highest fold change compared to expression in the positive control.

Metabolite	**Fold change**	**P-value**	**Description**	**Functional class**
1,2-Dimyristoyl-sn-glycero-3-phosphoethanolamine	5.2857E-10	2.3839E-10	Phosphoethanolamine	Membrane phospholipid
DL-beta-Hydroxybutyric Acid	7.8449E-09	1.4671E-08	Fatty acid	Other
L-Cystine	7.2536E-09	6.7618E-07	Amino acid	Amino acid
Riboflavin	5.6969E-09	2.4617E-08	Protein cofactor	Other
Uridine-5'-monophosphate	4.9281E-09	8.0544E-09	End product of purine/pyrimidine synthesis	Metabolite of interest
Deoxyribose	4.5935E-09	1.9937E-09	DNA backbone	DNA/RNA component
Halosulfuron-methyl	3.6259E-09	8.0984E-08	Organic compound	Other
Amentoflavone	1.5262E-09	4.5616E-06	Flavonoid	Other
Uridine	4.2384E-08	2.3573E-05	Pyrimidine synthesis intermediate	Purine/pyrimidine component
PE 32:01	3.3342E-08	3.5469E-07	Phosphatidylethanolamine	Membrane phospholipid
Xanthine	1.8571E-08	1.372E-05	Purine degradation product	Purine/pyrimidine component
Theophylline	1.6579E-08	7.7233E-08	Xanthine derivative	Purine/pyrimidine component
Lactose	1.4903E-08	3.1959E-06	Disaccharide	Other
D-(+)-2-Phosphoglyceric Acid	1.6915E-07	9.9827E-09	Glycolysis substrate	Other
Adenosine	0.0010595	0.037799	Amino acid	Amino acid
Shikimic Acid	0.0027204	0.044597	Amino acid precursor	Amino acid
1,2-Dipentadecanoyl-sn-glycero-3-phosphoethanolamine	0.027509	0.0071931	phosphoethanolamine	Membrane phospholipid
1-Palmitoyl-2-oleoyl-sn-glycero-3-phosphoethanolamine	0.051984	0.0029422	phosphoethanolamine	Membrane phospholipid
PC (16:1/16:1) (del9-cis)	0.077402	0.0077377	Phosphatidylcholine	Membrane phospholipid

Ophthalmate	0.08046	0.002071	Organic compound	Other
N-Acetyl-L-aspartic Acid	0.082518	0.013495	Amino acid derivative	Amino acid
PC 32:01	0.11126	0.013072	Phosphatidylcholine	Membrane phospholipid
L-(+)-Lactic Acid	0.14321	0.045775	End product of carbohydrate fermentation	Other
PE 36:02	0.14676	0.000971	Phosphatidylethanolamine	Membrane phospholipid
Itaconate	0.1756	0.0002811	Fatty acid	Other
PE 35:01	0.21515	0.034322	Phosphatidylethanolamine	Membrane phospholipid
PE 38:05	0.27765	0.0041923	Phosphatidylethanolamine	Membrane phospholipid
N-Methylaspartate	0.41888	0.025885	Amino acid derivative	Amino acid
Elaidate	0.42891	0.047173	Fatty acid	Other
Tyramine	2.067	0.0024777	Amino acid	Amino acid
Cer 40:00 OH	37737000	1.8883E-07	Ceramide	Membrane component

6.4 Discussion

In the previous experimental chapters, there was a large focus on how fullerenes and their derivatives alter the growth characteristics of various microorganisms. In this chapter, a metabolomics approach was used to determine how exposure to the most relevant of these conditions changes the metabolic profile of both *E. coli* and the anaerobic isolate to narrow down the physiological effect fullerenes have on these organisms.

6.4.1 nC_{60} induces minor metabolomic changes to *E. coli*

In Chapter 5, I showed that fullerene C_{60} had no discernible effect on the growth of *E. coli*, but that UV-C_{60} was slightly inhibitory, reducing both cell number and growth rate. The results of the metabolomics analysis of *E. coli* grown with C_{60} and UV-C_{60} do seem to reflect this; while the UV-C_{60} condition generated a total of 40 significantly expressed metabolites, indicating a significant effect, there are only very minor differences between the C_{60} condition and the positive control. Deoxyribose, the sugar backbone of DNA, and uracil, an RNA nucleotide, are both significantly downregulated in the C_{60} condition. It is known that a common general stress response in bacteria involves a decrease in nucleotide biosynthesis

(Gasch et al., 2000), therefore a reduction in uracil could indicate that the *E. coli* in this condition are experiencing cellular stress. Similarly, a common stress response may involve a notable increase in protein synthesis to replace damaged cellular components, resulting in a decrease in free deoxyribose and uracil as these are used up in transcriptional processes (Fasnacht & Polacek, 2021; Foster, 2005). In Chapter 5 I found nC_{60} to have no effect on the growth of *E. coli*, as neither the growth rate nor maximum cell density was affected. This suggests that although the metabolomics results from this chapter show that *E. coli* experiences cellular stress in response to nC_{60} exposure, this stress response is not sufficient to cause a reduction in growth. This is a very interesting result as it may imply that although nC_{60} imposes some sort of energy demand on the cells, it doesn't ultimately slow down the growth rate.

6.4.2 UV-C_{60} exposure alters *E. coli* phospholipid expression

In the UV-C_{60} condition, there is a total of 40 differentially expressed metabolites, which reflects the larger difference we expect as a result of the UV-C_{60} inhibition. Ten of the 40 metabolites with significant fold changes in the UV-C_{60} condition are membrane phospholipids or other membrane components. Several previous studies assessing the physiological impact of fullerenes on various bacterial species have shown that all of the species studied changed their membrane phospholipid composition in response to fullerene exposure (Fang et al., 2007; Riding et al., 2012). Given this, it is not surprising that 25% of the total significantly altered *E. coli* metabolites in this condition are phospholipids or similar. The exact manner of the compositional changes observed in previous studies varies depending on the species studied, with *P. putida, B. subtilus* and *P. fluorescens* all increasing different classes of phospholipids (Fang et al., 2007; Riding et al., 2012). For example, it was found that *P. putida* had decreased levels of unsaturated fatty acids and increased expression of cyclopropane fatty acids in response to nC_{60} exposure, while *B. subtilis* demonstrated a different response by increasing the expression of iso- and anteiso-branched fatty acids (Fang et al., 2007). In this study, the *E. coli* grown with UV-C_{60} under- or over-expressed a total of eight phospholipids compared to the positive control. The three upregulated phospholipids were a phosphorylethanolamine and two phosphatidylcholines, one with a carboxylic acid functional group (behenic acid) and one which is classified as a lysophospholipid due to its polar head. The five upregulated phospholipids consisted of two phosphatidylserines and three phosphatidylcholines. Phosphatidylcholine therefore appears in both the up- and down-regulated phospholipid groups, while all of the phosphatidylserines in the dataset are downregulated and only phosphorylethanolamine is upregulated. There does not appear to be a clear differentiation across the two groups regarding polarity and charge, as both the down- and upregulated groups contain zwitterionic and negatively charged phospholipids (van Hoogevest et al., 2021). In other words, there is no obvious trend in the type of phospholipid that is altered in each condition. Therefore, although it is clear that UV-C_{60} exposure does significantly alter membrane phospholipid expression in *E. coli*, further exploration into the phenomenon is needed to understand the exact biological reasons for this observation.

6.4.3 UV-C_{60} affects amino acid expression in *E. coli*

A second noticeable trend in the *E. coli* UV-C_{60} condition is that out of the 40 significant metabolites, 15 are amino acids or amino acid derivatives. Interestingly, it is often observed that bacteria undergoing a stress response will accumulate free amino acids (Jozefczuk et al., 2010), probably because when a cell is under stress it starts to degrade proteins either as a mechanism of eliminating damaged proteins, or to increase the availability of amino acids to synthesise new survival proteins (Mandelstam, 1963; Willetts, 1967). However, in the *E. coli* dataset, only six out of the 15 significant amino acids are upregulated, with the remaining nine all being under-expressed, which is contrary to the hypothesis that ubiquitously over-expressed amino acids are a sign of cellular stress. It is more likely in this case that the highly complex metabolic pathways involving various amino acids and intermediates are negatively impacted by the UV-C_{60} inhibition which is causing each intermediate to be either over or underproduced in a pathway-specific manner. Given that the *E. coli* in this condition are experiencing stress as evidenced by the growth inhibition observed in Chapter 5, these patterns of amino acid changes may reflect metabolic rearrangements in amino acid synthesis resulting from exposure to UV-C_{60}. The growth data combined with the metabolomic analysis therefore further indicates that UV-C_{60} exposure induces a stress response in *E. coli*.

6.4.4 *E. coli* experiences oxidative stress in response to UV-C_{60}

Methionine is an essential amino acid which is synthesised *de novo* by most bacteria (Ravanel et al., 1998). There are two major pathways involving methionine, the methionine synthesis and the methionine salvage pathways, which play a central role in bacterial metabolism (Albers, 2009; Ravanel et al., 1998). In the synthesis pathway, methionine is generated from inorganic sulphate and cysteine (Ravanel et al., 1998), whereas in the methionine salvage pathway, methionine is broken down into 5'-methylthioadenosine (MTA) as a way of recycling cellular sulphur (Albers, 2009). Interestingly, previous studies have found methionine levels to significantly decrease in *E. coli* after exposure to oxidative stress, almost certainly because methionine itself is extremely sensitive to oxidation (Jozefczuk et al., 2010). Although methionine isn't identified in the *E. coli* UV-C_{60} dataset, MTA is both present and highly upregulated compared to the expression levels in the positive control, which suggests the methionine salvage pathway is being overexpressed in response to UV-C_{60} exposure. Additionally, homoserine, which is a precursor in methionine synthesis, is significantly downregulated in the dataset, further supporting the hypothesis that methionine synthesis is being suppressed, resulting in increased activation of the methionine salvage pathway in response to oxidative stress exerted on the *E. coli* by the UV-C_{60}.

There is some literature available detailing the metabolomic response of *E. coli* to various external stressors, such as oxidative stress, but it is limited as most studies investigating markers of cellular stress do so using transcriptomic or proteomic profiles and do not look at metabolomic factors. However, in 2010, Jozefczuk et al were able to identify several significantly under- or over-expressed metabolites in *E. coli* after exposure to oxidative stress, the majority of which were involved in glycolysis, the pentose phosphate pathway or the TCA cycle. Ribose-5-phosphate is an intermediate in the pentose phosphate pathway and a precursor in nucleotide biosynthesis and is one of the identified metabolites involved in the *E. coli* response to oxidative stress (Jozefczuk et al., 2010). In my experiments, Ribose-5-phosphate is significantly upregulated in the *E. coli* after exposure to UV-C_{60}. However, Jozefczuk et al found this metabolite to be downregulated in response to oxidative stress, which is the opposite response observed here. A central intermediate in nucleotide biosynthesis is 5-phosphoribosyl-a-1-pyrophosphate (PRPP), which is generated directly from ribose-5-phosphate (Kilstrup et al., 2005). PRPP, however, as well as being important for nucleotide synthesis, is also a central component of a parallel nucleotide salvage pathway, which functions to ‘rescue’ damaged nucleobases and nucleosides (Kilstrup et al., 2005). It is therefore possible that the increase in ribose-5-phosphate in the *E. coli* exposure to UV-C_{60} is an indirect indicator of the nucleotide salvage pathway which is activated in response to insufficient levels of nucleotides as a result of cellular stress damage. Although Jozefczuk et al still observed a decrease rather than an increase, this is, to the best of my knowledge, the only study which has characterised the metabolomic response of *E. coli* to oxidative stress and therefore until more studies are carried out, we cannot be sure that this response is consistent and ubiquitous.

Ribose-5-phosphate is the only significant metabolite in the *E. coli* UV-C_{60} dataset which was also identified as a stress indicator in the Jozefczuk et al study. However, the lack of additional oxidative stress indicators may be explained by the volatile nature of many of these metabolites; in addition to identifying them, Jozefczuk et al showed that the metabolites expressed in response to oxidative stress are highly transient and that prolonged stress exposure of 24 hours lead to them being almost completely eliminated (Jozefczuk et al., 2010). Since the *E. coli* in this chapter were incubated with UV-C_{60} for exactly 24 hours before metabolite extraction, it is possible that the cells did experience a more significant stress response that was undetectable by the time the extractions were done.

A decrease in nucleotide biosynthesis is a prominent generic stress response observed in many different types of bacterial species (Gasch et al., 2000). In the *E. coli* UV-C_{60} condition, xanthine was one of the significantly upregulated metabolites identified. Xanthine is a key byproduct of purine degradation in bacteria (Brychkova et al., 2008; Marro et al., 1997), so its overexpression in this condition suggests the *E. coli* exposed to UV-C_{60} are undergoing increased purine degradation. Similarly, dihydroorotic acid, which is an intermediate in pyrimidine synthesis (Peters et al., 1990) is significantly downregulated, indicating that pyrimidine synthesis is being suppressed. Both the upregulation of xanthine and the downregulation of dihydroorotic acid indicate that there is indeed a notable decrease in nucleotide biosynthesis when *E. coli* is exposed to UV-C_{60}. This result further indicates that *E. coli* are undergoing a stress response induced by exposure to UV-C_{60}.

6.4.5 Summary of the *E. coli* metabolomic response to fullerenes

Aqueous nC_{60} does not have a large effect on the metabolic profile of *E. coli,* provided glucose is available as a carbon source. As previously discussed, there is evidence that a subcritical stress response is triggered by nC_{60} exposure, but this is not enough to significantly impact the overall growth of *E. coli*, as demonstrated in Chapter 5. When *E. coli* is grown with UV-C_{60}, a much bigger metabolomic difference is observed in which multiple membrane components and amino acids are under or over-expressed. No specific stress response metabolites are detected; however, this is likely due to the transient nature of these metabolites and not necessarily evidence that no stress response occurred. The overexpression of MTA in the UV-C_{60} condition indicates that the methionine salvage pathway is activated by exposure to UV-C_{60}, which is likely due to the methionine synthesis pathway being suppressed due to oxidative stress. Although the metabolic profile of *E. coli* exposed to UV-C_{60} alone is not conclusive evidence of oxidative stress, this data combined with the growth data in Chapter 5 does provide a convincing explanation for the inhibition of *E. coli* by UV-irradiated C_{60}.

6.4.6 Anaerobic isolate alters membrane properties in response to UV-C_{60}

In Chapter 4, I showed that the anaerobic isolate obtained from a pre-exposed mixed community is capable of utilising UV-degraded C_{60} as a carbon source. When grown only on UV-C_{60} the metabolic profile of this isolate is distinctly different from the positive control, as well as the other conditions in which glucose is also available. This is likely because glucose is a more preferential carbon source and therefore when it is available, the isolate growth is essentially identical to the positive control, which also grows on glucose as the carbon source. Therefore, we see very few metabolic changes in the C_{60} and UV-C_{60} conditions with glucose, but a large and distinct change once the glucose is removed and the only carbon source is UV-C_{60}.

When the anaerobic isolate is grown with UV-C_{60} as a sole carbon source, there are 31 metabolites which become significantly under- or overexpressed compared to when it is grown on glucose. A major trend in this group of significant metabolites is the large proportion of phospholipids that are differentially expressed, as nine out of the 31 metabolites are classed as membrane-associated components, eight of which are phospholipids and one of which is a ceramide. Interestingly, all of the phospholipids identified are downregulated, while the ceramide is highly upregulated. The alteration of membrane phospholipid composition has been observed previously in *E. coli* exposed to nC_{60} (Fang et al., 2007; Riding et al., 2012), as well as being observed in this study in the *E. coli* cultures, so it is not unexpected that many phospholipids would also be altered in the anaerobic isolate. All bacteria can alter their membrane phospholipid composition in order to regulate fluidity in response to external factors and stress (Rowlett et al., 2017; Zhang & Rock, 2008), so the under-expression of certain phospholipids may indicate exposure to UV-C_{60} is causing some cellular stress.

It has been previously observed that the concentration of ceramides in bacterial outer membranes increases in response to stress (Zou & Johnston, 2010). It has also been suggested that increased ceramide concentration causes a cellular membrane to become more permeable to large compounds and increases its rigidity (Alonso & Goñi, 2018). Significant overexpression of the ceramide in the anaerobic isolate after growth with UV-C_{60} may therefore indicate that the isolate is adapting to utilising UV-C_{60} by increasing the membrane permeability to larger carbon fragments- however the increase in permeability may also be a coincidence arising from an increase in membrane rigidity as a response to stress.

6.4.7 Growth on UV-C_{60} suppresses nucleotide biosynthesis and energy generation in anaerobic isolate

Growth with UV-C_{60} as the sole carbon source results in the downregulation of several DNA and RNA-related metabolites in the anaerobic isolate. One of the most common and prominent stress responses observed in many species of bacteria is a reduction in nucleotide biosynthesis (Gasch et al., 2000), therefore the under-expression of these DNA and RNA components may immediately indicate the cells in this condition are experiencing stress. Many bacteria produce both purines and pyrimidines *de novo* from free nucleotides and produce uridine-5'-monophosphate (UMP) as an end product of this synthesis pathway

(Kilstrup et al., 2005). In the anaerobic isolate grown with UV-C_{60} as a carbon source, UMP is significantly downregulated compared to growth on glucose. This suggests that the entire pyrimidine and purine synthesis pathway is being suppressed, which is further supported by the downregulation of several other purines and pyrimidines, as well as deoxyribose, in the same condition. It is clear from this data that there is a decrease in nucleotide biosynthesis when the anaerobic isolate is grown on UV-C_{60}, and although no reduction in growth was observed in Chapter 4, this is likely a result of the cells experiencing stress. Whether this stress is a direct result of UV-C_{60} exposure, or due to being grown on a less-accessible carbon source, however, is not clear.

In addition to the downregulation of nucleotide synthesis components, five out of the 31 significant metabolites in the anaerobic isolate UV-C_{60} condition are associated with cellular replication. In the Jozefczuk et al study discussed previously, it was found that different types of cellular stress consistently resulted in a decrease in metabolites involved in glycolysis, the pentose phosphate pathway and the TCA cycle (Jozefczuk et al., 2010). In the anaerobic isolate, 2-phosphoglyceric acid, a key product in glycolysis, is significantly downregulated after UV-C_{60} exposure. Additional central energy-generating metabolites such as nicotinate, the precursor for NAD^+ and $NADP^+$, ADP and AMP, which are precursors for ATP, are also significantly downregulated (Cancino-Diaz et al., 2023). The under-expression of these metabolites is further evidence that the anaerobic isolate grown with UV-C_{60} experiences cellular stress and suggests that although the UV-C_{60} is accessible as a carbon source, it simultaneously exerts some form of stress onto the isolate.

Interestingly, this is not the first time C_{60} has been observed to simultaneously be used as a carbon source by, and also toxic to a microorganism. The 2020 Wang et al study identified the aerobic species *Labrys sp.* WJW to be capable of growing on C_{60} as a sole carbon source (Wang et al., 2020). In this study it was found that within the biofilm, the cells growing on the surface of the C_{60} aggregates had reduced viability, probably because these cells had direct contact with the C_{60} surface. Although in this chapter it is the UV-degraded C_{60} that is used as a carbon source while eliciting a stress response, rather than pristine C_{60}, the Wang et al study is further evidence that the 'toxic carbon source' observation is a recurring phenomenon.

6.4.8 UV-C_{60} does not induce oxidative stress in anaerobic isolate

In the MTA recycling pathway discussed previously, the amino acid cysteine is generated from homocysteine, which is synthesised from methionine; this is the only known pathway for the synthesis of cysteine (Werge et al., 2021). In the anaerobic isolate grown with UV-C_{60}, cysteine is significantly downregulated. Spermine, which is a key intermediate in polyamine synthesis and therefore also in the MTA recycling pathway (Albers, 2009), is also significantly downregulated. The downregulation of these two key metabolites indicates the MTA recycling pathway is being under-expressed in the anaerobic isolate when it is grown with UV-C_{60} as a carbon source. In the *E. coli* condition, the MTA synthesis pathway was downregulated while the MTA recycling pathway was upregulated, which indicated the bacteria were experiencing oxidative stress. In the anaerobic isolate, however, there is no evidence that the MTA synthesis pathway is being suppressed, and the MTA recycling pathway is downregulated. Additionally, none of the oxidative stress-specific metabolites identified by Jozefczuk et al (2012) are present. Therefore, while the anaerobic isolate may show other signs of stress, there is no evidence of a specific oxidative stress response.

6.4.9 Evidence for biodegradation pathway activation in the anaerobic isolate grown with UV-C_{60}

The results discussed so far suggest that the anaerobic isolate, while able to grow on UV-C_{60} as a carbon source, also experiences some form of cellular stress, however, there is no evidence of this stress response corresponding to oxidative stress as there is with *E. coli* grown under the same conditions. Since UV-C_{60} is likely not as biologically accessible to the anaerobic isolate as glucose, the stress responses observed may be simply due to a low level of carbon starvation which is enough to trigger a metabolomic stress response but not sufficient to significantly reduce growth of the cultures. A 2006 study which sought to characterise the metabolomic response to nutrient starvation in bacteria previously identified fructose bisphosphate as a key metabolite which becomes downregulated in response to glucose starvation (Brauer et al., 2006). Fructose bisphosphate is present in the anaerobic isolate dataset, however, it is very slightly upregulated, not downregulated, although this is not statistically significant therefore we can consider the expression level to be unchanged in the isolate grown on UV-C_{60} compared to growth on glucose. Another glucose starvation metabolite identified by Brauer et al was AMP, which was found to be highly upregulated in

E. coli experiencing carbon starvation. Again, while AMP is present in the isolate dataset, we observe the opposite of this as AMP is slightly downregulated, but not significantly so, after growth on UV-C_{60} as the carbon source. The expression levels of these two metabolites therefore indicate there is no evidence of carbon starvation in the anaerobic isolate when is it grown with UV-C_{60} as the sole carbon source, which indicates starvation is not the cause of the possible stress response discussed.

Polycyclic aromatic hydrocarbons (PAHs) are a class of complex organic compounds which contain 2 or more fused benzene rings (Haritash & Kaushik, 2009; Peng et al., 2008). Due to their aromatic structure, PAHs are considered closely related to fullerenes and may be particularly relevant analogues to UV-degraded fullerenes in which the cage structure is broken. Although most PAH-degrading bacteria will preferentially use aerobic catabolic pathways, anaerobic degradation of PAHs has been observed (Carmona et al., 2009; Ghosal et al., 2016). Bacteria grown on PAHs as carbon sources have been found to produce certain dioxygenase enzymes which play a critical role in PAH biodegradation, and these enzymes produce salicylic acid and catechol compounds as byproducts (Ghosal et al., 2016). In the anaerobic isolate grown with UV-C_{60} as a carbon source, two catechol compounds, 3,4-Dihydroxymandelate and catechin, are upregulated (563040 and 2962800 times, respectively). The upregulation of these compounds suggests that they may be produced in this condition as a result of the overexpression of dioxygenase enzymes, which may indicate biodegradation pathways similar to those involved in PAH degradation are activated in response to UV-C_{60} being the only available carbon source. Neither 3,4-Dihydroxymandelate and catechin are considered significantly upregulated, however, as both have P-values > 0.05 when compared to the expression levels in the positive control. We therefore cannot definitively say that these catechols are upregulated in the UV-C_{60} condition, however their presence in the dataset and the large fold change observed is enough evidence to suggest the possibility of dioxygenase enzyme activity. Since the PAHs are expected to be structurally similar to UV-degraded C_{60}, it is likely that the anaerobic isolate is capable of activating pathways similar or identical to those involved in PAH degradation in order to utilise UV-C_{60} as a carbon source.

6.4.10 Summary of the anaerobic isolate metabolomic response to fullerenes

In Chapter 4 I showed that when the anaerobic isolate is grown with UV-C_{60} as the sole carbon source, there is no reduction in growth, which suggests the UV-degradation products provide an accessible carbon source for this microorganism. The results discussed in this chapter show that there are several key differences in the metabolomic profile of the isolate when it is grown with the UV-C_{60} compared to growth on glucose, which is not surprising given the difference in molecular structure between fullerenes and glucose. After growth with UV-C_{60}, the isolate changes its membrane composition by downregulating several membrane phospholipids and upregulating a ceramide, which may increase membrane rigidity. This results in increased membrane permeability, which although could be a physiological response to allow ingestion of larger carbon compounds, could also indicate the cells are experiencing some kind of stress. The downregulation of several DNA and RNA components indicates that nucleotide synthesis is being suppressed, which is a common general stress response in bacteria and further indicates that UV-C_{60} exposure may induce a stress response in the isolate. However, there are no signs of a specific oxidative stress response, and no evidence that the isolate is experiencing carbon starvation due to limited accessibility of the UV-degradation products. In fact, there is strong evidence that degradation pathways which are involved in PAH degradation are also being activated in the anaerobic isolate in order to allow it to degrade UV-C_{60}. Therefore, although UV-C_{60} does impose some stress on the anaerobic isolate, it is simultaneously used as a carbon source which allows the cultures to achieve a similar level of growth as they do on glucose.

6.5 Conclusions

This chapter examines the metabolomic response of both *E. coli* and the anaerobic isolate when grown on C_{60} and UV-C_{60} to provide a detailed metabolic analysis of the microbial response to fullerenes. A summary of the key findings presented in this chapter is provided in Table 6.4.

Table 6.4: Summary of the evidence for different metabolic responses observed with *E. coli* and the anaerobic isolate after exposure to UV-C_{60}

	E. coli:	**Anaerobic isolate:**
Membrane composition	Multiple membrane phospholipids up- or down-regulated after UV-C_{60} exposure	Multiple membrane phospholipids downregulated and one ceramide upregulated after UV-C_{60} exposure
General cellular stress response	Significant alteration of amino acid synthesis pathways and suppression of nucleotide biosynthesis after UV-C_{60} exposure	Significant alteration of amino acid synthesis pathways and suppression of nucleotide biosynthesis after UV-C_{60} exposure
Oxidative stress	Overexpression of the methionine savage pathway in response to UV-C_{60} exposure	No evidence of oxidative stress
Metabolic utilisation of UV-C_{60}	No evidence for degradation of UV-C_{60}	Activation of complex organic degradation pathways

E. coli was grown with both C_{60} and UV-C_{60}, with additional glucose as a carbon source, and an analysis of the biological response to the C_{60}-toxicity previously observed is presented. The anaerobic isolate obtained from the community in Chapter 4 was grown with UV-C_{60}, which was previously shown to function as a sole carbon source for this isolate, and a proposed pathway for its biodegradation is presented.

Native nC_{60} exposure resulted in very minor changes in metabolomic expression levels in *E. coli*, which is consistent with the growth results discussed in Chapter 5. Although *E. coli* may experience a small amount of stress resulting in the downregulation of deoxyribose and uracil, this is not enough to significantly inhibit growth provided an additional carbon source is available. UV-C_{60}, on the other hand, has a much larger effect on the metabolomic expression in the *E. coli* cultures, which is not surprising given the observed inhibition that UV-C_{60} exposure induced in the Chapter 5 experiments. The metabolomic analysis of *E. coli* after growth with UV-C_{60} indicates that a large number of phospholipids are either under or over-expressed, which is consistent with previous literature detailing the effects of C_{60} on bacterial membranes. The alteration of several amino acid expression levels, as well as the suppression of nucleotide biosynthesis and the methionine synthesis pathway, indicates that *E. coli* experiences oxidative stress in response to UV-C_{60} exposure, all of which is consistent with the previous growth data.

In Chapter 4, the anaerobic isolate was found to be capable of using UV-C_{60} as a sole carbon source. In this chapter, the metabolomic analysis confirms that there is supportive evidence for this utilisation at the metabolic level. Evidence of dioxygenase enzyme activity suggests that similar pathways involved in PAH degradation in other bacterial species are activated by the anaerobic isolate in response to UV-C_{60} to allow for its biodegradation, indicating that UV-degraded C_{60} is metabolised by the same metabolic pathways involved in the utilisation of other complex aromatic compounds. However, despite the anaerobic isolates' clear ability to grow on UV-C_{60} as the carbon source, the suppression of nucleotide biosynthesis may indicate the cells simultaneously experience stress when exposed to UV-C_{60}. There is no evidence of carbon starvation, which indicates this stress is not caused by a limited ability to utilise the carbon source. These results therefore give an interesting insight into how a single carbon source may simultaneously provide a food stock and an environmental stressor to a single microorganism.

To summarise, this chapter provides a comprehensive analysis of the metabolomic response of relevant microorganisms to C_{60} and UV-C_{60}. Evidence is provided to support the observation that while native C_{60} has little to no effect on *E. coli*, UV-C_{60} exerts oxidative stress which results in inhibited growth. Additionally, this chapter provides the first metabolomic explanation for the pathways involved in the anaerobic biodegradation of UV-degraded C_{60}. Interestingly, evidence was also found of UV-C_{60} exerting some form of cellular stress while simultaneously being used as a carbon source by the anaerobic isolate. These results may therefore point towards a paradigm shift concerning the link between carbon availability and habitability, as, while it is commonly assumed that organic-rich environments are habitable, these results suggest that biologically accessible carbon sources may also pose limitations on microbial growth. The accessibility of carbon compounds for utilisation by microbes may be far more complex than previously considered.

Chapter 7 Concluding remarks

With this thesis, I aimed to investigate how microorganisms on the early Earth may have utilised extra-terrestrial organics from meteorites as carbon and energy sources. More specifically, I sought to explore how fullerenes may have impacted early life on Earth to better understand how the influx of extra-terrestrial organics may affect the origin and evolution of microbial life on other rocky exoplanets. This knowledge will not only contribute to the current understanding of the metabolic development of primitive microorganisms and their available energy sources but will also improve our understanding of the link between carbon availability and habitability. To this end, in this thesis, I established the effect that fullerenes and their derivatives have on both anaerobic and aerobic environmentally relevant microorganisms and presented a comprehensive analysis of the underlying metabolic processes involved in these responses.

7.2 Summary

Chapter 4, the first experimental chapter in this thesis, aimed to explore the effects of fullerene C_{60}, C_{70}, and their fullerol derivatives on an anaerobic microbial community that was previously selected to grow on raw meteorite material as a carbon source. The results presented in this chapter indicate that the community can utilise C_{60} as a sole carbon source, but that the larger fullerene C_{70} is inhibitory. A single isolate derived from the anaerobic community is not able to use C_{60} as a carbon source once it is cultured alone outside of the community environment. However, when C_{60} is degraded under UV light, the degradation products provide an accessible carbon source for this isolate. Both C_{60}- and C_{70}-fullerol are inhibitory to the anaerobic community and the isolate, and this toxicity increases under visible or UV light exposure.

Chapter 5 assesses the effect of the fullerenes, fullerols and UV-degraded fullerenes on the model aerobic species *E. coli*, as well as two environmentally derived species of *Pseudomonas*, to provide an aerobic comparison to the results obtained in Chapter 4. The aim of this chapter was to determine if the responses observed in Chapter 4 are unique to anaerobic microorganisms, or if these responses are innate to all microorganisms. The results in this chapter indicate that fullerenes C_{60} and C_{70} have no effect on the growth of *E. coli*, but that they are inhibitory to both species of *Pseudomonas*. The UV-degraded C_{60} was inhibitory to *E. coli*. Fullerol, however, had no effect on the growth of *E. coli* and actually enhanced the growth of both *Pseudomonas* species by increasing the growth rate and maximum culture density.

Chapter 6 constitutes the last experimental chapter of this thesis. This chapter provides a metabolomic study of the response of *E. coli* and the anaerobic isolate to fullerene C_{60} and UV-degraded C_{60}. The aim of this metabolomic analysis was to identify any metabolic pathways activated by the anaerobic isolate in response to using UV-degraded C_{60} as a carbon source, with growth on non-accessible pristine C_{60} for comparison. The metabolomic response of *E. coli* was analysed under the same conditions to provide a comparison to a well-characterised model organism. Interestingly, despite not showing any growth inhibition, *E. coli* demonstrated a subcritical stress response after exposure to C_{60}. UV-degraded C_{60} had a much larger metabolic effect on *E. coli*; large changes in membrane phospholipid composition, restructuring of amino acid pathways and suppression of nucleotide biosynthesis and the methionine synthesis pathways all indicate *E. coli* experiences oxidative stress in response to UV-C_{60} exposure. The anaerobic isolate results, however, demonstrate that there is activation of the same metabolic pathways which are involved in the degradation of other complex aromatic organics in different bacterial species, which indicates the anaerobic isolate uses the same pathways to degrade UV-C_{60}. Interestingly, however, the suppression of nucleotide biosynthesis in response to UV-C_{60} exposure indicates that the anaerobic isolate is simultaneously experiencing a subcritical stress response while also able to utilise UV-C_{60} as a carbon source.

7.2 Key findings

Across the results detailed in all three experimental chapters, there are several recurring key findings that are continuously highlighted. The first key finding is that fullerene size appears to be highly important for biological accessibility, with smaller fullerenes providing more accessible carbon sources and larger fullerenes not only becoming inaccessible, but also inhibitory with increasing size and concentration.

On the early Earth, and also on the surface of many other young exoplanets, any organic compounds present are subject to extreme environmental conditions such as strong short-wave UV irradiation in an anoxic environment. When fullerenes are exposed to these conditions in a laboratory setting, the degradation products provide an accessible carbon source for anaerobic microorganisms, even if they are unable to utilise the non-irradiated parent fullerene. However, the same UV-degradation products are highly inhibitory to aerobic microorganisms. This indicates that while anoxic UV exposure increases fullerene accessibility for anaerobic species, it increases the toxicity of fullerenes towards aerobic species, which has important implications for the toxicity of fullerenes in the environment on the modern Earth. Although the accessibility of UV-degraded fullerenes indicates that fullerenes on the early Earth may have provided a source of carbon and energy for primitive anaerobic microorganisms, the metabolic response shows this response is more complicated, as the UV-degradation products, as well as being utilised as a carbon source, also induce a subcritical stress response.

The water-soluble fullerene derivates, fullerols, are inhibitory to the anaerobic microorganisms tested in this thesis, increasingly so when exposed to UV or visible light. However, they either have no effect on, or actually enhance the growth of the aerobic species. This phenomenon is observed when facultative anaerobic *E. coli* is grown without oxygen, which indicates the presence or absence of oxygen is not responsible for this discrepancy in response. These results demonstrate that while fullerols are toxic to obligate anaerobic microorganisms, aerobic species appear to have evolved a resistance to fullerol oxidation via the adaptations they innately possess for living in an oxic environment.

All of the key findings discussed throughout this thesis highlight not only how different the aerobic and anaerobic response to fullerenes is, but how multifaceted the correlation between carbon availability and habitability may be. The aerobic response to fullerenes discussed throughout Chapters 5 and 6 has important implications for the effects of anthropogenic fullerenes on modern microbes in the environment. The anaerobic response indicates that primitive terrestrial microbes, as well as life on other young planets, may be capable of utilising fullerenes as a carbon source, while simultaneously indicating that organic-rich environments are not necessarily ubiquitously habitable and that long-term utilisation of these organics may have deleterious effects on microorganisms.

7.3 Future work

This thesis provides a comprehensive analysis of the physiological and metabolomic effects that fullerenes and their environmentally relevant derivatives have on both aerobic and anaerobic microorganisms grown in isolation and in a complex community. However, there are still many conflicting results in the available literature due to the wide range of experimental approaches employed to assess the microbial response to fullerenes. The responses documented in the experimental chapters of this thesis indicate the importance of further cohesive research into the effect of fullerenes on different microorganisms to establish how ubiquitous the trends observed in this thesis are across a metabolically diverse collection of species, and how closely linked these responses are to the type of primary microbial respiration.

The metabolomic work detailed in this thesis provides, to the best of my knowledge, the first overview of the metabolic effect of fullerenes on microorganisms. The results of this study validate the merit of further investigating the observed phenomenon where environmentally relevant fullerene degradation products are simultaneously used as sole carbon sources while inducing a subcritical stress response. In order to understand how this relationship affects the ability of carbon-rich extra-terrestrial environments to support life, it is important to study the long-term effects of growth with UV-degraded fullerenes on anaerobic microorganisms. Continuous exposure to subcritical stress may either reduce growth over extended periods, or it could lead to an evolutionary shift that enhances microbial resistance to these environmental stresses. These outcomes have very different implications for evaluating the potential for life on organic-rich exoplanets.

Bibliography

Akter, T., Barile, C., & Ahammad, A. J. S. (2022). Chapter 23—Introduction and overview of carbon nanomaterial-based sensors for sustainable response. In J. G. Manjunatha & C. M. Hussain (Eds.), *Carbon Nanomaterials-Based Sensors* (pp. 395–416). Elsevier. https://doi.org/10.1016/B978-0-323-91174-0.00018-4

Albers, E. (2009). Metabolic characteristics and importance of the universal methionine salvage pathway recycling methionine from 5’-methylthioadenosine. *IUBMB Life*, *61*(12), 1132–1142. https://doi.org/10.1002/iub.278

Alexander, C. M. O. D., Cody, G. D., De Gregorio, B. T., Nittler, L. R., & Stroud, R. M. (2017). The nature, origin and modification of insoluble organic matter in chondrites, the major source of Earth’s C and N. *Chemie Der Erde*, *77*(2), 227–256. https://doi.org/10.1016/j.chemer.2017.01.007

Alonso, A., & Goñi, F. M. (2018). The Physical Properties of Ceramides in Membranes. *Annual Review of Biophysics*, *47*(Volume 47, 2018), 633–654. https://doi.org/10.1146/annurev-biophys-070317-033309

An, H., & Jin, B. (2015). Fullerenols and Fullerene Alter Cell Growth and Metabolisms of Escherichia coli. *Journal of Biomedical Nanotechnology*, *11*(7), 1261–1268. https://doi.org/10.1166/jbn.2015.2070

Auwerter, L. C. C., Ouki, S. K., Asaadi, M., & Shana, A. (2017). Effects of nanosized titanium dioxide (TiO2) and fullerene (C60) on wastewater microorganisms activity. *Journal of Water Process Engineering*, *16*, 35–40. https://doi.org/10.1016/j.jwpe.2016.12.006

Avanasi, R., Jackson, W. A., Sherwin, B., Mudge, J. F., & Anderson, T. A. (2014). C60 fullerene soil sorption, biodegradation, and plant uptake. *Environmental Science and Technology*, *48*(5), 2792–2797. https://doi.org/10.1021/es405306w

Badireddy, A. R., Hotze, E. M., Chellam, S., Alvarez, P., & Wiesner, M. R. (2007). Inactivation of Bacteriophages via Photosensitization of Fullerol Nanoparticles. *Environmental Science and Technology*, *41*(18), 6627–6632. https://doi.org/10.1021/ES0708215

Becker, L., & Bunch, T. E. (1997). Fullerenes, fulleranes and polycyclic aromatic hydrocarbons in the Allende meteorite. *Meteoritics and Planetary Science*, *32*(4), 479–487. https://doi.org/10.1111/j.1945-5100.1997.tb01292.x

Becker, L., Bunch, T. E., & Allamandola, L. J. (1999). Higher fullerenes in the Allende meteorite. *Nature*, *400*(6741), 227–228. https://doi.org/10.1038/22250

Becker, L., Poreda, R. J., & Bunch, T. E. (2000). Fullerenes: An extraterrestrial carbon carrier phase for noble gases. *Proceedings of the National Academy of Sciences*, *97*(7), 2979–2983. https://doi.org/10.1073/PNAS.97.7.2979

Benzerara, K., Chapon, V., Moreira, D., López-García, P., Guyot, F., & Heulin, T. (2006). Microbial diversity on the Tatahouine meteorite. *Meteoritics and Planetary Science*, *41*(8), 1249–1265. https://doi.org/10.1111/j.1945-5100.2006.tb00519.x

Berné, O., Cox, N. L. J., Mulas, G., & Joblin, C. (2017). Detection of buckminsterfullerene emission in the diffuse interstellar medium. *Astronomy & Astrophysics*, *605*, L1. https://doi.org/10.1051/0004-6361/201630325

Berry, T. D., Clavijo, A. P., Zhao, Y., Jafvert, C. T., Turco, R. F., & Filley, T. R. (2016). Soil microbial response to photo-degraded C60 fullerenes. *Environmental Pollution*, *211*, 338–345. https://doi.org/10.1016/j.envpol.2015.12.025

Berry, T. D., Filley, T. R., Clavijo, A. P., Bischoff Gray, M., & Turco, R. (2017). Degradation and Microbial Uptake of C60 Fullerols in Contrasting Agricultural Soils. *Environmental Science and Technology*, *51*(3), 1387–1394. https://doi.org/10.1021/acs.est.6b04637

Blattner, F. R., Plunkett, G., Bloch, C. A., Perna, N. T., Burland, V., Riley, M., Collado-Vides, J., Glasner, J. D., Rode, C. K., Mayhew, G. F., Gregor, J., Davis, N. W., Kirkpatrick, H. A., Goeden, M. A., Rose, D. J., Mau, B., & Shao, Y. (1997). The Complete Genome Sequence of Escherichia coli K-12. *Science*, *277*(5331), 1453–1462. https://doi.org/10.1126/science.277.5331.1453

Botta, O., & Bada, J. L. (2002). Extraterrestrial organic compounds in meteorites. *Surveys in Geophysics*, *23*(5), 411–467. https://doi.org/10.1023/A:1020139302770

Brant, J. A., Labille, J., Robichaud, C. O., & Wiesner, M. (2007). Fullerol cluster formation in aqueous solutions: Implications for environmental release. *Journal of Colloid and Interface Science*, *314*(1), 281–288. https://doi.org/10.1016/J.JCIS.2007.05.020

Brauer, M. J., Yuan, J., Bennett, B. D., Lu, W., Kimball, E., Botstein, D., & Rabinowitz, J. D. (2006). Conservation of the metabolomic response to starvation across two divergent microbes. *Proceedings of the National Academy of Sciences*, *103*(51), 19302–19307. https://doi.org/10.1073/pnas.0609508103

Brunet, L., Lyon, D. Y., Hotze, E. M., Alvarez, P. J. J., & Wiesner, M. R. (2009). Comparative Photoactivity and Antibacterial Properties of C60 Fullerenes and

Titanium Dioxide Nanoparticles. *Environmental Science and Technology*, *43*(12), 4355–4360. https://doi.org/10.1021/ES803093T

Brychkova, G., Fluhr, R., & Sagi, M. (2008). Formation of xanthine and the use of purine metabolites as a nitrogen source in Arabidopsis plants. *Plant Signaling & Behavior*, *3*(11), 999–1001.

Buseck, P. R. (2002). Geological fullerenes: Review and analysis. *Earth and Planetary Science Letters*, *203*(3–4), 781–792. https://doi.org/10.1016/S0012-821X(02)00819-1

Cami, J., Bernard-Salas, J., Peeters, E., & Malek, S. E. (2010). Detection of C60and C70 in a young planetary nebula. *Science*, *329*(5996), 1180–1182. https://doi.org/10.1126/SCIENCE.1192035/SUPPL_FILE/CAMI.SOM.PDF

Campbell, E. K., Holz, M., Gerlich, D., & Maier, J. P. (2015). Laboratory confirmation of C60+ as the carrier of two diffuse interstellar bands. *Nature 2015 523:7560*, *523*(7560), 322–323. https://doi.org/10.1038/nature14566

Cancino-Diaz, M. E., Guerrero-Barajas, C., Betanzos-Cabrera, G., & Cancino-Diaz, J. C. (2023). Nucleotides as Bacterial Second Messengers. *Molecules*, *28*(24), 7996. https://doi.org/10.3390/molecules28247996

Candian, A., Gomes Rachid, M., MacIsaac, H., Staroverov, V. N., Peeters, E., & Cami, J. (2019). Searching for stable fullerenes in space with computational chemistry. *Monthly Notices of the Royal Astronomical Society*, *485*(1), 1137–1146. https://doi.org/10.1093/mnras/stz450

Carboni, A., Helmus, R., Parsons, J. R., Kalbitz, K., & de Voogt, P. (2017). Incubation of solid state C60 fullerene under UV irradiation mimicking environmentally relevant

Extra-terrestrial fullerenes as a food source for microorganisms on the early Earth conditions. *Chemosphere*, *175*, 1–7. https://doi.org/10.1016/j.chemosphere.2017.01.149

Carmona, M., Zamarro, M. T., Blázquez, B., Durante-Rodríguez, G., Juárez, J. F., Valderrama, J. A., Barragán, M. J. L., García, J. L., & Díaz, E. (2009). Anaerobic Catabolism of Aromatic Compounds: A Genetic and Genomic View. *Microbiology and Molecular Biology Reviews*, *73*(1), 71–133. https://doi.org/10.1128/mmbr.00021-08

Chae, S. R., Hunt, D. E., Ikuma, K., Yang, S., Cho, J., Gunsch, C. K., Liu, J., & Wiesner, M. R. (2014). Aging of fullerene C60 nanoparticle suspensions in the presence of microbes. *Water Research*, *65*, 282–289. https://doi.org/10.1016/j.watres.2014.07.038

Chae, S.-R., Hotze, E. M., & Wiesner, M. R. (2009). Evaluation of the Oxidation of Organic Compounds by Aqueous Suspensions of Photosensitized Hydroxylated-C60 Fullerene Aggregates. *Environmental Science and Technology*, *43*(16), 6208–6213. https://doi.org/10.1021/ES901165Q

Chiang, L., Fung-Jou Lu, & Jaw-Town Lin. (1995). Free radical scavenging activity of water-soluble fullerenols. *Journal of the Chemical Society, Chemical Communications*, *0*(12), 1283–1284. https://doi.org/10.1039/C39950001283

Chuvilin, A., Kaiser, U., Bichoutskaia, E., Besley, N. A., & Khlobystov, A. N. (2010). Direct transformation of graphene to fullerene. *Nature Chemistry*, *2*(6), 450–453. https://doi.org/10.1038/nchem.644

Chyba, C. F., Thomas, P. J., Brookshaw, L., & Sagan, C. (1990). Cometary delivery of organic molecules to the early earth. *Science*, *249*(4967), 366–373. https://doi.org/10.1126/science.11538074

Extra-terrestrial fullerenes as a food source for microorganisms on the early Earth

Clish, C. B. (2015). Metabolomics: An emerging but powerful tool for precision medicine. *Cold Spring Harbor Molecular Case Studies*, *1*(1), a000588. https://doi.org/10.1101/mcs.a000588

Cnossen, I., Sanz-Forcada, J., Favata, F., Witasse, O., Zegers, T., & Arnold, N. F. (2007). Habitat of early life: Solar X-ray and UV radiation at Earth’s surface 4–3.5 billion years ago. *Journal of Geophysical Research: Planets*, *112*(E2), 2008. https://doi.org/10.1029/2006JE002784

Cockell, C. S. (1998). Biological Effects of High Ultraviolet Radiation on Early Earth-a Theoretical Evaluation. *J. Theor. Biol*, *193*.

Creegan, K. M., Robbins, J. L., Robbins, W. K., Millar, J. M., Sherwood, R. D., Tindall, P. J., Cox, D. M., Smith, A. B., McCauley, J. P., Jones, D. R., & Gallagher, R. T. (1992). Synthesis and Characterization of C60O, the First Fullerene Epoxide. *Journal of the American Chemical Society*, *114*(3), 1103–1105. https://doi.org/10.1021/JA00029A058/SUPPL_FILE/JA00029A058_SI_001.PDF

Deryabin, D. G., Davydova, O. K., Yankina, Z. Z., Vasilchenko, A. S., Miroshnikov, S. A., Kornev, A. B., Ivanchikhina, A. V., & Troshin, P. A. (2014). The activity of [60]fullerene derivatives bearing amine and carboxylic solubilizing groups against Escherichia coli: A comparative study. *Journal of Nanomaterials*, *2014*(January). https://doi.org/10.1155/2014/907435

Domínguez-Andrés, J., Eleveld, M., Renieris, G., Boltje, T. J., Mesman, R. J., Van Niftrik, L., Moons, S. J., Rettberg, P., Van Der Meer, J. W. M., Giamarellos-Bourboulis, E. J., Op Den Camp, H. J. M., De Jonge, M. I., & Netea, M. G. (2020). Growth on Carbohydrates from Carbonaceous Meteorites Alters the Immunogenicity of

Extra-terrestrial fullerenes as a food source for microorganisms on the early Earth Environment-Derived Bacterial Pathogens. *Astrobiology*, *20*(11), 1353–1362. https://doi.org/10.1089/ast.2019.2173

Duncan, L. K., Jinschek, J. R., & Vikesland, P. J. (2008). C60 colloid formation in aqueous systems: Effects of preparation method on size, structure, and surface charge. *Environmental Science and Technology*, *42*(1), 173–178. https://doi.org/10.1021/es071248s

Eaton, A., D., & Franson, M. A., H. (2005). *Standard methods for the examination of water & wastewater* (21st ed., Vol. 1). Washington, DC: American Public Health Association.

Ehrenfreund, P., Spaans, M., & Holm, N. G. (2011). The evolution of organic matter in space. *Philosophical Transactions of the Royal Society A: Mathematical, Physical and Engineering Sciences*, *369*(1936), 538–554. https://doi.org/10.1098/rsta.2010.0231

Fang, J., Lyon, D. Y., Wiesner, M. R., Dong, J., & Alvarez, P. J. J. (2007). Effect of a fullerene water suspension on bacterial phospholipids and membrane phase behavior. *Environmental Science and Technology*, *41*(7), 2636–2642. https://doi.org/10.1021/es062181w

Fasnacht, M., & Polacek, N. (2021). Oxidative Stress in Bacteria and the Central Dogma of Molecular Biology. *Frontiers in Molecular Biosciences*, *8*. https://doi.org/10.3389/fmolb.2021.671037

Fischer, R. A., Cottrell, E., Hauri, E., Lee, K. K. M., & Le Voyer, M. (2020). The carbon content of Earth and its core. *Proceedings of the National Academy of Sciences*, *117*(16), 8743–8749. https://doi.org/10.1073/pnas.1919930117

Flynn, G. J. (1996). The delivery of organic matter from asteroids and comets to the early surface of Mars. *Earth, Moon and Planets*, *72*(1–3), 469–474. https://doi.org/10.1007/BF00117551

Fortner, J. D., Lyon, D. Y., Sayes, C. M., Boyd, A. M., Falkner, J. C., Hotze, E. M., Alemany, L. B., Tao, Y. J., Guo, W., Ausman, K. D., Colvin, V. L., & Hughes, J. B. (2005). C60 in water: Nanocrystal formation and microbial response. *Environmental Science and Technology*, *39*(11), 4307–4316. https://doi.org/10.1021/es048099n

Foster, P. L. (2005). Stress responses and genetic variation in bacteria. *Mutation Research*, *569*(1–2), 3–11. https://doi.org/10.1016/j.mrfmmm.2004.07.017

Friedrich, D., Henkel, K., Richter, M., & Schmeißer, D. (2011). Fullerenol as Probed by Synchrotron X-ray Photoemission and Absorption Spectroscopy. *BioNanoScience 2011 1:4*, *1*(4), 218–223. https://doi.org/10.1007/S12668-011-0025-2

Gao, J., Wang, Y., Folta, K. M., Krishna, V., Bai, W., Indeglia, P., Georgieva, A., Nakamura, H., Koopman, B., & Moudgil, B. (2011). Polyhydroxy Fullerenes (Fullerols or Fullerenols): Beneficial Effects on Growth and Lifespan in Diverse Biological Models. *PLOS ONE*, *6*(5), e19976. https://doi.org/10.1371/JOURNAL.PONE.0019976

García-Hernández, D. A., Villaver, E., García-Lario, P., Acosta-Pulido, J. A., Manchado, A., Stanghellini, L., Shaw, R. A., & Cataldo, F. (2012). Infrared study of fullerene planetary nebulae. *The Astrophysical Journal*, *760*(2), 107. https://doi.org/10.1088/0004-637X/760/2/107

Extra-terrestrial fullerenes as a food source for microorganisms on the early Earth

Gasch, A. P., Spellman, P. T., Kao, C. M., Carmel-Harel, O., Eisen, M. B., Storz, G., Botstein, D., & Brown, P. O. (2000). Genomic Expression Programs in the Response of Yeast Cells to Environmental Changes□D. *Molecular Biology of the Cell*, *11*.

Gavalas, V. G., & Chaniotakis, N. A. (2000). [60]Fullerene-mediated amperometric biosensors. *Analytica Chimica Acta*, *409*(1–2), 131–135. https://doi.org/10.1016/S0003-2670(99)00887-9

Ghosal, D., Ghosh, S., Dutta, T. K., & Ahn, Y. (2016). Current state of knowledge in microbial degradation of polycyclic aromatic hydrocarbons (PAHs): A review. *Frontiers in Microbiology*, *7*(AUG). https://doi.org/10.3389/fmicb.2016.01369

González-toril, E., Martínez-frías, J., María, J., Gómez, G., Rull, F., & Amils, R. (2005). Chemolithoautotrophic Microorganisms. *Astrobiology*, *5*(3), 406–414.

Gronstal, A., Pearson, V., Kappler, A., Dooris, C., Anand, M., Poitrasson, F., Kee, T. P., & Cockell, C. S. (2009). Laboratory experiments on the weathering of iron meteorites and carbonaceous chondrites by iron-oxidizing bacteria. *Meteoritics and Planetary Science*, *44*(2), 233–247. https://doi.org/10.1111/j.1945-5100.2009.tb00731.x

Guldi, D. M., & Asmus, K. D. (1999). Activity of water-soluble fullerenes towards OH-radicals and molecular oxygen. *Radiation Physics and Chemistry*, *56*(4), 449–456. https://doi.org/10.1016/S0969-806X(99)00325-4

Hammond, M. R., & Zare, R. N. (2008). Identifying the source of a strong fullerene envelope arising from laser desorption mass spectrometric analysis of meteoritic insoluble organic matter. *Geochimica et Cosmochimica Acta*, *72*(22), 5521–5529. https://doi.org/10.1016/J.GCA.2008.08.008

Extra-terrestrial fullerenes as a food source for microorganisms on the early Earth

Hancock, D. E., Indest, K. J., Gust, K. A., & Kennedy, A. J. (2012). Effects of C 60 on the Salmonella typhimurium TA100 transcriptome expression: Insights into C 60-mediated growth inhibition and mutagenicity. *Environmental Toxicology and Chemistry*, *31*(7), 1438–1444. https://doi.org/10.1002/etc.1848

Haritash, A. K., & Kaushik, C. P. (2009). Biodegradation aspects of Polycyclic Aromatic Hydrocarbons (PAHs): A review. *Journal of Hazardous Materials*, *169*(1–3), 1–15. https://doi.org/10.1016/j.jhazmat.2009.03.137

Hotze, E. M., Badireddy, A. R., Chellam, S., & Wiesner, M. R. (2009). Mechanisms of Bacteriophage Inactivation via Singlet Oxygen Generation in UV Illuminated Fullerol Suspensions. *Environmental Science and Technology*, *43*(17), 6639–6645. https://doi.org/10.1021/ES901110M

Hotze, E. M., Labille, J., Alvarez, P., & Wiesner, M. R. (2008). Mechanisms of Photochemistry and Reactive Oxygen Production by Fullerene Suspensions in Water. *Environmental Science and Technology*, *42*(11), 4175–4180. https://doi.org/10.1021/ES702172W

Hou, W. C., & Jafvert, C. T. (2009). Photochemical transformation of aqueous C clusters in sunlight. *Environmental Science and Technology*, *43*(2), 362–367. https://doi.org/10.1021/es802465z

Hou, W.-C., Kong, L., Wepasnick, K. A., Zepp, R. G., Fairbrother, D. H., & Jafvert, C. T. (2010). Photochemistry of Aqueous C60 Clusters: Wavelength Dependency and Product Characterization. *Environmental Science and Technology*, *44*(21), 8121–8127. https://doi.org/10.1021/ES101230Q

Huang, F., Ge, L., Zhang, B., Wang, Y., Tian, H., Zhao, L., He, Y., & Zhang, X. (2014). A fullerene colloidal suspension stimulates the growth and denitrification ability of wastewater treatment sludge-derived bacteria. *Chemosphere*, *108*, 411–417. https://doi.org/10.1016/j.chemosphere.2014.02.042

Huang, L., Wang, M., Sharma, S., Sperandio, F., Maragani, S., Nayka, S., Chang, J., Hamblin, M., & Chiang, L. (2013). Decacationic [70]Fullerene Approach for Efficient Photokilling of Infectious Bacteria and Cancer Cells. *ECS Transactions*, *45*(20), 65–73. https://doi.org/10.1149/04520.0065ECST/XML

Hyung, H., Fortner, J. D., Hughes, J. B., & Kim, J. H. (2007). Natural organic matter stabilizes carbon nanotubes in the aqueous phase. *Environmental Science and Technology*, *41*(1), 179–184. https://doi.org/10.1021/es061817g

Jothi, L., Jayakumar, N., Jaganathan, S. K., & Nageswaran, G. (2018). Ultrasensitive and selective non-enzymatic electrochemical glucose sensor based on hybrid material of graphene nanosheets/graphene nanoribbons/nickel nanoparticle. *Materials Research Bulletin*, *98*, 300–307. https://doi.org/10.1016/j.materresbull.2017.10.020

Jozefczuk, S., Klie, S., Catchpole, G., Szymanski, J., Cuadros-Inostroza, A., Steinhauser, D., Selbig, J., & Willmitzer, L. (2010). Metabolomic and transcriptomic stress response of Escherichia coli. *Molecular Systems Biology*, *6*(1), 364. https://doi.org/10.1038/msb.2010.18

Kamat, J. P., Devasagayam, T. P. A., Priyadarsini, K. I., & Mohan, H. (2000). Reactive oxygen species mediated membrane damage induced by fullerene derivatives and its possible biological implications. *Toxicology*, *155*(1–3), 55–61. https://doi.org/10.1016/S0300-483X(00)00277-8

Extra-terrestrial fullerenes as a food source for microorganisms on the early Earth

Kilstrup, M., Hammer, K., Ruhdal Jensen, P., & Martinussen, J. (2005). Nucleotide metabolism and its control in lactic acid bacteria. *FEMS Microbiology Reviews*, *29*(3), 555–590. https://doi.org/10.1016/j.fmrre.2005.04.006

Kokubo, K., Shirakawa, S., Kobayashi, N., Aoshima, H., & Oshima, T. (2011). Facile and scalable synthesis of a highly hydroxylated water-soluble fullerenol as a single nanoparticle. *Nano Research*, *4*(2), 204–215. https://doi.org/10.1007/s12274-010-0071-z

Kong, L., Tedrow, O., Chan, Y. F. (Kyle), & Zepp, R. G. (2009). Light-Initiated Transformations of Fullerenol in Aqueous Media. *Environmental Science and Technology*, *43*(24), 9155–9160. https://doi.org/10.1021/ES901839Q

Kroto, H. (1988). Space, stars, C60, and soot. *Science*, *242*(4882), 1139–1145. https://doi.org/10.1126/science.242.4882.1139

Kwok, S. (2019). Organics in the solar system. *Research in Astronomy and Astrophysics*, *19*(4). https://doi.org/10.1088/1674

Kyzyma, O. A., Avdeev, M. V., Bolshakova, O. I., Melentev, P., Sarantseva, S. V., Ivankov, O. I., Korobov, M. V., Mikheev, I. V., Tropin, T. V., Kubovcikova, M., Kopcansky, P., Korolovych, V. F., Aksenov, V. L., & Bulavin, L. A. (2019). State of aggregation and toxicity of aqueous fullerene solutions. *Applied Surface Science*, *483*, 69–75. https://doi.org/10.1016/j.apsusc.2019.03.167

Lee, J., Cho, M., Fortner, J. D., Hughes, J. B., & Kim, J. H. (2009). Transformation of aggregated C60 in the aqueous phase by UV irradiation. *Environmental Science and Technology*, *43*(13), 4878–4883. https://doi.org/10.1021/es8035972

Li, Q., Mahendra, S., Lyon, D. Y., Brunet, L., Liga, M. V., Li, D., & Alvarez, P. J. J. (2008). Antimicrobial nanomaterials for water disinfection and microbial control: Potential applications and implications. *Water Research*, *42*(18), 4591–4602. https://doi.org/10.1016/J.WATRES.2008.08.015

Litasova, E. V., Iljin, V. V., Sokolov, A. V., Vasilyev, V. B., Dumpis, M. A., & Piotrovskiy, L. B. (2016). The biodegradation of fullerene C60 by myeloperoxidase. *Doklady Biochemistry and Biophysics*, *471*(1), 417–420. https://doi.org/10.1134/S1607672916060119

Lu, Y., Pang, Z., & Xia, J. (2023). Comprehensive investigation of pathway enrichment methods for functional interpretation of LC-MS global metabolomics data. *Briefings in Bioinformatics*, *24*(1), bbac553. https://doi.org/10.1093/bib/bbac553

Lyon, D. Y., Adams, L. K., Falkner, J. C., & Alvarez, P. J. J. (2006). Antibacterial activity of fullerene water suspensions: Effects of preparation method and particle size. *Environmental Science and Technology*, *40*(14), 4360–4366. https://doi.org/10.1021/es0603655

Lyon, D. Y., Brunet, L., Hinkal, G. W., Wiesner, M. R., & Alvarez, P. J. J. (2008). Antibacterial Activity of Fullerene Water Suspensions (nC60) Is Not Due to ROS-Mediated Damage. *Nano Letters*, *8*(5), 1539–1543. https://doi.org/10.1021/NL0726398

Lyon, D. Y., Fortner, J. D., Sayes, C. M., Colvin, V. L., & Hughes, J. B. (2005). Bacterial cell association and antimicrobial activity of a C60 water suspension. *Environmental Toxicology and Chemistry*, *24*(11), 2757–2762. https://doi.org/10.1897/04-649R.1

Extra-terrestrial fullerenes as a food source for microorganisms on the early Earth

Ma, J., Guo, R., & Tan, X. (2020). Aqueous photochemistry of fullerol revisited: Energy transfer vs. Electron transfer processes probed by Rhodamine B degradation. *Journal of Photochemistry and Photobiology A: Chemistry*, *397*, 112600. https://doi.org/10.1016/J.JPHOTOCHEM.2020.112600

Maier, J. P., & Campbell, E. K. (2017). Fullerenes in Space. *Angewandte Chemie - International Edition*, *56*(18), 4920–4929. https://doi.org/10.1002/anie.201612117

Mandelstam, J. (1963). Protein turnover and its function in the economy of the cell. *Annals of the New York Academy of Sciences*, *102*(3), Article 3. https://doi.org/10.1111/j.1749-6632.1963.tb13664.x

Marro, P. J., Baumgart, S., Delivoria-Papadopoulos, M., Zirin, S., Corcoran, L., McGaurn, S. P., Davis, L. E., & Clancy, R. R. (1997). Purine Metabolism and Inhibition of Xanthine Oxidase in Severely Hypoxic Neonates Going onto Extracorporeal Membrane Oxygenation. *Pediatric Research*, *41*(4), 513–520. https://doi.org/10.1203/00006450-199704000-00010

Mautner, M. N. (1997). Biological potential of extraterrestrial materials—1. Nutrients in carbonaceous meteorites, and effects on biological growth. *Planetary and Space Science*, *45*(6), 653–661. https://doi.org/10.1016/s0032-0633(97)00017-2

Mautner, M. N., Conner, A. J., Killham, K., & Deamer, D. W. (1997). Biological potential of extraterrestrial materials. *Icarus*, *129*(1), 245–253. https://doi.org/10.1006/icar.1997.5786

Mautner, M. N., Leonard, R. L., & Deamer, D. W. (1995). Meteorite organics in planetary environments: Hydrothermal release, surface activity, and microbial utilization.

Extra-terrestrial fullerenes as a food source for microorganisms on the early Earth *Planetary and Space Science*, *43*(1–2), 139–147. https://doi.org/10.1016/0032-0633(94)00205-6

Milojevic, T., Zebec, Z., & Schimak, M. P. (2020). Cultivation With Powdered Meteorite (NWA 1172) as the Substrate Enhances Low-Temperature Preservation of the Extreme Thermoacidophile Metallosphaera sedula. *Frontiers in Astronomy and Space Sciences*, *7*(July), 1–8. https://doi.org/10.3389/fspas.2020.00037

Nasim, K., & Hamblin, M. R. (2017). Can microbial cells develop resistance to oxidative stress in antimicrobial photodynamic inactivation? *Drug Resistance Updates : Reviews and Commentaries in Antimicrobial and Anticancer Chemotherapy*, *31*, 31. https://doi.org/10.1016/j.drup.2017.07.003

Navarro, D. A., Kookana, R. S., McLaughlin, M. J., & Kirby, J. K. (2015). Fullerol as a Potential Pathway for Mineralization of Fullerene Nanoparticles in Biosolid-Amended Soils. *Environmental Science and Technology Letters*, *3*(1), 7–12. https://doi.org/10.1021/ACS.ESTLETT.5B00292

Nyberg, L., Turco, R. F., & Nies, L. (2008). Assessing the impact of nanomaterials on anaerobic microbial communities. *Environmental Science and Technology*, *42*(6), 1938–1943. https://doi.org/10.1021/es072018g

Orgel, L. E. (1998). The origin of life: A review of facts and speculation. *The Nature of Life: Classical and Contemporary Perspectives from Philosophy and Science*, *0004*(December), 121–128. https://doi.org/10.1017/CBO9780511730191.012

Otsuka, M., Kemper, F., Cami, J., Peeters, E., & Bernard-Salas, J. (2014). Physical properties of fullerene-containing Galactic planetary nebulae. *Monthly Notices of the Royal Astronomical Society*, *437*(3), 2577–2593. https://doi.org/10.1093/MNRAS/STT2070

Extra-terrestrial fullerenes as a food source for microorganisms on the early Earth

Ouyang, K., Dai, K., Walker, S. L., Huang, Q., Yin, X., & Cai, P. (2016). Efficient Photocatalytic Disinfection of Escherichia coli O157:H7 using C 70-TiO 2 Hybrid under Visible Light Irradiation. *Nature Publishing Group*. https://doi.org/10.1038/srep25702

Panina, L. K., Kurochkin, V. E., Bogomolova, E. V., Evstrapov, A. A., & Spitsyna, N. G. (1997). Biotransformation of fullerenes. *Doklady Akademii Nauk*, *357*(2), 275–277.

Pasek, M., & Lauretta, D. (2008). Extraterrestrial flux of potentially prebiotic C, N, and P to the early earth. *Origins of Life and Evolution of Biospheres*, *38*(1), 5–21. https://doi.org/10.1007/s11084-007-9110-5

Peng, R. H., Xiong, A. S., Xue, Y., Fu, X. Y., Gao, F., Zhao, W., Tian, Y. S., & Yao, Q. H. (2008). Microbial biodegradation of polyaromatic hydrocarbons. *FEMS Microbiology Reviews*, *32*(6), 927–955. https://doi.org/10.1111/j.1574-6976.2008.00127.x

Peng, Z., Liu, X., Zhang, W., Zeng, Z., Liu, Z., Zhang, C., Liu, Y., Shao, B., Liang, Q., Tang, W., & Yuan, X. (2020). Advances in the application, toxicity and degradation of carbon nanomaterials in environment: A review. *Environment International*, *134*, 105298. https://doi.org/10.1016/j.envint.2019.105298

Pérez, S., Farré, M. la, & Barceló, D. (2009). Analysis, behavior and ecotoxicity of carbon-based nanomaterials in the aquatic environment. *TrAC - Trends in Analytical Chemistry*, *28*(6), 820–832. https://doi.org/10.1016/j.trac.2009.04.001

Peters, G. J., Schwartsmann, G., Nadal, J. C., Laurensse, E. J., van Groeningen, C. J., & Pinedo, H. M. (1990). *In Vivo Inhibition of the Pyrimidine de Novo Enzyme Dihydroorotic Acid*.

Extra-terrestrial fullerenes as a food source for microorganisms on the early Earth

Picache, J. A., Rose, B. S., Balinski, A., Leaptrot, K. L., Sherrod, S. D., May, J. C., & McLean, J. A. (2018). Collision cross section compendium to annotate and predict multi-omic compound identities †Electronic supplementary information (ESI) available. See DOI: 10.1039/c8sc04396e. *Chemical Science*, *10*(4), 983–993. https://doi.org/10.1039/c8sc04396e

Pickering, K. D., & Wiesner, M. R. (2005). Fullerol-Sensitized Production of Reactive Oxygen Species in Aqueous Solution. *Environmental Science and Technology*, *39*(5), 1359–1365. https://doi.org/10.1021/ES048940X

Pičmanová, M., Moses, T., Cortada-Garcia, J., Barrett, G., Florance, H., Pandor, S., & Burgess, K. (2022). Rapid HILIC-Z ion mobility mass spectrometry (RHIMMS) method for untargeted metabolomics of complex biological samples. *Metabolomics: Official Journal of the Metabolomic Society*, *18*(3), 16. https://doi.org/10.1007/s11306-022-01871-1

Pikuta, E. V., & Hoover, R. B. (2012). Microbiological study of the Murchison CM2 meteorite. *Instruments, Methods, and Missions for Astrobiology XV*, *8521*, 852105. https://doi.org/10.1117/12.929815

Piotrovskiy, L. B., Litasova, E. V., Sokolov, A. V., Iljin, V. V., Utsal, V. A., & Zhurkovich, I. K. (2020). Degradation of fullerene C60 by human myeloperoxidase and some reaction products. *Fullerenes Nanotubes and Carbon Nanostructures*, *28*(3), 196–201. https://doi.org/10.1080/1536383X.2019.1686620

Ravanel, S., Gakière, B., Job, D., & Douce, R. (1998). The specific features of methionine biosynthesis and metabolism in plants. *Proceedings of the National Academy of Sciences of the United States of America*, *95*(13), 7805–7812.

Extra-terrestrial fullerenes as a food source for microorganisms on the early Earth

Riding, M. J., Martin, F. L., Trevisan, J., Llabjani, V., Patel, I. I., Jones, K. C., & Semple, K. T. (2012). Concentration-dependent effects of carbon nanoparticles in gram-negative bacteria determined by infrared spectroscopy with multivariate analysis. *Environmental Pollution*, *163*, 226–234. https://doi.org/10.1016/j.envpol.2011.12.027

Rowlett, V. W., Mallampalli, V. K. P. S., Karlstaedt, A., Dowhan, W., Taegtmeyer, H., Margolin, W., & Vitrac, H. (2017). Impact of Membrane Phospholipid Alterations in Escherichia coli on Cellular Function and Bacterial Stress Adaptation. *Journal of Bacteriology*, *199*(13), e00849-16. https://doi.org/10.1128/JB.00849-16

Ruoff, R. S., Tse, D. S., Malhotra, R., & Lorents, D. C. (1993). Solubility of C60 in a variety of solvents. *Journal of Physical Chemistry*, *97*(13), 3379–3383. https://doi.org/10.1021/j100115a049

Sabbah, H., Carlos, M., Jenniskens, P., Shaddad, M. H., Duprat, J., Goodrich, C. A., & Joblin, C. (2022). Detection of Cosmic Fullerenes in the Almahata Sitta Meteorite: Are They an Interstellar Heritage? *The Astrophysical Journal*, *931*, 91. https://doi.org/10.3847/1538-4357/ac69dd

Sanchís, J., Aminot, Y., Abad, E., Jha, A. N., Readman, J. W., & Farré, M. (2018). Transformation of C60 fullerene aggregates suspended and weathered under realistic environmental conditions. *Carbon*, *128*, 54–62. https://doi.org/10.1016/j.carbon.2017.11.060

Sayes, C. M., Fortner, J. D., Guo, W., Lyon, D., Boyd, A. M., Ausman, K. D., Tao, Y. J., Sitharaman, B., Wilson, L. J., Hughes, J. B., West, J. L., & Vicki L. Colvin. (2004). The Differential Cytotoxicity of Water-Soluble Fullerenes. *Nano Letters*, *4*(10), 1881–1887. https://doi.org/10.1021/NL0489586

Extra-terrestrial fullerenes as a food source for microorganisms on the early Earth

Schönheit, P., Buckel, W., & Martin, W. F. (2016). On the Origin of Heterotrophy. *Trends in Microbiology*, *24*(1), 12–25. https://doi.org/10.1016/j.tim.2015.10.003

Schreiner, K. M., Filley, T. R., Blanchette, R. A., Bowen, B. B., Bolskar, R. D., Hockaday, W. C., Masiello, C. A., & Raebiger, J. W. (2009). White-rot basidiomycete-mediated decomposition of C60 fullerol. *Environmental Science and Technology*, *43*(9), 3162–3168. https://doi.org/10.1021/es801873q

Seixas, A. F., Quendera, A. P., Sousa, J. P., Silva, A. F. Q., Arraiano, C. M., & Andrade, J. M. (2022). Bacterial Response to Oxidative Stress and RNA Oxidation. *Frontiers in Genetics*, *12*, 821535. https://doi.org/10.3389/fgene.2021.821535

Semenov, K. N., Charykov, N. A., Postnov, V. N., Sharoyko, V. V., Vorotyntsev, I. V., Galagudza, M. M., & Murin, I. V. (2016). Fullerenols: Physicochemical properties and applications. *Progress in Solid State Chemistry*, *44*(2), 59–74. https://doi.org/10.1016/j.progsolidstchem.2016.04.002

Steele, A., Goddard, D. T., Stapleton, D., Toporski, J. K. W., Peters, V., Bassinger, V., Sharples, G., Wynn-Williams, D. D., & McKay, D. S. (2000). Investigations into an unknown organism on the martian meteorite Allan Hills 84001. *Meteoritics and Planetary Science*, *35*(2), 237–241. https://doi.org/10.1111/j.1945-5100.2000.tb01772.x

Stoker, C. R., Boston, P. J., Mancinelli, R. L., Segal, W., Khare, B. N., & Sagan, C. (1990). Microbial metabolism of tholin. *Icarus*, *85*(1), 241–256. https://doi.org/10.1016/0019-1035(90)90114-O

Sun, Y. P., Ma, B., Bunker, C. E., & Liu, B. (1995). All-Carbon Polymers (Polyfullerenes) from Photochemical Reactions of Fullerene Clusters in Room-Temperature Solvent

Extra-terrestrial fullerenes as a food source for microorganisms on the early Earth Mixtures. *Journal of the American Chemical Society*, *117*(51), 12705–12711. https://doi.org/10.1021/JA00156A007

Tait, A. W., Wilson, S. A., Tomkins, A. G., Gagen, E. J., Fallon, S. J., & Southam, G. (2017). Evaluation of meteorites as habitats for terrestrial microorganisms: Results from the Nullarbor Plain, Australia, a Mars analogue site. *Geochimica et Cosmochimica Acta*, *215*, 1–16. https://doi.org/10.1016/j.gca.2017.07.025

Tang, Y. J., Ashcroft, J. M., Chen, D., Min, G., Kim, C.-H., Murkhejee, B., Larabell, C., Keasling, J. D., & Chen, F. F. (2007). Charge-Associated Effects of Fullerene Derivatives on Microbial Structural Integrity and Central Metabolism. *American Chemical Society*, *7*(3). https://doi.org/10.1021/nl063020t

Taylor, R., Parsons, J. P., Avent, A. G., Rannard, S. P., Dennis, T. J., Hare, J. P., Kroto, H. W., & Walton, D. R. M. (1991). Degradation of C60 by light. *Nature*, *351*(6324), 277. https://doi.org/10.1038/351277A0

Tegos, G. P., Demidova, T. N., Arcila-Lopez, D., Lee, H., Wharton, T., Gali, H., & Hamblin, M. R. (2005). Cationic fullerenes are effective and selective antimicrobial photosensitizers. *Chemistry & Biology*, *12*(10), 1127–1135. https://doi.org/10.1016/J.CHEMBIOL.2005.08.014

Tielens, A. G. G. M. (2013). The molecular universe. *Reviews of Modern Physics*, *85*(3), 1021–1081. https://doi.org/10.1103/RevModPhys.85.1021

Tong, Z. H., Bischoff, M., Nies, L. F., Carroll, N. J., Applegate, B., & Turco, R. F. (2016). Influence of fullerene (C60) on soil bacterial communities: Aqueous aggregate size and solvent co-introduction effects. *Scientific Reports*, *6*(May), 1–9. https://doi.org/10.1038/srep28069

Extra-terrestrial fullerenes as a food source for microorganisms on the early Earth

Trevors, J. T. (2010). Suitable microscopic entropy for the origin of microbial life: Microbiological methods are challenges. *Journal of Microbiological Methods*, *83*(3), 341–344. https://doi.org/10.1016/j.mimet.2010.05.012

Tsao, N., Luh, T. Y., Chou, C. K., Chang, T. Y., Wu, J. J., Liu, C. C., & Lei, H. Y. (2002). In vitro action of carboxyfullerene. *Journal of Antimicrobial Chemotherapy*, *49*(4), 641–649. https://doi.org/10.1093/jac/49.4.641

van Hoogevest, P., Tiemessen, H., Metselaar, J. M., Drescher, S., & Fahr, A. (2021). The Use of Phospholipids to Make Pharmaceutical Form Line Extensions. *European Journal of Lipid Science and Technology*, *123*(4), 2000297. https://doi.org/10.1002/ejlt.202000297

Vileno, B., Sienkiewicz, A., Lekka, M., Kulik, A. J., & Forró, L. (2004). In vitro assay of singlet oxygen generation in the presence of water-soluble derivatives of C60. *Carbon*, *42*(5–6), 1195–1198. https://doi.org/10.1016/J.CARBON.2003.12.042

Waajen, A. C., Prescott, R., & Cockell, C. S. (2022). Meteorites as Food Source on Early Earth: Growth, Selection, and Inhibition of a Microbial Community on a Carbonaceous Chondrite. *Astrobiology*, *22*(5), 495–508. https://doi.org/10.1089/ast.2021.0089

Wang, J., Ma, Q., Zhang, Z., Diko, C. S., & Qu, Y. (2020). Biogenic fenton-like reaction involvement in aerobic degradation of C60 by Labrys sp. WJW. *Environmental Pollution*, *272*, 115300. https://doi.org/10.1016/j.envpol.2020.115300

Werge, M. P., McCann, A., Galsgaard, E. D., Holst, D., Bugge, A., Albrechtsen, N. J. W., & Gluud, L. L. (2021). The Role of the Transsulfuration Pathway in Non-Alcoholic

Extra-terrestrial fullerenes as a food source for microorganisms on the early Earth

Fatty Liver Disease. *Journal of Clinical Medicine*, *10*(5), Article 5. https://doi.org/10.3390/jcm10051081

Willetts, N. S. (1967). Intracellular protein breakdown in non-growing cells of Escherichia coli. *The Biochemical Journal*, *103*(2), 453–461. https://doi.org/10.1042/bj1030453

Zhang, Q. L., O'Brien, S. C., Heath, J. R., Liu, Y., Curl, R. F., Kroto, H. W., & Smalley, R. E. (1986). Reactivity of large carbon clusters: Spheroidal carbon shells and their possible relevance to the formation and morphology of soot. *Journal of Physical Chemistry*, *90*(4), 525–528. https://doi.org/10.1021/j100276a001

Zhang, Y.-M., & Rock, C. O. (2008). Membrane lipid homeostasis in bacteria. *Nature Reviews Microbiology*, *6*(3), 222–233. https://doi.org/10.1038/nrmicro1839

Zhao, L., Ji, Y., Sun, P., Li, R., Xiang, F., Wang, H., Ruiz-Martinez, J., & Yang, Y. (2018). Effects of individual and complex ciprofloxacin, fullerene C60, and ZnO nanoparticles on sludge digestion: Methane production, metabolism, and microbial community. *Bioresource Technology*, *267*(May), 46–53. https://doi.org/10.1016/j.biortech.2018.07.024

Zou, S., & Johnston, L. J. (2010). Ceramide-enriched microdomains in planar membranes. *Current Opinion in Colloid & Interface Science*, *15*(6), 489–498. https://doi.org/10.1016/j.cocis.2010.06.003